LANDING AUTOPILOT DESIGN
FOR AN UAV

A THESIS SUBMITTED TO
THE GRADUATE SCHOOL OF NATURAL AND APPLIED SCIENCES
OF
MIDDLE EAST TECHNICAL UNIVERSITY

BY

MERVE HANKÖYLÜ

IN PARTIAL FULFILLMENT OF THE REQUIREMENTS
FOR
THE DEGREE OF MASTER OF SCIENCE
IN
ELECTRICAL AND ELECTRONICS ENGINEERING

FEBRUARY 2011

Approval of the thesis:

LANDING AUTOPILOT DESIGN FOR AN UAV

submitted by **MERVE HANKÖYLÜ** in partial fulfillment of the requirements for the degree of **Master of Science in Electrical and Electronics Engineering Department, Middle East Technical University** by,

Prof. Dr. Canan Özgen ----------
Dean, Graduate School of **Natural and Applied Sciences**

Prof. Dr. İsmet Erkmen ----------
Head of Department, **Electrical and Electronics Eng.**

Prof. Dr. M. Kemal Leblebicioğlu ----------
Supervisor, **Electrical and Electronics Eng. Dept., METU**

Examining Committee Members:

Prof. Dr. M. Kemal Özgören ----------
Mechanical Engineering Dept., METU

Prof. Dr. M. Kemal Leblebicioğlu ----------
Electrical and Electronics Engineering Dept., METU

Assist. Prof. Dr. Afşar Saranlı ----------
Electrical and Electronics Engineering Dept., METU

Assist. Prof. Dr. İlkay Yavrucuk ----------
Aerospace Engineering Dept., METU

Assist. Prof. Dr. S. Emre Tuna ----------
Electrical and Electronics Engineering Dept., METU

Date: 10.02.2011

I hereby declare that all information in this document has been obtained and presented in accordance with academic rules and ethical conduct. I also declare that, as required by these rules and conduct, I have fully cited and referenced all material and results that are not original to this work.

Name, Last name: Merve HANKÖYLÜ

Signature:

ABSTRACT

LANDING AUTOPILOT DESIGN FOR AN UAV

Hanköylü, Merve
M.Sc., Department of Electrical and Electronics Engineering
Supervisor: Prof. Dr. M. Kemal Leblebicioğlu

February 2011, 107 pages

In this thesis, a landing autopilot for an UAV (IAI Pioneer RQ-2) is designed based on a nonlinear MATLAB model implemented with MATLAB/Simulink. In order to control the movement of the UAV at lateral and longitudinal axes, a speed, an altitude, a heading angle (direction) and a yaw rate controllers are designed. Controller design procedure is started with determination of different trim points of the aircraft. Next, the corresponding initial states and initial inputs are obtained. The model is linearized about those trim points and the gain values are determined. The resultant gain scheduled controller is used on the non-linear model.

The response of the aircraft to these controllers is tested in a constrained landing area that is constructed with respect to applicable aviation regulations. The aircraft position is investigated whether it is inside or outside of this safe landing area. If it is inside, an optimized landing path set is obtained. The steepest descent method is used for multidimensional search and parabolic fit method is used for one dimensional search (as line search) in the optimization phase.

In case it is outside the defined landing area a special algorithm which takes the aircraft into the desired region is applied. In addition, the area is allowed to move as much as possible depending on the situation with special regards to the length of the runway. Also a lateral position controller is designed in order to provide the reach of the aircraft to the main landing path.

Keywords: Landing autopilot, optimized landing path, lateral position controller

ÖZ

BİR İNSANSIZ HAVA ARACI İÇİN İNİŞ OTOPİLOTU TASARIMI

Hanköylü, Merve
Yüksek Lisans, Elektrik ve Elektronik Mühendisliği Bölümü
Tez Yöneticisi: Prof. Dr. M. Kemal Leblebicioğlu

Şubat 2011, 107 sayfa

Bu tez çalışmasında insansız bir hava aracının (İHA) (IAI Pioneer RQ-2) doğrusal olmayan MATLAB modeli için MATLAB/Simulink ile iniş otopilotu tasarımı gerçekleştirilmiştir. İHAnın hareketini yatay ve dikey eksenlerde kontrol etmek için hız, yükseklik, baş açısı (uçağın yönü) ve yönelim açısı değişme hızı kontrolcüsü tasarlanmıştır. Kontrolcülerin tasarımları için önce uçağın farklı trim noktaları bulunup başlangıç durum ve giriş değerleri elde edilmiştir. Daha sonra model doğrusallaştırılıp kontrolcüler için kazançlar elde edilmiştir. Bu kazanç değerleri kazanç planlama metodu ile doğrusal olmayan modele uygulanmıştır.

Uçağın bu kontrolcülere olan tepkileri genel havacılık kurallarına göre tasarlanıp sınırlandırılmış bir iniş alanında denenmiştir. Daha sonra uçağın bu belirlenen alana göre konumu değerlendirilmiştir. İçinde olduğu durumlar için optimize edilmiş iniş yolları seti elde edilmiştir. Optimizasyon sırasında çok boyutlu arama olarak “en hızlı iniş” ve adım uzunluğunu bulmak için “parabolic yaklaşım” adı verilen tek boyutlu bir arama metodu kullanılmıştır.

Uçağın alanın dışında olması durumu için basit bir yaklaşma prosedürü uygulanmıştır. İlaveten pistin kısıtları ile ilgili varsayımlar göz önünde bulundurularak bahsedilen güvenli alanın mümkün olduğunca hareket etmesi sağlanmıştır. Ayrıca uçağın iniş esnasında asıl iniş yolunu yakalayabilmesi için bir yatay eksen pozisyon kontrolcüsü tasarlanmıştır.

Anahtar kelimeler: İniş otopilotu, optimize edilmiş iniş yolları, yatay eksen pozisyon kontrolcüsü

To my parents and my sisters for their endless love and support…

ACKNOWLEDGEMENTS

First, I extend my deepest graduate to my supervisor, Prof. Dr. Kemal Leblebicioğlu, for his encouragements, advices, guidance, and helpfulness throughout this research work. Also, I would like to thank my colleague at this project Seçkin Arıbal for his valuable contributions, at all part of this work.

I would like to express my special thanks to Dr. Volkan Nalbantoğlu, for his guidance and suggestions that provided the start of the design activities in the thrust phase and for his patience. I would like to thank Burak Durmaz and Hakan Tiftikçi for their technical support about controller design process of the thesis. I would like to thank my colleague from TAI, Mehtap Tüysüz for her technical support about the flight procedures. I also would like to thank Murat Karani Önal and Anıl Demirel for reflecting their researcher personality on some problems during my thesis work and for logistical support. In addition, I would like to thank all these persons for their patience, perceptions and spending time for me.

And, I would like to thank all members of my so crowded family and my best girl-friends for their endless moral support and trust in me.

At the end, I wish to express my special thanks to “TUBİTAK” for their scholarship.

TABLE OF CONTENTS

ABSTRACT. iv
ÖZ. vi
ACKNOWLEDGEMENTS ix
TABLE OF CONTENTS x
LIST OF FIGURES xii
LIST OF TABLES. xvii
LIST OF ABBREVIATIONS, SYMBOLS AND SUBSCRIPTS.. xviii

CHAPTERS

1. INTRODUCTION 1
    1.1. Literature Survey. 1
    1.2. Problem Statement. 3
        1.2.1. Objectives of the Thesis 5
        1.2.2. Organization of the Thesis 6
2. LANDING AUTOPILOT. 7
    2.1. Phases of Flight 7
        2.1.1. Flight Procedures. 9
    2.2. General Design Information. 9
    2.3. Landing Path Design Approach. 12
3. DESIGN OF CONTROLLER. 16
    3.1. Trimming. 18
    3.2. Linear Model. 22
    3.3. Design of the Landing Autopilot. 28
        3.3.1. Longitudinal Controllers 28
            3.3.1.1. Speed Controller. 29
            3.3.1.2. Altitude Controller. 30
        3.3.2. Lateral Controller 31
            3.3.2.1. Direction Controller 31
            3.3.2.2. Yaw Rate Controller 33

3.4. Non-linear Model Control 35
3.5. Pole Placement Method. 40
3.6. Gain Scheduling. 43
4. PATH (TRAJECTORY) OPTIMIZATION. 49
4.1. Interpolation for Landing Paths 60
5. MISSING PATH APPROACH 67
6. LATERAL POSITION CONTROLLER 76
6.1. Cross Track Error Control 79
6.2. Lateral Track Controller. 82
7. SHIFTING LANDING PATH. 86
8. WIND EFFECT. 89
9. CONCLUSIONS 101
REFERENCES 104

LIST OF FIGURES

FIGURES

Figure 1 General Concept of an Autopilot 4
Figure 2 Relation of Autopilot, Navigation System and FMS 5
Figure 3 Phases of Flight 9
Figure 4 IAI Pioneer RQ-2 10
Figure 5 Approach and Landing Phases on Runway Representation.....12
Figure 6 Y and Z Axis Minimum Tolerances.....14
Figure 7 Y and Z Axis Maximum Tolerances.....14
Figure 8 Coverage of the Tolerance Angles.....15
Figure 9 General Model of IAI Pioneer UAV.....17
Figure 10 Trimmed flight 20
Figure 11 Disturbed Flight.....20
Figure 12 Nonlinear Model Linearization Setup in MATLAB.....22
Figure 13 Representation of Perturbation Variables on the Body-fixed Reference Frame of the Aircraft 25
Figure 14 Block Diagram of the Speed Controller 29
Figure 15 Step Response of the Speed Controller (on Linear Model) 29
Figure 16 Block Diagram of the Altitude Controller.....30
Figure 17 Step Response of the Altitude Controller (on Linear Model).....31
Figure 18 Block Diagram of the Direction Controller 32
Figure 19 Step Response of the Heading Controller (on Linear Model) 33
Figure 20 Block Diagram of the Yaw Rate Controller 33
Figure 21 Response of the Yaw Rate Controller for Sensor Input 34
Figure 22 Block Diagram of the Lateral Motion Autopilot.....34
Figure 23 Response of the System to Airspeed Signal (Non-linear Model, 1st case) 36
Figure 24 Response of the System to Altitude Signal (Non-linear Model, 1st case) .36
Figure 25 Response of the System to Heading Signal (Non-linear Model, 1st case)36
Figure 26 Response of System to Speed Signal (Non-linear Model, 2nd case).....37

Figure 27 Response of System to Altitude Signal (Non-linear Model, 2nd case) 37
Figure 28 Response of System to Heading Signal (Non-linear Model, 2nd case).....37
Figure 29 Angle of Attack and Sideslip Angle Responses (Non-linear Model, 2nd case).....38
Figure 30 Pitch Rate and Pitch Angle Responses (Non-linear Model, 2nd case).....38
Figure 31 Roll Rate, Yaw Rate and Roll Angle Responses (Non-linear Model, 2nd case).....39
Figure 32 Throttle and Elevator Deflections (Non-linear Model, 2nd case) 39
Figure 33 Aileron and Rudder Deflections (Non-linear Model, 2nd case) 39
Figure 34 General Form of Pole Placement Method 40
Figure 35 Pole Placement Application for Lateral Control on the Model.....41
Figure 36 The Response of Heading Pole Placement Controller (1st Signal).....42
Figure 37 The Response of Heading Pole Placement Controller (2nd Signal).....42
Figure 38 The Response of Heading Pole Placement Controller (3rd Signal) 43
Figure 39 Response of System to Speed Signal (with Gain Sch. 1st case).....44
Figure 40 Response of System to Altitude Signal (with Gain Sch. 1st case) 44
Figure 41 Response of System to Heading Signal (with Gain Sch. 1st case).....45
Figure 42 Response of System to Altitude Signal (with Gain Sch. 2nd case) 45
Figure 43 Response of System to Speed Signal (with Gain Sch. 2nd case).....46
Figure 44 Changing of Altitude Controller Gains 46
Figure 45 Angle of Attack and Sideslip Angle Responses (with Gain Sch. 2nd case) 47
Figure 46 Pitch Rate and Pitch Angle Responses (with Gain Sch. 2nd case).....47
Figure 47 Roll Rate, Yaw Rate and Roll Angle Responses (with Gain Sch. 2nd case) 47
Figure 48 Throttle and Elevator Deflections (with Gain Sch. 2nd case) 48
Figure 49 Aileron and Rudder Deflections (with Gain Sch. 2nd case).....48
Figure 50 Representation of Steepest Descent Method [27] 52
Figure 51 Optimized Heading Reference Signals at 49 m Altitude Area.....54
Figure 52 Response of System to Reference Heading Signal at y-axis (at 49 m)....54
Figure 53 Optimized Altitude Reference Signals at 49 m Altitude Area 54
Figure 54 Response of System to Reference Altitude Signal at z-axis (at 49 m).....55
Figure 55 Optimized Heading Reference Signals at 75 m Altitude Area.....56

Figure 56 Response of System to Reference Heading Signal at y-axis (at 75 m)....56
Figure 57 Optimized Altitude Reference Signals at 75 m Altitude Area.....57
Figure 58 Response of System to Reference Altitude Signal at z-axis (at 75 m).....57
Figure 59 Optimized Heading Reference Signals at 102 m Altitude Area.....58
Figure 60 Response of System to Reference Heading Signal at y-axis (at 102 m)..59
Figure 61 Optimized Altitude Reference Signals at 102 m Altitude Area.....59
Figure 62 Response of System to Reference Altitude Signal at z-axis (at 102 m)...60
Figure 63 Interpolated Reference Heading Signal for First Initial Position.....63
Figure 64 Response of System to Reference Heading Signal at y-axis for First Initial Position.....63
Figure 65 Interpolated Reference Heading Signal for Second Initial Position.....64
Figure 66 Response of System to Reference Heading Signal at y-axis for Second Initial Position 64
Figure 67 Interpolated Reference Heading Signal for Third Initial Position.....65
Figure 68 Response of System to Reference Heading Signal at y-axis for Third Initial Position 65
Figure 69 Interpolated Heading Signal for Fourth Initial Position.....66
Figure 70 Response of System to Reference Heading Signal at y-axis for Fourth Initial Position 66
Figure 71 Planned Missing Path Approach Flight Path (Top View) 67
Figure 72 Planned Missing Path Approach Flight Path (Side View) 68
Figure 73 Lateral Movement of Aircraft for First Initial Position 71
Figure 74 Response of System to Speed Controller for First Initial Position.....71
Figure 75 Response of System to Altitude Controller for First Initial Position 71
Figure 76 Lateral Movement of Aircraft for Second Initial Position 72
Figure 77 Response of System to Speed Controller for Second Initial Position.....73
Figure 78 Response of System to Altitude Controller for Second Initial Position 73
Figure 79 Response of System to Direction Controller for Second Initial Position ...73
Figure 80 Lateral Movement of Aircraft for Second Initial Positions with Landing Path.....74
Figure 81 Response of System to Altitude Controller for Second Initial Position with Landing Path 74

Figure 82 Response of System to Speed Controller for Second Initial Position with Landing Path 75
Figure 83 Response of System to Direction Controller for Second Initial Position with Landing Path 75
Figure 84 Response of System to Direction Controller with Lateral Position Controller 77
Figure 85 Followed Path by the Aircraft During Replacement 78
Figure 86 Response of System to Speed Controller with Lateral Position Controller 78
Figure 87 Response of System to Altitude Controller with Lateral Position Controller 78
Figure 88 Simulink Model of Cross Track Error Controller 79
Figure 89 Cross Track Error Compansation Psi Angle Result 80
Figure 90 Cross Track Error Compansation y-axis Result.....80
Figure 91 Response of System to Altitude Signal 80
Figure 92 Response of System to Speed Signal 80
Figure 93 Angle of Attack and Sideslip Angle Responses 81
Figure 94 Roll Rate, Yaw Rate and Roll Angle Responses 81
Figure 95 Pitch Rate and Pitch Angle Responses 81
Figure 96 Throttle and Elevator Deflections 82
Figure 97 Aileron and Rudder Deflections.....82
Figure 98 Desired Performance of the Lateral Track Controller 82
Figure 99 Geometrical Representatiton of the Lateral Track Controller 83
Figure 100 Simulink Model of the Lateral Track Controller 84
Figure 101 Result of the y-axis Position for the Lateral Track Controller 85
Figure 102 Response of System to the Direction Controller for Lateral Track Controller 85
Figure 103 Result of x-axis Position for the Lateral Track Controller 85
Figure 104 Improper Response of System to the Speed Controller (Wind Effect) ...90
Figure 105 Improper Response of System to the Altitude Controller (Wind Effect)..90
Figure 106 Improper Response of System to the Direction Controller (Wind Effect)91
Figure 107 y-axis Result of System (Wind Effect) 91
Figure 108 Proper Response of System to the Speed Controller (Wind Effect).....92

Figure 109 Proper Response of System to the Altitude Controller (Wind Effect) 93
Figure 110 Proper Response of System to the Direction Controller (Wind Effect) ...93
Figure 111 y-axis Result of System (Wind Effect) 93
Figure 112 Sideslip Angle Response 94
Figure 113 Roll Rate, Yaw Rate and Roll Angle Responses 94
Figure 114 Angle of Attack, Pitch Rate and Pitch Angle Responses 95
Figure 115 Throttle and Elevator Deflections 95
Figure 116 Aileron and Rudder Deflections.....95
Figure 117 Response of 1st Linear System to Speed Controller with Wind Input 97
Figure 118 Response of 1st Linear System to Altitude Controller with Wind Input ...97
Figure 119 Response of 1st Linear System to Direction Controller with Wind Input .98
Figure 120 y-axis Response of 1st Linear Model with Wind Input 98
Figure 121 Response of 2nd Linear System to Speed Controller with Wind Input 99
Figure 122 Response of 2nd Linear System to Altitude Controller with Wind Input...99
Figure 123 Response of 2nd Linear System to Direction Controller with Wind Input 99
Figure 124 y-axis Response of 2nd Linear Model with Wind Input 100

LIST OF TABLES

TABLES

Table 1 Specifications of IAI Pioneer RQ-2 11
Table 2 Input and Output Parameters of the Nonlinear Model.....17
Table 3 Representation of Variables of Trimmed and Perturbed Flight Conditions..18
Table 4 Variables of Perturbed Flight Condition.....19
Table 5 Optimization Starting Points Data Set 50
Table 6 Data Set for 49 m Altitude Area.....53
Table 7 Data Set for 75 m Altitude Area.....55
Table 8 Data Set for 102 m Altitude Area.....58
Table 9 First Initial Position for Interpolation Algorithm 62
Table 10 Second Initial Position for Interpolation Algorithm 64
Table 11 Third Initial Position for Interpolation Algorithm 65
Table 12 Fourth Initial Position for Interpolation Algorithm 66
Table 13 Generalized Representation of Missing Path Approach Path Waypoints..70
Table 14 First Initial Position for Missing Path Aproach Scenario.....70
Table 15 Second Initial Position for Missing Path Aproach Scenario.....72
Table 16 Test Results of Shifting Safe Landing Corridor Algorithm.....88

LIST OF ABBREVIATIONS, SYMBOLS AND SUBSCRIPTS

DA: Direct to Altitude

İHA: İnsansız Hava Aracı

FAF: Final Approach Fix

FAR: Federal Aviation Rules

FMS: Flight Management System

GPA: Glide Path Angle

g: gravity

IAF: Initial Approach Fix

ICAO: International Civil Aviation Organization

IFR: Instrument Flight Rules

ILS: Instrument Landing System

KIAS: Knots Indicated Airspeed

m: mass

N: Newton

NAVAID: Navigational Aid

PID: Proportional-Integral-Derivative

RNAV: Area Navigation

RF: Radius to Fix

SAR: Search and Rescue

TAI: Turkish Aerospace Industries

TD: Touch Down

UAV: Unmanned Aerial Vehicle

VFR: Visual Flight Rules

Vs: Stall Speed

Wpt: Waypoint

I_x moment of inertia in roll

I_y moment of inertia in pitch

I_z moment of inertia in yaw

I_{xz} product of inertia about x and z axis

SUBSCRIPTS

a aerodynamic effects

g gravitational effect

c movement of aerodynamic controls

p power effect

d atmospheric disturbances

CHAPTER 1

INTRODUCTION

Today's most important issues are UAVs which will provide so many benefits in military missions and civilian uses. Especially, their sizes, performance specifications and hardware loaded on them are changing their intended usage areas.

As it is known, these remote controlled or autonomous vehicles are frequently used in the missions such as surveillance and monitoring. Among other primary functions are remote sensing, transportation and scientific research. In addition to the price issue the autonomy degree and mission capabilities are the most important differences between UAVs [1]. Depending on the development of international relationships, common uses of these vehicles are spying for possible military precautions of enemy countries or terroristic attacks and also for reconnaissance flights during natural disasters [2].

Additionally, UAVs have many advantages.

- They have wide usage area and mission profile which will not be realized with piloted aircraft.
- They have low cost and simple design (e.g., the systems for surveillance of human beings are not required) [3].

1.1. Literature Survey

As stated in [4] the first Automatic Landing System (ALS) for aircrafts was made in 1965. After this date the use of the system has become widespread in the design of the aircrafts. It depends on the Instrument Landing System (ILS) coverage area that guides the aircraft for appropriate position, altitude etc. It also seemed that an

automatic landing system is smoother than the manual landing. But the capability of the system is limited with the safety envelope.

The statistics about flight accidents shows that 67% of the accidents are due to human factors as the primary cause and 5% are attributed to weather factors. With respect to the flight phases, 47% accidents occur during the final approach or landing of aircrafts [4].

Landing is one of the most difficult parts of a flight. Aircraft pilots have to consider the aircraft instruments and also they need to be sensitive to the environment changes. This is important because if the flight envelope gets over the limits of the installed ALS, the pilot have to take the control. But as we have already mentioned this will increase the accident possibility. Due to these problems (envelope limitation, human factors), special landing algorithms have been developed based on intelligent techniques like fuzzy logic, neural network and adaptive systems [29].

Practically, classical control methods are still being used for the landing job and they have been used in this thesis work as well. PID controllers will be employed in the vertical axis controller [5], and also in the design of controllers to deal with the lateral and longitudinal axis effects [3], [6].

When we look at the aircraft dynamics we can see that the landing control law is a nonlinear control problem. Accordingly, utilization of only a linear controller will not be sufficient to cover whole operation envelopes [7]. During the controller design the most important problem is the necessity of calculation of different gain values [8]. Changes of one of the controller parameters especially speed or altitude controller parameters may make the controller gains invalid. For these reasons most of the ALS systems are generated by the gain scheduling method [4]. However, again, to improve the system robustness some fuzzy logic or adaptive controllers are frequently tried [9].

In addition to the vertical axis movement of the aircraft the lateral movement is also a very important part of the landing and all phases of the flight. So there are many studies about lateral position control (guidance). The main idea is to produce the direction command in order to adjust aircraft position according to the reference

point or line coming from the guidance block. Actually, the reference line during the landing guidance phase represents the desired course of the aircraft [10]. In principle the way point guidance method is used to obtain the reference line but there are many other methods [10], [11], [12], [13].

Lateral position control brings path planning issues that are also very important to guide the aircraft during landing. In general the purpose of path planning here is to generate an effective path to avoid known or unknown obstacles and regenerate the flight path in response to changing state of the aircraft [14].

It should be noted that the attributed missions to the UAVs (military or civilians) require a powerful trajectory generation and guidance capability. In civil systems only some linear trajectory generation methods are being used. But these studies continue to be used especially for military applications which are sufficiently complex and comprehensive with high technology which cannot be available to be used in civil researches [2]. Generally different optimization methods (e.g., steepest descent based or genetic algorithms) [15], [16] can be used for path/trajectory optimization and they are used widely in order to avoid collision of the aircrafts, to construct minimum energy paths, etc. In particular, especially for the landing problem, the required reference signals for the autopilots of the aircraft can be generated based on optimal control theory while regarding time constraints or performance parameters of the aircraft [17], [18]. In this thesis an application of optimal path generation for landing is presented.

1.2. Problem Statement

In this study the main concern is designing an autopilot that considers the approach and landing phase of an UAV (unmanned aerial aircraft). This controller should control both lateral and longitudinal axis movement of the aircraft. These are required because of the fact that, during the approach phase, the aircraft have to reach a suitable landing path.

After development of controller mechanism the robustness of the system will be improved, regarding varying system parameters which may cause bad results if not determined in a special way. This means that the controller gains that are generated for one initial speed value may not be capable enough to control the aircraft states at another possible speed value. For this purpose the gain scheduling method is applied.

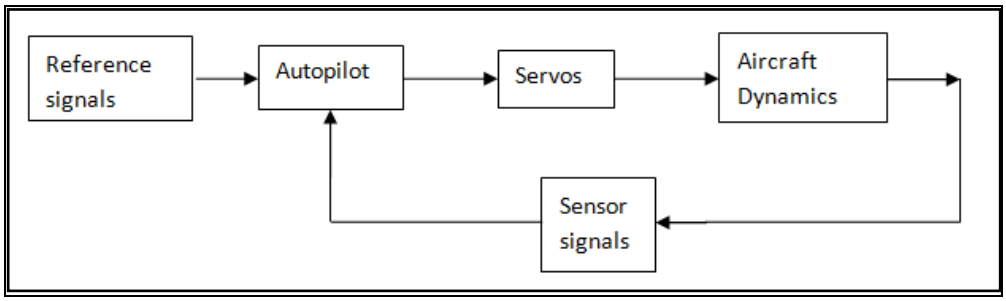

Figure 1 General Concept of an Autopilot

Another important problem is determining a safe movement area for the air vehicle which covers suitable landing paths regarding performance parameters. This area will be generated by vertical and horizontal tolerance angles around a basic approach and landing path (the source of tolerances are NavAid instruments, especially ILS and GS). It is called as the safe landing corridor in this study. The most suitable landing paths for tracking in this area will be obtained by optimization procedures according to limits and performance parameters of the air vehicle.

Then, backward and forward movement capability (movement on x-axis) is added to the safety landing corridor. Also, by the help of this idea the movement area of the aircraft will be expanded with regards to the desired runway length at x-axis. Otherwise the corridor will be shifted as far away as you want.

If the UAV is outside of safe landing corridor (the aircraft will not necessarily be inside the corridor despite the corridor shifting action) some general approach procedures (missing path approach) will be applied.

In order to provide the movement of the aircraft at lateral axis reference signals (guidance) will be provided. The required waypoints and related signals will be provided by a Flight Management System (FMS) with RNAV (area navigation). Regarding system requirements a lateral navigation system will be enough for this study.

To talk about the purposes of the study effectively, the generalized form of the problems stated above is represented with a block diagram here. As it is mentioned this is a generalized representation. In this thesis work some parts are applied in detail, some are not.

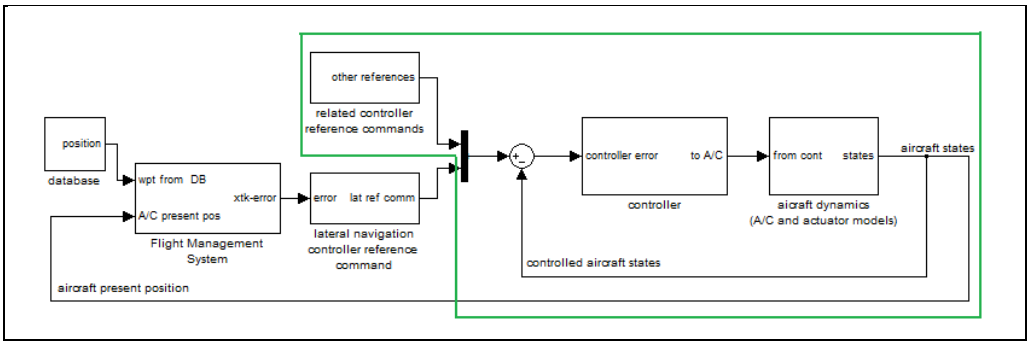

Figure 2 Relation of Autopilot, Navigation System and FMS

1.2.1. Objectives of the Thesis

First of all, notice that the main concern is controlling the aircraft properly while landing (represented on Figure 2 with the blocks in coverage) in this thesis. The remaining part on the figure 2 is considered as lateral position controller in the thesis (where FMS and RNAV applications are studied limited).

At the first step the purpose is designing an autopilot that provides the control of the aircraft at both lateral and longitudinal axes for different initial states (different trim points). In order to realize this aim the aircraft is trimmed at suitably chosen points. Then aircraft is linearized at those trim points. Related controllers will be designed for linear aircraft models and the obtained controller gains are transferred to the non-linear aircraft model.

In this thesis another important issue is generating acceptable paths and corresponding reference signals for the state controllers. For the longitudinal axis, reference altitude signal (approach and landing path) and for the lateral axis, reference heading signal (lateral movement path) will be produced.

The development of a safe landing corridor which will be determined by the vertical and horizontal axis angle tolerances is another issue. The aircraft position inside and outside this area should be considered. Acceptable landing paths for different initial points regarding both altitude and lateral deviation on y-axis will be produced by optimization algorithms. For initial states outside this area different methods will be applied. One of them is the missing path approach procedure (limited application). The other one is shifting the safe landing corridor on x-axis and covering the initial position states of the aircraft. Also, for lateral axis movement lateral position controller is designed which produces the heading reference signal.

At the end the system response due to wind effect is tested and the observed results are given.

1.2.2. Organization of the Thesis

The organization of this thesis is as follows. Chapter 2 explains some flight science and dynamics principles and their relation with the project. Also, approach and landing trajectories and some important limitations/constraints are given in this chapter. In chapter 3 the controller design and their generalized models are represented. Then, gain scheduling method in order to provide satisfactory responses of the aircraft at each acceptable state is covered in chapter 3. In chapter 4, path (trajectory) optimization issue is explained. An essential procedure, missing path approach is considered in chapter 5. Chapter 6 explains the lateral position control methods. In order to expand the movement area of the aircraft and coverage area of the safe landing corridor, shifting the landing corridor issue is considered in chapter 7. At the end the effect of environmental conditions (crosswind disturbance) is considered in chapter 8. Chapter 9 represents conclusions and recommendations for future works.

CHAPTER 2

LANDING AUTOPILOT

This chapter defines some important aviation terms which will be used frequently in this thesis. Also it explains some initial design approaches about the landing autopilot which will be detailed in the following chapters.

2.1. Phases of Flight

Firstly, we will examine all main phases of flight. Then we will consider our subject, approach and landing phase. These definitions are given by ICAO (International Civil Aviation Organization) for commercial aircrafts in order to develop a common understanding in world-wide and to make clear the related safety studies for everybody [19].

1. Standing:

   Before taxi phase, the aircraft is still waiting into gate or parking area. Engine start-up/shutdown is realized at this step.

2. Pushback/Towing:

   The aircraft starts to move from gate or parking area to runway with assistance. Otherwise it is accepted as in the TAXI phase.

3. Taxi:

   The movement of aircraft on runway before take-off or after landing phase with its own power.

4. Take-off:

It is started at take-off power application and ended at a decided altitude (35 ft for commercial aircraft) with realization of gear-up action.

5. Climb:

This phase starts at the end of take-off and finishes when it reaches a sufficiently high altitude (1000 ft for commercial aircraft regarding VFR (Visual Flight Rules) pattern).

6. En-route:

This phase covers another climbing movement up to the cruise altitude, cruise phase, changing cruise phase (climb/descent at any altitude out of defined climb and descent phase values) and descent phase up to IAF (Initial Approach Fix). Note that descent phase end point will be changed according to the VFR or IFR (Instrument Flight Rules) flight.

7. Approach:

The coverage of this phase, for IFR and VFR flight is different. In general for IFR this phase continues between IAF and flare begin point and for VFR case, it starts at VFR pattern (or 1000ft altitude, which is earlier), ends at flare begin point. Also, the missing path approach procedure is another part of the approach. The details will be given in the following chapters.

8. Landing:

This phase considers the duration of flight that covers the flare begin point, touchdown and landing taxi. According to the FAR requirements landing starts at 50 ft (V = 1.3Vs – 1.3 times stall speed (Vs)) above runway and finishes at the end of flare (V = 1.25Vs) [20].

Note that, our project covers both approach and landing phases. When it is said “landing” in the remaining part of the thesis, it should be understood as it includes these two phases.

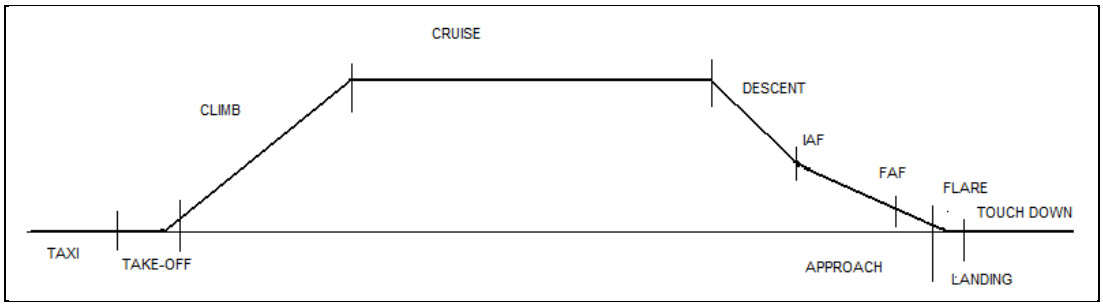

Figure 3 Phases of Flight

2.1.1. Flight Procedures

According to the type of the aircraft there are many other procedures that are performed in flight (hold patterns, p-turns, SAR (Search and Rescue) patterns etc.). In general, these procedures include defined waypoints, and aircraft follows these points due to the flight plan.

Under this title we are interested in only the missing path approach procedure that will be realized when the aircraft does not remain in a safe landing attitude.

Missing path approach is realized when the aircraft cannot make appropriate approach and landing. Then the aircraft have to follow a new procedure which is similar to en-route phase. The aircraft climbs at a special altitude, then turns to reach the desired position and descents to the final approach point (FAF-Final Approach Fix) and starts the approach phase. The suitable values of climb and descent altitudes and turn direction (bank angle) will be changed according to aircraft type and applicable flight rules for them.

2.2. General Design Information

Non-linear model of IAI Pioneer RQ-2 type UAV is used in this landing autopilot design thesis. Related stability derivatives and specifications about the UAV are also found at [33].

The generalized specifications of IAI Pioneer RQ-2 type UAV are given in Table 1.

Figure 4 IAI Pioneer RQ-2

We constructed an autopilot in order to control the aircraft during the landing phase. For this purpose we defined controlling commands and critical initial states. Then, UAV model is considered in order to find trimming values and linear model state space matrices at these critical points. At the end the autopilots are designed for linear models and the obtained controller gains are applied on the non-linear aircraft model.

For a good landing performance we considered both lateral and vertical navigation performances of the aircraft. Thus, we try to control speed, altitude and lateral attitude (direction) of the aircraft [6], [8]. We designed PID type controllers for all state controllers. Also pole placement method is applied to the heading controller in order to evaluate and test the performance of the heading PID controller.

As it can be seen from the controller performance the air vehicle motions are decoupled. When we observed non-linear system simulations, any change at airspeed values causes unacceptable results for all controlled states especially for altitude. According to the performance parameters of UAV (Table 1) the critical operating speed values are defined as 60 m/s maximum and 30 m/s minimum. Then gain scheduling method is applied for 30 m/s and 60 m/s airspeed values (Please see Chapter 3 for details).

In order to work as much realistic as possible we considered landing scenarios and defined some constraints about runway, airspace and aircraft performance.

Table 1 Specifications of IAI Pioneer RQ-2

Specifications of IAI Pioneer RQ-2:	
Weight	451.9 pounds
Fuel	47 liters 100 Octane AVGAS
Lenght	14 feet
Width	16.9 feet
Height	3.3 feet
Engine	26-HP magneto ignition, crankcase scavenged, horizontally opposed, simultaneous firing two-stroke directly coupled to a 29-inch fixed 18 degree pitch wooden laminate propeller.
Service Ceiling	12,000 feet
Absolute Ceiling	15,000 feet
Maximum Range	185+ KM
Maximum Endurance	5+ hours
Maximum Authorized Airspeed	110 KIAS (Knots Indicated Airspeed)
Minimum Speed	55 KIAS (Still Air) 60 KIAS (Rough Air) 65 KIAS (MIAG Autopilot software limit)
Stall Speed	40-45 KIAS
Cruise Speed	70 KIAS

A decision making mechanism is prepared, which considers initial position (altitude and lateral attitude) of the aircraft and the length of the runway. This decision making process evaluates the aircraft position with respect to the safe landing corridor regarding corridor shifting option. For acceptable cases (aircraft is inside the defined landing area), a set of appropriate landing paths is obtained by using optimization algorithms.

Also cross track error control and lateral track control methods are applied on the controlled aircraft model in order to reach the associated landing path on y-axis.

We have preferred to study the approach and landing phases. According to the literature survey there is not much non-military study available about landing of an air vehicle. It is the most important part of any flight; but it requires so much financial and occupational supports. Also, the complexity of the controller algorithm that considers both lateral and longitudinal axes is another cause that reduces the interest. Mostly control of one of the axes is preferable.

2.3. Landing Path Design Approach

As mentioned before, for each flight phase there are some defined parameters and limitations which are acceptable for all air vehicles in order to enable a standard flight.

When we consider the landing phase, some parameters are defined according to total landing distance (lateral and vertical distance) and aircraft performance. These parameters are glide path angle, altitude constraints and speed constraints and also lateral distance tolerances depending on properties of the runway.

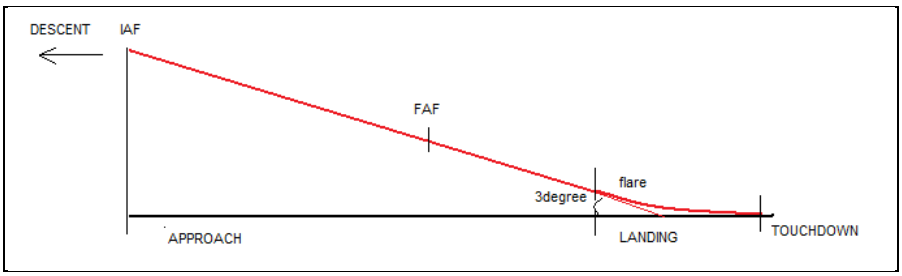

Figure 5 Approach and Landing Phases on Runway Representation

The acceptable glide path angle (GPA) value is between -2.5 and -3.5 degrees [21]. We chose the glide path angle in our application as -3.0 degrees. Actually, by the help of basic trigonometric calculations, due to constraint values (altitude or

assumed runway distance) we can determine altitude value or length of the runway. We decided approximately 100 m as the maximum height which will be appropriate for the landing phase. Basically, with these features (maximum height and GPA) we generated the main landing path. But also the deviations will be considered in this study. This issue is considered in Chapter 4 in detail.

As mentioned in [22] speed value at the top of the landing phase (at FAF-final approach fix) is 1.3Vs for commercial aircraft and 1.2Vs for military aircraft. At the touchdown this speed reduces to 1.15Vs for commercial aircraft and 1.1Vs for military aircraft. The difference between speed values at mentioned fixes is at most 0.15Vs. In this thesis, for such kind of an UAV we can use same speed values for all parts of the flight and we decided to fix speed value at 30 m/s throughout landing.

Due to the decided maximum landing altitude (100 m) and glide path angle (-3.0 degrees) we can calculate maximum required runway distance (assigned as x axis for this application) as approximately 1942 m. We defined the width of the runway (assigned as y axis for this application) as 13.71 m. Note that all of these values are assumptions coming from the performance and physical specifications of given the UAV.

During the landing phase, in order to compensate for possible acceptable deviations at lateral and longitudinal axes we tried to construct a landing corridor. We defined maximum and minimum angular tolerance values for each axis.

We defined the high lateral tolerance angle value as 5.0 degrees (coverage of an ILS); also the low lateral tolerance angle value is chosen as 0.41 degrees. The chosen high longitudinal tolerance angles are +0.5 degrees for upward and -1.5 degrees for downward (Figure 6 and Figure 7) According to these angular tolerances a corridor is drawn that is appropriate for safe landing [21].

On this corridor we pointed out some different altitude constraints and corresponding lateral areas. These constraints are assigned as starting points for different landing conditions. Also these areas and related conditions are considered at path (trajectory) optimization chapter one by one. See Chapter 4 for details.

The mentioned altitude constraints are 49 m, 75 m and 102 m (Figure 8). The lateral axis distances will be calculated by the tolerance angle values but on the given figures (Figure 6 and Figure 7) these values are written greater than the calculated values. In this theoretical study we tried to cover a larger area. Also in the optimization chapter we used these given lateral axis values.

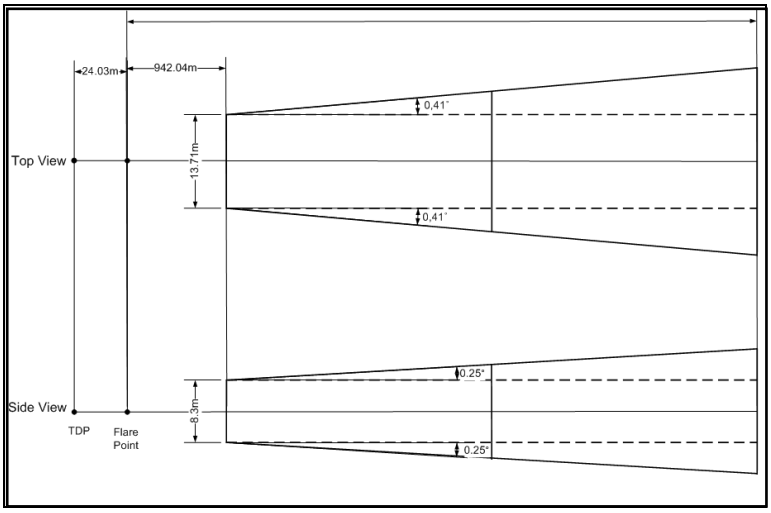

Figure 6 Y and Z Axis Minimum Tolerances

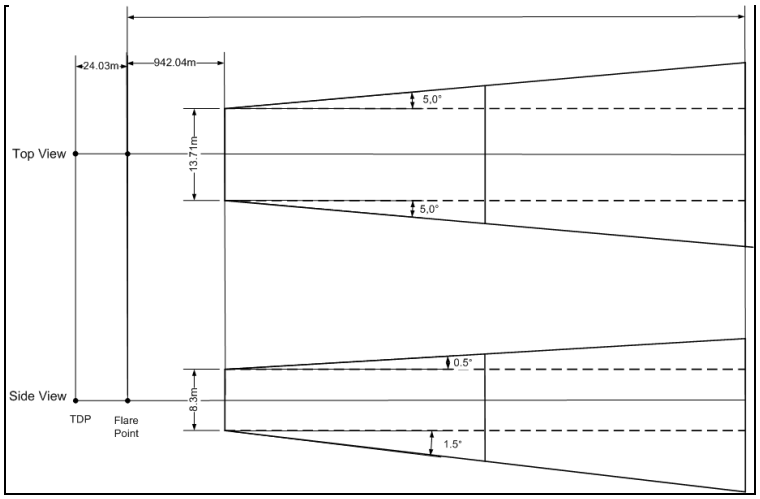

Figure 7 Y and Z Axis Maximum Tolerances

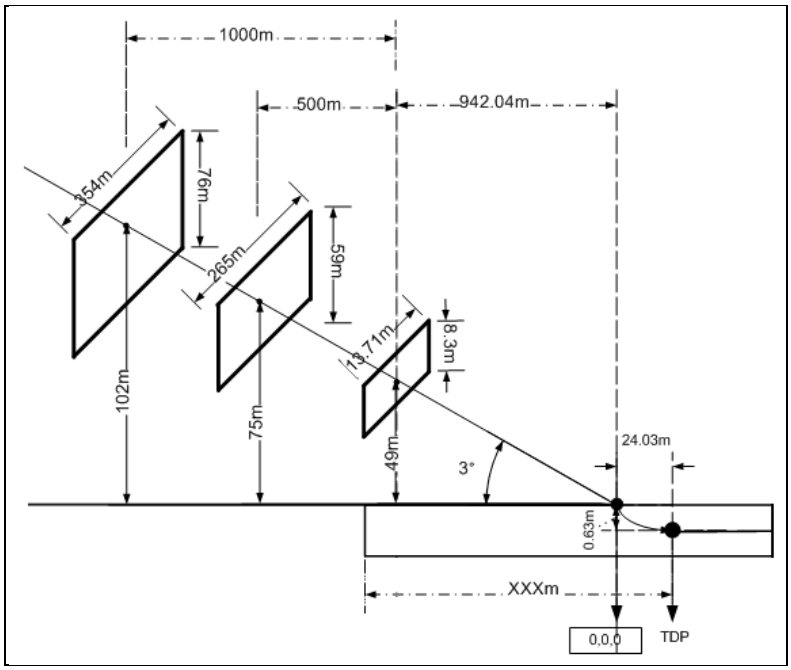

Figure 8 Coverage of the Tolerance Angles

CHAPTER 3

DESIGN OF CONTROLLER

In this thesis the main issue is designing a landing autopilot for an unmanned aerial vehicle. Through the low mass of the vehicle, lower Reynolds numbers, and light wing loading of the aircraft, stabilization of an UAV is more difficult [6]. We tried to control UAV movement states and explained the studies in the following paragraphs.

We used MATLAB/Simulink programming language during all system design activities and coded some auxiliary MATLAB/m-files. For the landing phase, we designed airspeed and altitude controllers to control the longitudinal axis states and a direction controller (heading controller) to control the lateral axis states of UAV. As references, some thesis works, and some well-known books about automatic flight control issue have been investigated during the design of all control logics.

We have used 6-DoF nonlinear model of IAI Pioneer RQ-2 type UAV that is implemented in a MATLAB library. According to the general controller design idea, first, we have designed the autopilots for linear models of the UAV. By the help of tools in the MATLAB library we have trimmed the aircraft due to initial states (speed, altitude and gamma) and obtained initial states and initial inputs at the trimmed point. These initial states are used during the linearization of the non-linear UAV model. For this purpose MATLAB Linearization Tool is used and state-space matrices of linearized UAV models have been obtained. As mentioned previously, initially, we have designed controllers for these linear models. Then, they have been applied on the non-linear model of the UAV.

The general MATLAB model of the aircraft is given in Figure 9. The input and output components of the model are tabulated in Table 2. Each component will be detailed in following sections.

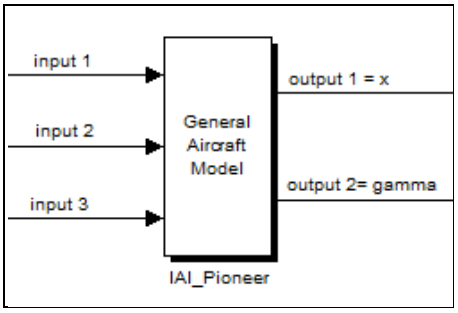

Figure 9 General Model of IAI Pioneer UAV

Table 2 Input and Output Parameters of the Nonlinear Model

inputs		outputs		
Input_1	01 Uwind (m/s)	Output_1 (x, states)	01 V (m/s)	airspeed
	02 Vwind (m/s)		02 alpha (rad)	angle of attack
	03 Wwind (m/s)		03 beta (rad)	sideslip angle
	04 Uwind_dot (m/s2)		04 p (rad/s)	roll rate
	05 Vwind_dot (m/s2)		05 q (rad/s)	pitch rate
	06 Wwind_dot (m/s2)		06 r (rad/s)	yaw rate
Input_2	07 Fx (N)		07 psi (rad)	heading angle
	08 Fy (N)		08 theta (rad)	pitch angle
	09 Fz (N)		09 phi (rad)	roll angle
	10 Mx (N)		10 xe (m)	X coordinate
	11 My (N)		11 ye (m)	Y coordinate
	12 Mz (N)		12 ze (m)	altitude
Input_3	13 delta elevators (rad)	Output_2	gamma (rad)	glide path angle
	14 delta ailerons (rad)			
	15 delta rudder (rad)			
	16 delta stabs/flaps (rad)			

3.1. Trimming

Trimming of an aircraft can be done as the solution of any system at equilibrium points, where all dynamical equations are set to zero. Equilibrium condition will be provided when force/moment equations are balanced [8]. Related representation from reference [8] is given below.

$$X_0 - mg\, sin\theta = 0 \qquad [3.1]$$

$$Z_0 + mg\, cos\theta = 0 \qquad [3.2]$$

$$Y_0 = L_0 = M_0 = N_0 = 0 \qquad [3.3]$$

When the trimmed flight condition is perturbed, the force and moment balance on the aircraft is upset. Then the resultant transient motion is defined in terms of the perturbation variables [23]. The summary about trimmed and perturbed flight components are given in Table 3.

Table 3 Representation of Variables of Trimmed and Perturbed Flight Conditions

	Trimmed equilibrium			**Perturbed equilibrium**		
Aircraft axis	ox	oy	oz	ox	oy	oz
Force	0	0	0	X	Y	Z
Moment	0	0	0	L	M	N
Linear velocity	U_e	V_e	W_e	U	V	W
Angular velocity	0	0	0	p	q	r
Attitude	0	θ_e	0	ϕ	θ	ψ

Note: Please see List of Abbreviations, Symbols and Subscripts for the remaining components that are not given in the tables.

The explanations for variables of perturbed flight condition are given in Table 4.

Table 4 Variables of Perturbed Flight Condition

X	Axial “drag” force	Sum of the components of aerodynamics, thrust and weight forces
Y	Side (lateral) force	
Z	Normal “lift” force	
L	Rolling moment	Sum of the components of aerodynamics, thrust and weight forces
M	Pitching moment	
N	Yawing moment	
p	Roll rate	Components of angular velocity
q	Pitch rate	
r	Yaw rate	
U	Axial velocity	Total linear velocity components of the cg
V	Lateral velocity	
W	Normal velocity	

Note that the components of the total linear velocity perturbations (U, V, W) are given by the sum of the steady state equilibrium components and the transient perturbation components (u, v, w). Thus,

$$\begin{aligned} U &= U_e + u \\ V &= V_e + v \\ W &= W_e + w \end{aligned} \qquad [3.4]$$

The difference between a trimmed flight and a disturbed flight [23] is represented in Figures 10 and 11.

The maintenance of trimmed equilibrium requires the correct simultaneous adjustment of the motional variables in all six degrees of freedom and is dependent on airspeed or Mach number, flight path angle, airframe configuration, weight and centre of gravity (cg) position. When these parameters are changed during a typical

flight, trim adjustments will be repeated as required. This is a disadvantage for the design activities, because at different airspeed values the aircraft will produce different initial angle of attack values. This means that, for an effective controller design only one trim point will not be enough.

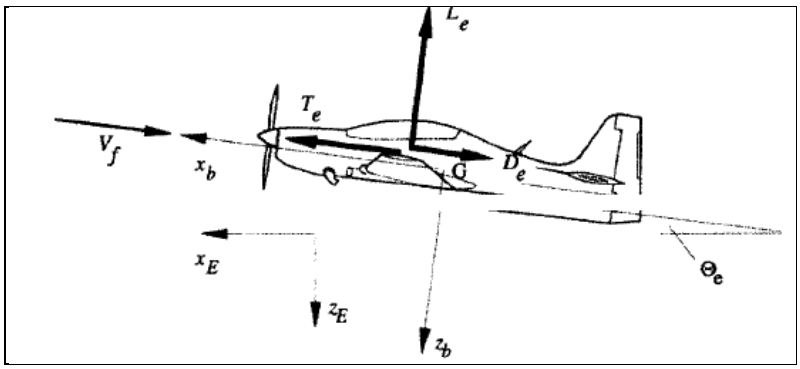

Figure 10 Trimmed flight

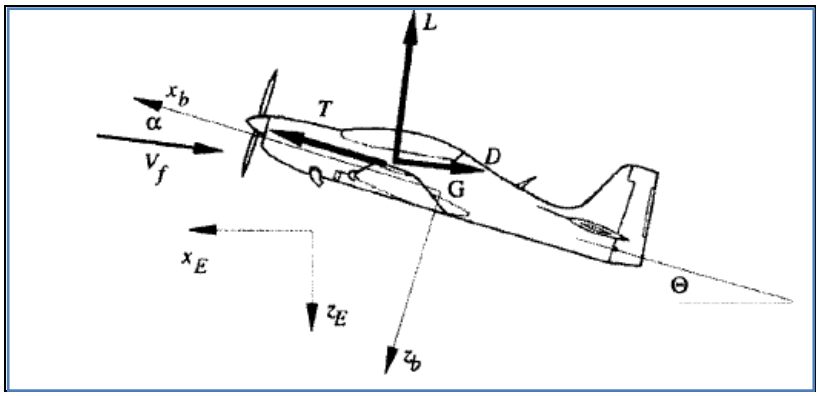

Figure 11 Disturbed Flight

This step is repeated for different trim points in order to increase the robustness of the controller. Because as it is seen from the simulation results, when we change initial airspeed value the response of the controlled system becomes unacceptable. So, we concluded to use gain scheduling method by using airspeed value as the scheduling variable. The details will be given at Gain Scheduling subchapter.

For given initial flight conditions (speed, altitude, and gamma), the initial values of all considered aircraft states and initial input values (i.e., alpha, theta, thrust, and elevators) are obtained by using the given trimming tool in MATLAB library. Note that, these findings will be used during the generation of linear UAV model and control of the non-linear model of the aircraft.

Next, we have defined critical values for speed, altitude, and gamma and assigned them as trim points. Actually, as mentioned before the only critical state is airspeed value. We used maximum and minimum cruising speed values (60 m/s and 30 m/s) as trim points. According to a level flight condition, altitude value is defined as 60 m (average) and gamma (GPA: Glide Path Angle) is defined as zero for each case.

Related outputs of trimming tool are initial states of aircraft and initial controller inputs. See Table 2 for their explanations. By the help of initial state values we obtained linear models of the UAV. See the next subchapter for details.

States of the model are; $x0 = [V\ alpha\ beta\ p\ q\ r\ psi\ theta\ phi\ xe\ ye\ H]$;

Inputs of the model are;

$$u0 = [Fx, Fy, Fz, Mx, My, Mz, del_elev, del_ail, del_rud, del_stabs/flaps]$$

Trimming at V0 =30 m/s, H0 = 60 m, GPA = 0 and the results are;

x0 = [30 0.1753 0 0 0 0 0 0.1753 0 0 0 60];

u0 = [309.8742 0 0 0 0 0 0.145603 0 0 0]

Trimming at V0 = 60 m/s, H0 = 60 m, GPA = 0 and the results are;

x0 = [60 -0.0200 0 0 0 0 0 -0.0200 0 0 0 60]

u0 = [21 0.2210 0 0 0 0 0 -0.1009 0 0 0]

Notice that, according to the simulation results which are represented in the following chapters, these two trim points are enough to provide the control of the system properly.

3.2. Linear Model

After obtaining trim results for the non-linear model of the UAV the autopilot design is performed. For this purpose (as a general design approach), initially, the autopilot has been designed for the linear model of the aircraft. In order to find state space model of linearized aircraft models we have used MATLAB/Linearization Tool. We have realized the linearization step two times due to the existence of two trim points which are defined in the previous chapter. The basic linearization setup in MATLAB Simulink is given in Figure 12.

Note that the linear model will be generated by the known equations of motions and stability derivatives of the aircraft. The stability derivatives of this UAV can be found in [33]. First, we can consider the theoretical way of linearization of a non-linear aircraft model. The given equations are based on reference [23].

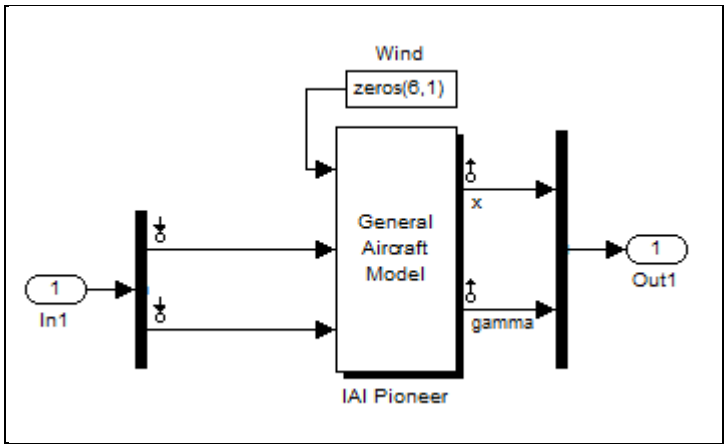

Figure 12 Nonlinear Model Linearization Setup in MATLAB

The initial form of the equations of motion is based on Newton's second law [23], [36];

Mass*acceleration = disturbing force

$$\sum \vec{F} = m\vec{a} = m\dot{V} \qquad [3.5]$$

where,

$$\vec{a} = \left.\frac{d\vec{V}}{dt}\right|_b = \left.\frac{d\vec{V}}{dt}\right|_e - w_{be} \times \vec{V} \qquad [3.6]$$

“e” represents earth frame, “b” represents body frame of aircraft, “w” represents angular velocity of the body.

For the rotational degrees of freedom the mass and acceleration become moment of inertia and angular acceleration, respectively whilst the disturbing force becomes the disturbing moment or torque.

The moment equations are represented by the rotational form of Newton’s second law of motion. Moment equation is the Euler’s Equations for a rigid body [36].

$$\vec{M} = \left.\frac{dH}{dt}\right|_b + \omega_{be} \times H \qquad [3.7]$$

“b” represents body frame of aircraft, “w” represents angular velocity of the body.

The equations given below show the generalized form of equations of motion. The right hand side (RHS) represents the disturbing force and moments. These disturbing forces and moments usually occur through aerodynamic effects, gravitational effects, movement of aerodynamic controls, power effects and the effects of atmospheric disturbances.

$$\begin{aligned} m(\dot{U} - rV + qW) &= X_a + X_g + X_c + X_p + X_d \\ m(\dot{V} - pW + rU) &= Y_a + Y_g + Y_c + Y_p + Y_d \\ m(\dot{W} - qU + pV) &= Z_a + Z_g + Z_c + Z_p + Z_d \end{aligned} \qquad [3.8]$$

$$\begin{aligned} I_x\dot{p} - (I_y - I_z)qr - I_{xz}(pq + \dot{r}) &= L_a + L_g + L_c + L_p + L_d \\ I_y\dot{q} - (I_x - I_z)pr + I_{xz}(p^2 - r^2) &= M_a + M_g + M_c + M_p + M_d \\ I_z\dot{r} - (I_x - I_y)pq + I_{xz}(qr - \dot{p}) &= N_a + N_g + N_c + N_p + N_d \end{aligned} \qquad [3.9]$$

These non-linear equations have complex mathematical solutions due to the disturbance terms. After the linearization phase, the equations are converted to a simpler form so that they are much easier to solve. Linearization is simply accomplished by constraining the motion of the aircraft to small perturbations about the trim conditions.

Here we have summarized the initial assumptions that make these equations simpler and eliminate nonlinear disturbance components (linearization) [23].

Assumptions related with Left Hand Side (LHS) of equations [3.8] and [3.9] are

- A trimmed flight which means perturbation components are deleted (eqn. [3.1]). In that case only Ue, Ve, We terms remain.
- There is no sideslip. Ve is deleted.

Assumptions related with Right Hand Side (RHS) of equations [3.8] and [3.9] are

- Steady-state atmospheric conditions (no atmospheric disturbance).
- Gravitational terms are disregarded out of X and Z forces due to the resolving weight components into the disturbed body axes.
- Only higher order derivative terms are encountered (Aerodynamic stability derivatives).
- Aerodynamic coupling and aerodynamic control derivatives are negligibly small due to the decoupling of lateral and longitudinal motions.
- Level flight and the reference axes are wind or stability axes.

The simpler forms of longitudinal equations of motion are;

$$\begin{aligned} &m\dot{u} - q\tilde{X}_q - \tilde{X}_u u - \tilde{X}_w w - \tilde{X}_{\dot{w}}\dot{w} + mg\theta = \tilde{X}_\eta \eta + \tilde{X}_\tau \tau \\ &\dot{w}(m - \tilde{Z}_{\dot{w}}) - q(mU_e + \tilde{Z}_q) - \tilde{Z}_u u - \tilde{Z}_w w = \tilde{Z}_\eta \eta + \tilde{Z}_\tau \tau \\ &I_y \dot{q} - \tilde{M}_u u - \tilde{M}_w w - \tilde{M}_q q - \tilde{M}_{\dot{w}}\dot{w} = \tilde{M}_\eta \eta + \tilde{M}_\tau \tau \end{aligned} \qquad [3.10]$$

The simpler forms of lateral equations of motion are;

$$
\begin{aligned}
&m\dot{v} - p\tilde{Y}_p + r(mU_e - \tilde{Y}_r) - \tilde{Y}_v v - mg\phi = \tilde{Y}_\xi \xi + \tilde{Y}_\zeta \zeta \\
&I_x \dot{p} - I_{xz}\dot{r} - \tilde{L}_v v - \tilde{L}_p p - \tilde{L}_r r = \tilde{L}_\xi \xi + \tilde{L}_\zeta \zeta \\
&I_z \dot{r} - I_{xz}\dot{p} - \tilde{N}_v v - \tilde{N}_p p - \tilde{N}_r r = \tilde{N}_\xi \xi + \tilde{N}_\zeta \zeta
\end{aligned}
\qquad [3.11]
$$

In general, for a meaningful representation these equations are written in the state-space form, because matrix representation of these equations is more adequate for mathematical solutions.

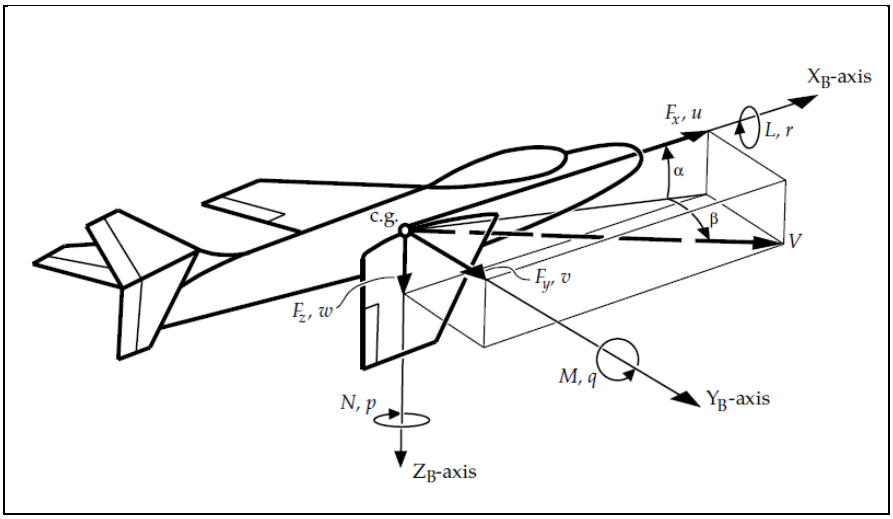

Figure 13 Representation of Perturbation Variables on the Body-fixed Reference Frame of the Aircraft

Generalized state space forms of equations of motion are given below [23].

$$x'(t) = Ax(t) + Bu(t) \qquad [3.12]$$

$$y(t) = Cx(t) + Du(t) \qquad [3.13]$$

$$x(0) = x0 \qquad [3.14]$$

where, **x,** the state vector (*n*)

u, the control vector (*m*)

A, the system matrix (*n* * *n*)

B, the control matrix (*n* * *m*)

y, output vector (column vector of r)

C, output matrix (*r* * *n*)

D, direct matrix (*r* * *m*)

x(0) = trim results

For the following matrix representations we used references [6], [24], [25]. The simplest forms of decoupled longitudinal equations are given next, where the states and control vectors are given in equations [3.15] and [3.16].

$$x^T(t) = [u \quad w \quad q \quad \theta] \qquad [3.15]$$

$$u^T = [\eta \quad \tau] = [\delta E \ \delta T] \qquad [3.16]$$

$$\begin{bmatrix} \dot{u} \\ \dot{w} \\ \dot{q} \\ \dot{\theta} \end{bmatrix} = \begin{bmatrix} X_u & X_w & 0 & -g\cos\theta_0 \\ Z_u & Z_w & U_0 & 0 \\ M_u + M_{\dot{w}} Z_u & M_w + M_{\dot{w}} Z_w & M_q + M_{\dot{w}} U_0 & 0 \\ 0 & 0 & 1 & 0 \end{bmatrix} \begin{bmatrix} u \\ w \\ q \\ \theta \end{bmatrix} + \begin{bmatrix} X_{\delta E} & X_{\delta T} \\ Z_{\delta E} & Z_{\delta T} \\ M_{\delta E} + M_{\dot{w}} Z_{\delta E} & M_{\delta T} + M_{\dot{w}} Z_{\delta T} \\ 0 & 0 \end{bmatrix} \begin{bmatrix} \delta E \\ \delta T \end{bmatrix} \qquad [3.17]$$

$$y(t) = \begin{bmatrix} 1 & 0 & 0 & 0 \\ 0 & 1 & 0 & 0 \\ 0 & 0 & 1 & 0 \\ 0 & 0 & 0 & 1 \\ 0 & -1 & 0 & U_0 \end{bmatrix} \begin{bmatrix} u \\ w \\ q \\ \theta \\ h \end{bmatrix} \qquad [3.18]$$

The simplest forms of decoupled lateral equations are given next, where states and controls vectors are given in equations [3.19] and [3.20];

$$x^T(t) = [v \quad p \quad r \quad \phi \quad \psi] \qquad [3.19]$$

$$u^T = [\xi \quad \zeta] = [\delta A \ \delta R] \qquad [3.20]$$

$$\begin{bmatrix} \dot{v} \\ \dot{p} \\ \dot{r} \\ \dot{\phi} \\ \dot{\psi} \end{bmatrix} = \begin{bmatrix} Y_v & 0 & U_0 & g\cos\theta_0 & 0 \\ L_v & L_p & N_r & 0 & 0 \\ N_v & N_p & N_r & 0 & 0 \\ 0 & 1 & 0 & 0 & 0 \\ 0 & 0 & 1 & 0 & 0 \end{bmatrix} \begin{bmatrix} v \\ p \\ r \\ \phi \\ \psi \end{bmatrix} + \begin{bmatrix} 0 & Y_{\delta R} \\ L_{\delta A} & L_{\delta R} \\ N_{\delta A} & N_{\delta R} \\ 0 & 0 \\ 0 & 0 \end{bmatrix} \begin{bmatrix} \delta A \\ \delta R \end{bmatrix} \qquad [3.21]$$

$$y(t) = Ix(t) = \begin{bmatrix} 1 & 0 & 0 & 0 & 0 \\ 0 & 1 & 0 & 0 & 0 \\ 0 & 0 & 1 & 0 & 0 \\ 0 & 0 & 0 & 1 & 0 \\ 0 & 0 & 0 & 0 & 1 \end{bmatrix} \begin{bmatrix} v \\ p \\ r \\ \phi \\ \psi \end{bmatrix} \qquad [3.22]$$

As we have mentioned before we have obtained the proper state space matrices by the help of MATLAB/ Linearization Tool and a sample of the state space matrices are given here (belongs to second trim states).

A=

-0,05419	-4,13001	0	0	8,57E-14	0	0	-9,80647	0	0	0	0,000156
-0,00547	-2,61798	0	0	0,980052	0	0	8,61E-13	0	0	0	1,57E-05
0	0	-0,44392	-0,02936	0	-0,99957	0	0	0,16337	0	0	0
0	0	-20,1036	-12,9726	0	8,101234	0	0	0	0	0	0
5,18E-06	-79,23	0	0	-6,2533	0	0	0	0	0	0	-1,49E-08
0	0	32,4047	-0,57841	0	-2,94089	0	0	0	0	0	0
0	0	0	0	0	1,000431	0	0	0	0	0	0
0	0	0	0	1	0	0	0	0	0	0	0
0	0	0	1	0	-0,02938	0	0	0	0	0	0
1	1,27E-09	0	0	0	0	0	1,37E-10	0	0	0	0
0	0	60	0	0	0	60	0	1,76183	0	0	0
-1,61E-13	-60	0	0	0	0	0	60	0	0	0	0

B =

0,00525	0	-0,00015	0	0,00E+00	0	-0,5854	0	0	0
2,57E-06	0	8,74E-05	0	0	0	-0,2174	0,00E+00	0	0
0	8,75E-05	0	0	0	0	0	0,103527	0	0
0	0	0	0,02135	0	-0,00127	0	-110,536	2,16528	0
0,00E+00	0	0	0	0,010995	0	-65,776	0	0	0
0	0	0	-0,00127	0	0,00905	0	12,31607	-26,3823	0
0	0	0	0	0	0	0	0	0	0
0	0	0	0	0	0	0	0	0	0
0	0	0	0	0	0	0	0	0	0
0	0,00E+00	0	0	0	0	0	0,00E+00	0	0
0	0	0	0	0	0	0	0	0	0
0,00E+00	0	0	0	0	0	0	0	0	0

C=

$$\begin{matrix}
1 & 0 & 0 & 0 & 0 & 0 & 0 & 0 & 0 & 0 & 0 & 0 \\
0 & 1 & 0 & 0 & 0 & 0 & 0 & 0 & 0 & 0 & 0 & 0 \\
0 & 0 & 1 & 0 & 0 & 0 & 0 & 0 & 0 & 0 & 0 & 0 \\
0 & 0 & 0 & 1 & 0 & 0 & 0 & 0 & 0 & 0 & 0 & 0 \\
0 & 0 & 0 & 0 & 1 & 0 & 0 & 0 & 0 & 0 & 0 & 0 \\
0 & 0 & 0 & 0 & 0 & 1 & 0 & 0 & 0 & 0 & 0 & 0 \\
0 & 0 & 0 & 0 & 0 & 0 & 1 & 0 & 0 & 0 & 0 & 0 \\
0 & 0 & 0 & 0 & 0 & 0 & 0 & 1 & 0 & 0 & 0 & 0 \\
0 & 0 & 0 & 0 & 0 & 0 & 0 & 0 & 1 & 0 & 0 & 0 \\
0 & 0 & 0 & 0 & 0 & 0 & 0 & 0 & 0 & 1 & 0 & 0 \\
0 & 0 & 0 & 0 & 0 & 0 & 0 & 0 & 0 & 0 & 1 & 0 \\
0 & 0 & 0 & 0 & 0 & 0 & 0 & 0 & 0 & 0 & 0 & 1 \\
0 & 0 & 0 & 0 & 0 & 0 & 0 & 0 & 1 & 0 & 0 & 0
\end{matrix}$$

D = $(0)_{13\times10}$

The 13th output state represents gamma (glide path angle).

For decoupled model the longitudinal states are $x_{longitudinal} = [V, \alpha, q, \theta, H\ ]$,

and the lateral states are $x_{lateral} = [\beta, p, r, \Psi, \phi, xe, ye]$.

3.3. Design of the Landing Autopilot

After finding the state space matrices of linearized aircraft models (two linear models), we have designed autopilots for these models separately. The purpose of the autopilots is controlling airspeed, altitude and direction states of the aircraft using PID controllers. The following steps give the details of the design of a landing autopilot. In this case we limited the deflections of the control surfaces (elevator, aileron and rudder) at ±30 degrees turn and throttle at 0-450 N.

3.3.1. Longitudinal Controllers

In order to control speed and the movement of aircraft at longitudinal axes (deviations at altitude) longitudinal controllers are designed. These controllers have inner and outer loops. The outer loops use altitude or airspeed error signals in order to produce reference command signals for inner loops. The inner loops use command signal errors and produce the deflection commands which are sent to control components (elevator and throttle for this case).

3.3.1.1. Speed Controller

When we started to simulate the system it seemed that the speed controller is the most important part of this controller design process, because the speed value is very effective on the stability of the other aircraft states. The main idea of the speed controller is changing the thrust by throttle actuator in order to control the speed. That is, throttle deflection is sent to the aircraft model. A PID controller is used to control the speed signal [8].

The basic block diagram representation of the designed speed controller is given in Figure 14.

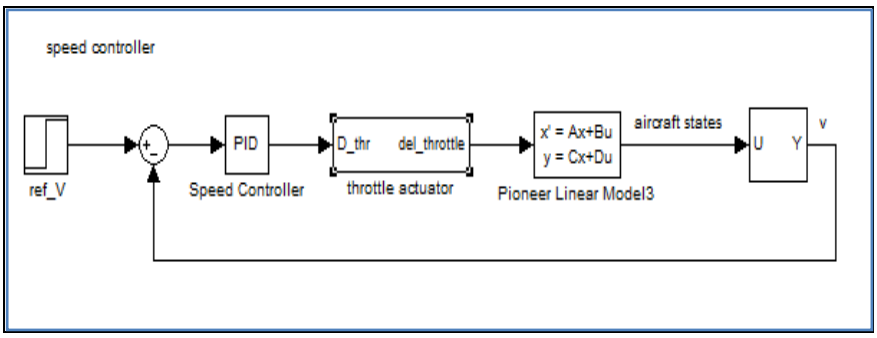

Figure 14 Block Diagram of the Speed Controller

Then we have observed the step response of this speed controller for the linear model of the UAV. As it is seen from Figure 15 the control of speed signal is provided for the considered linear aircraft model.

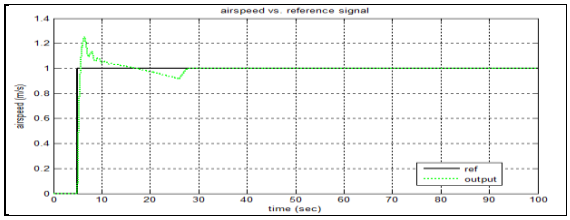

Figure 15 Step Response of the Speed Controller (on Linear Model)

3.3.1.2. Altitude Controller

Altitude controller is another important issue of the landing phase due to continuous descending trend. Especially altitude control depends to control of the pitch angle. One of the methods of controlling altitude is holding a proper pitch angle (constant pitch angle, e.g., GPA = 3 degree). But, considering the change of altitude (distance at z-axis) directly is more practical. According to this approach we can observe the motion of the aircraft at longitudinal axis more clearly [8].

Thus, height control or height hold system design is preferable. The height control is provided by considering inner loops and an outer loop. Inner loops control the pitch angle and the pitch rate and send the output signal to the elevator actuator model. Only proportional gain coefficients are used to provide control of these two signals.

The outer loop compares reference altitude signal with the altitude signal that is generated by the aircraft model. Note that, the reference altitude signal is generated manually according to the assumptions as mentioned in Chapter 2.3. There is no altitude information source on the model like radar altimeter or etc.

It produces a pitch angle command signal. The control of the system is provided with a PID controller.

The basic block diagram representation of the designed altitude controller is given in Figure 16.

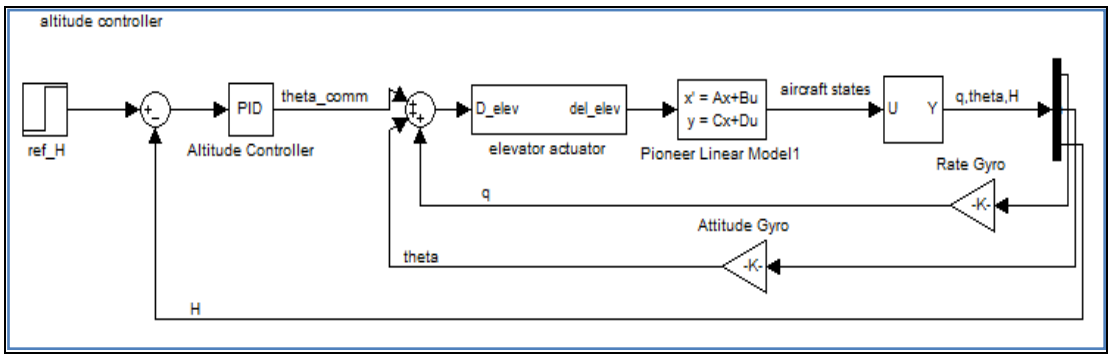

Figure 16 Block Diagram of the Altitude Controller

Then we have observed the step response of this altitude controller on the linear model of the UAV. As it is seen from Figure 17 the control of the altitude signal is sufficiently well for the considered linear aircraft model.

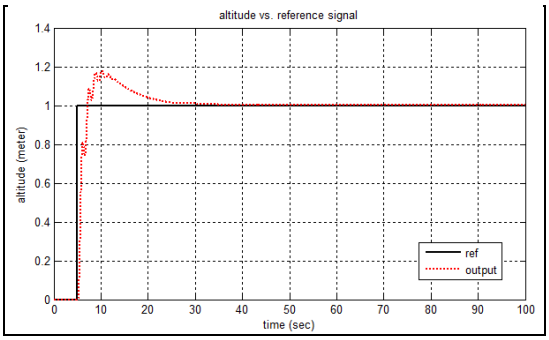

Figure 17 Step Response of the Altitude Controller (on Linear Model)

3.3.2. Lateral Controller

Lateral motion of an aircraft will be provided by two control surfaces, which are aileron and rudder. In order to compensate the deviations which are supposed to occur at lateral axis (x and y axis) a direction controller is required. Regarding this requirement we have designed a direction controller and an assisting yaw rate controller [8].

Also, the designed direction controller includes both inner and outer loops. The outer loop uses heading signal (yaw angle signal) error in order to produce the reference command signals for inner loops. The inner loops use command signal errors and produce the deflection commands which are sent to control components (aileron for this case). The aim of the yaw controller is driving the rudder servo.

3.3.2.1. Direction Controller

The first part of the lateral controller is direction controller. In this study, basically a yaw angle controller is designed as a direction controller [8], [10]. This kind of controller is needed to compensate the deviations or cross-track error that can occur

during movement of the aircraft at lateral axis. In addition the UAV may deviate from the landing path when it is in the safe landing corridor. In order to catch the desired path the aircraft have to change its direction.

The designed direction controller is composed of cascaded controller loops. The first inner loop is p (roll rate) controller which produces aileron deflection from the commanded roll rate signal. This commanded signal is sent from a higher level controller which controls phi (roll angle) signal with a proportional gain coefficient as p controller. Roll angle controller produces a commanded p signal by the help of a controller gain and sends it to the inner loop.

Then the outer loop controls psi (yaw angle) which compares the reference heading angle with the system output yaw angle. It produces a phi command signal with a gain coefficient.

The basic block diagram representation of the designed heading controller is given in Figure 18.

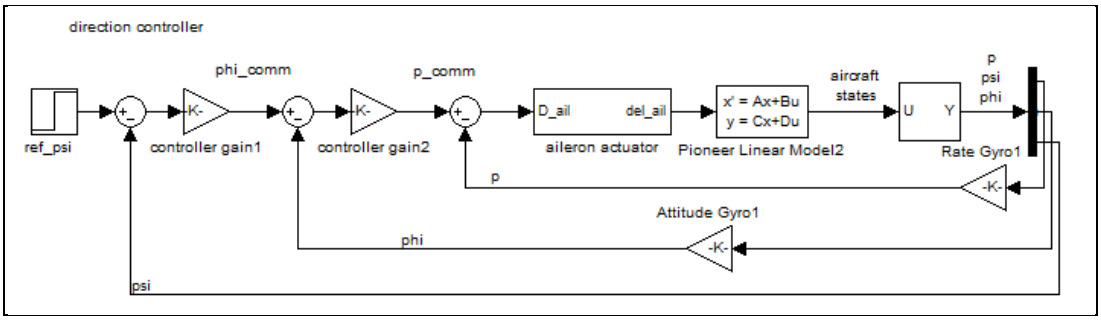

Figure 18 Block Diagram of the Direction Controller

Then we have observed the step response of this direction controller on the linear model of the UAV. As it is seen from Figure 19 the control of heading signal is sufficiently well for the considered linear aircraft model.

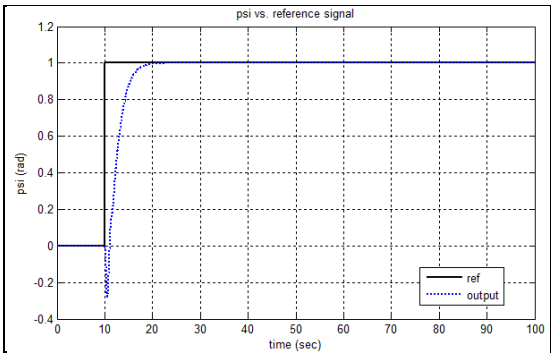

Figure 19 Step Response of the Heading Controller (on Linear Model)

3.3.2.2. Yaw Rate Controller

In order to complete the lateral motion control of the aircraft a yaw rate controller is added to system. This yaw rate controller provides deflection on rudder. The reference signal of the controller is the yaw rate signal which is obtained from the output states of the aircraft (sensor output).

The controller simply consists of a proportional gain. The block diagram representation of the yaw rate controller is given in Figure 20.

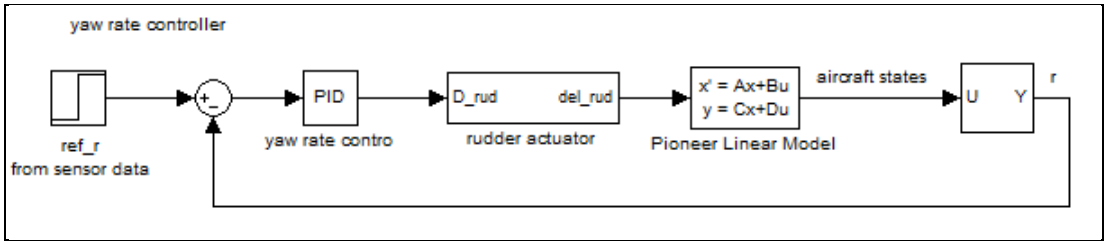

Figure 20 Block Diagram of the Yaw Rate Controller

The performance of the yaw rate controller is observed with the use of the direction controller. When we apply step input to the direction controller, the yaw rate controller response is observed and is given in Figure 21. As it is seen from this graph, yaw rate is changing when the direction controller is producing variable

commands. When the aircraft reaches the reference signal, a constant heading command signal is produced. For comparison please see Figure 19.

The combined block diagram representation of both direction and yaw rate controllers as the lateral motion autopilot is given in Figure 22.

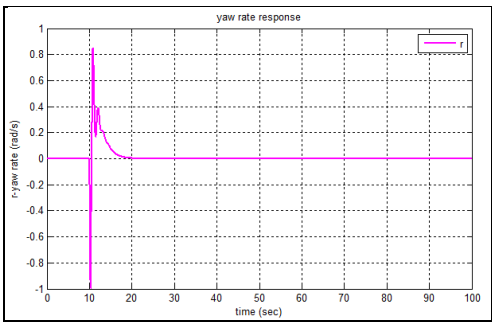

Figure 21 Response of the Yaw Rate Controller for Sensor Input

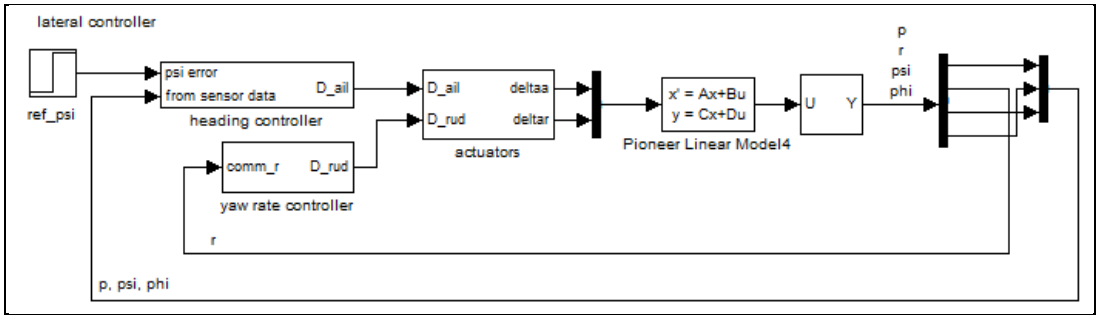

Figure 22 Block Diagram of the Lateral Motion Autopilot

We have completed the design of the landing autopilot for linear aircraft model and observed good controller results. Please remember that all these linear controller design activities are repeated for the other linear aircraft model. We can declare that, for the other linear model, similar good controller results are obtained. Those results are not presented here. But this idea will be verified by the help of the simulation results of the nonlinear model that includes gain scheduling. See chapter 3.6 for details.

3.4. Non-Linear Model Control

The designed landing autopilot according to the linear model of the UAV is applied to the nonlinear model of the UAV. During this transition the controller design parameters are not changed directly. But the related PID controller gains have to be adjusted again due to the characteristics of non-linear aircraft model and initial forces of throttle and elevator (obtained from the trimming state) have been added.

Initially, we have considered the linear aircraft model which is linearized at 30 m/s airspeed and related trim inputs. This defines initial states of system and initial forces of throttle and elevator. Initial states are 30 m/s airspeed, 60 m altitude. Initial throttle force is 309.8742 N and elevator force is 0.145603 N.

Then, we have tested the landing autopilot on the non-linear aircraft model with initial states (1st case). Assume that, the mission is holding the altitude at 60 m and holding the aircraft speed at 30 m/s without any lateral deviation. This means the aircraft have to follow 0 rad heading angle (reference psi is zero).

We have observed the responses of the states versus the reference signals. Results obtained for the controlled airspeed (Figure 23), altitude (Figure 24), and heading (Figure 25) signals are more or less expected. These results show that the model is controlled properly. In this given scenario, we used trim conditions as reference signals in order to show the controller gains obtained at trim conditions are working on non-linear model properly. The observations about other initial states are given in gain scheduling chapter and the following chapters.

Then we have generated a new flight scenario (2nd case). In this case, the UAV is descending from 60 m to 0 m, with 30 m/s constant speed and no lateral deviation (psi = 0 rad). Note that according to the defined speed value such a descending action takes approximately 40 seconds.

Additionally, we applied 0.1 rad instead of zero as the reference signal to the direction controller. When the corresponding responses of the system have been obtained, we have observed that the performances of the controllers are very good. The system responses are given in figures below (Figure 26, Figure 27, Figure 28).

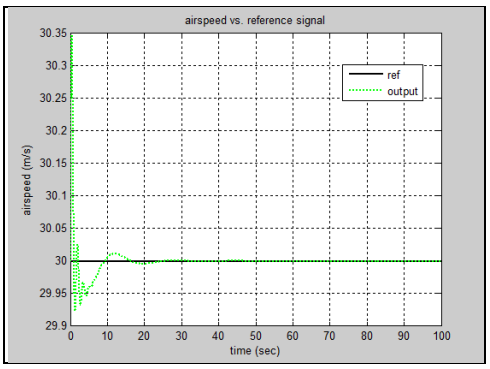

Figure 23 Response of the System to Airspeed Signal (Non-linear Model, 1st case)

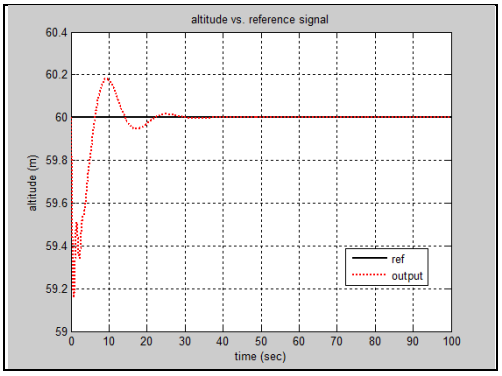

Figure 24 Response of the System to Altitude Signal (Non-linear Model, 1st case)

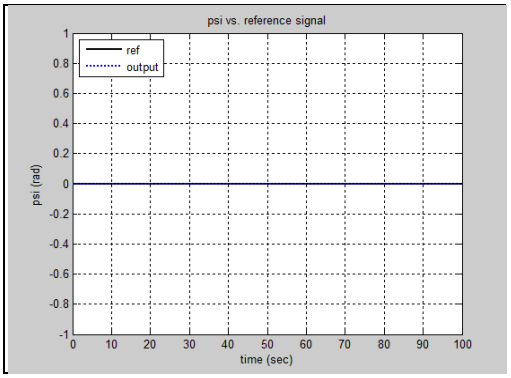

Figure 25 Response of the System to Heading Signal (Non-linear Model, 1st case)

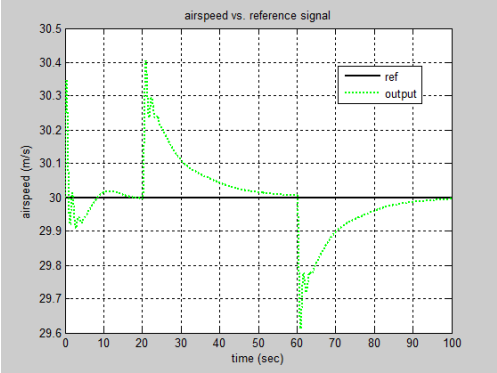

Figure 26 Response of System to Speed Signal (Non-linear Model, 2nd case)

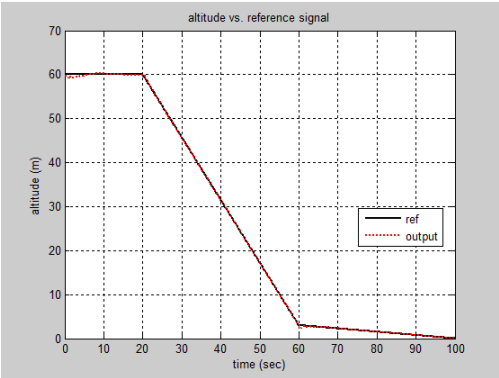

Figure 27 Response of System to Altitude Signal (Non-linear Model, 2nd case)

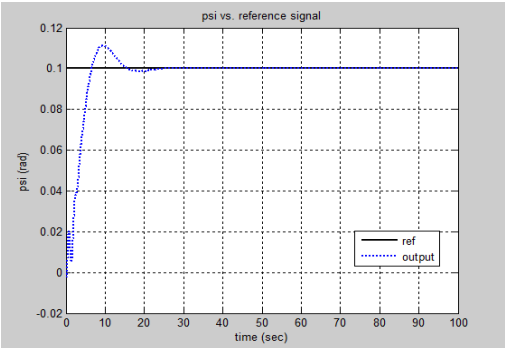

Figure 28 Response of System to Heading Signal (Non-linear Model, 2nd case)

As it is seen from the given simulation results for a constant speed value (30 m/s) the performance of the lateral and longitudinal controllers are well. But when we change the speed value we observed unacceptable results that are not given here.

Similarly this step is repeated for the other linear aircraft model (linearized at 60 m/s airspeed) and again results which are satisfactory have been obtained for those (60 m/s speed and 60 m altitude) initial states. In order to provide the control of system states at different airspeed values (out of 30 m/s or 60 m/s) we have applied the gain scheduling method.

Responses of the other system states and controller surfaces are given below. Due to the reference altitude value change of the response of the longitudinal states can be seen. Also when we look at the response of the lateral axis components, up to the point where aircraft reaches the reference value the signals are changing. Then they become constant.

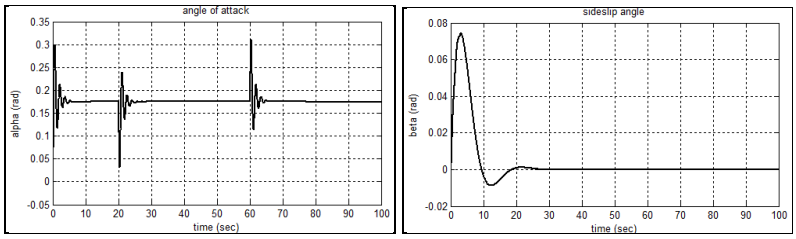

Figure 29 Angle of Attack and Sideslip Angle Responses (Non-linear Model, 2nd case)

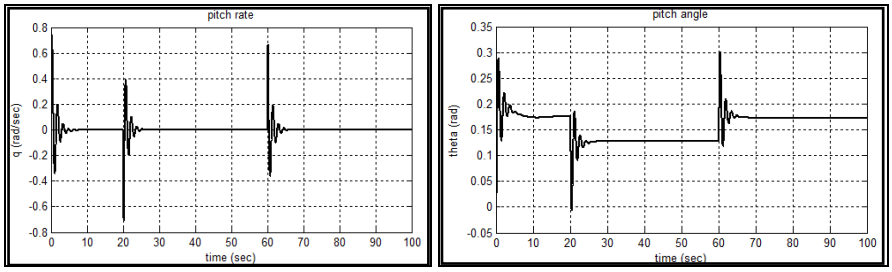

Figure 30 Pitch Rate and Pitch Angle Responses (Non-linear Model, 2nd case)

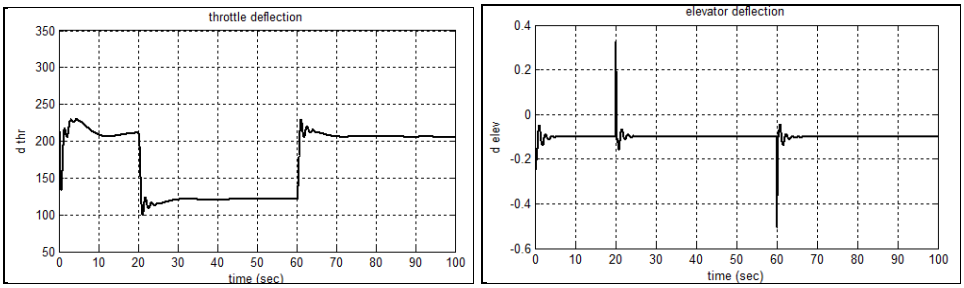

Figure 31 Throttle and Elevator Deflections (Non-linear Model, 2nd case)

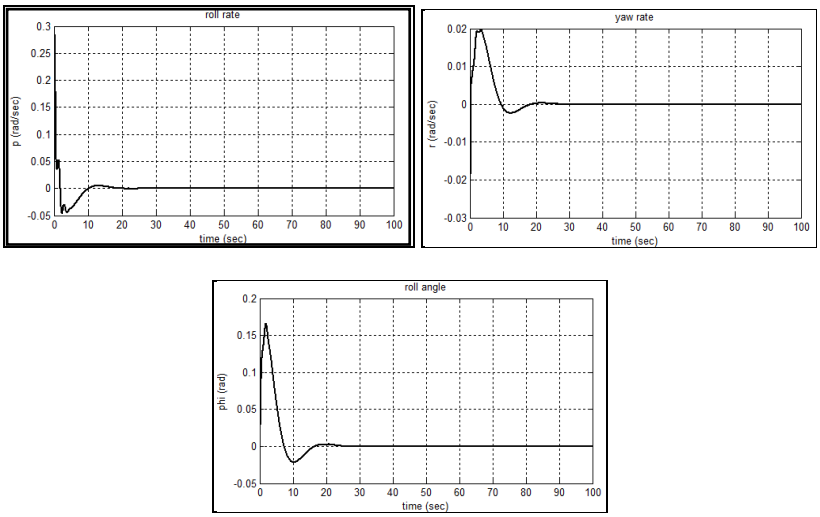

Figure 32 Roll Rate, Yaw Rate and Roll Angle Responses (Non-linear Model, 2nd case)

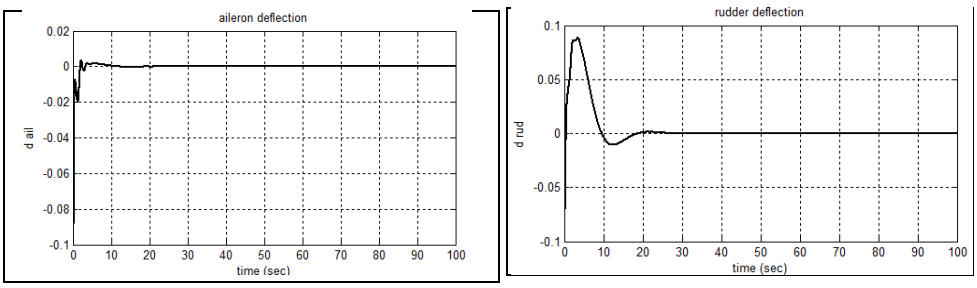

Figure 33 Aileron and Rudder Deflections (Non-linear Model, 2nd case)

3.5. Pole Placement Method

As mentioned in Subchapter 3.3 we have designed a direction controller with a PID controller structure. In order to ensure the performance of the controller we have yet designed another direction controller with pole placement method. The necessity of this study will be explained in Chapter 8 in detail.

As we know the places of poles of a system is effective on the stability and the response of the system. When we consider the poles, if all poles have negative real parts (on the left side of the s plane) the system is stable.

The poles of the system are considered separately. The purpose of this method is to pull such an unstable pole to an appropriate location in the left side of the s plane and thus providing system stability and acceptable system response [30]. The block diagram representation of the pole placement method is given in Figure 34.

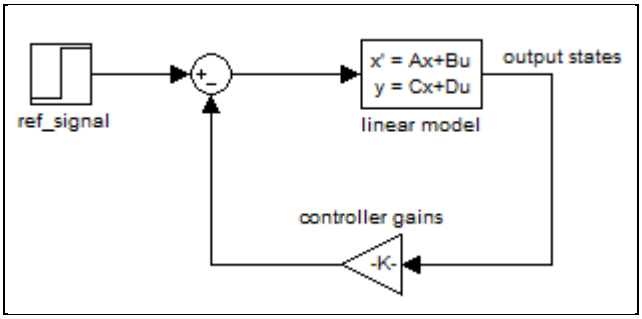

Figure 34 General Form of Pole Placement Method

According to the nature of this controller, it is first applied on the linear system state space model [31], [32]. The block diagram representation of the pole placement method on the linear aircraft model is given in Figure 35.

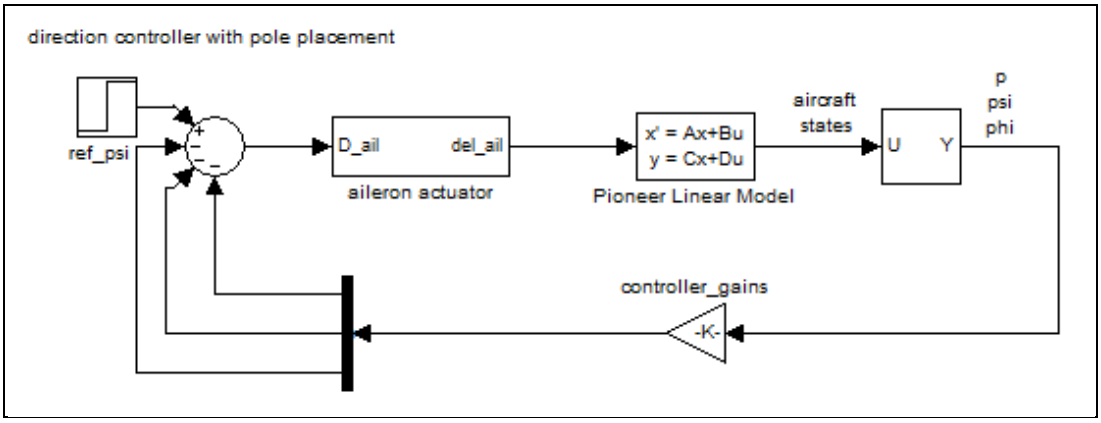

Figure 35 Pole Placement Application for Lateral Control on the Model

We have arranged the system state space matrices and have obtained direction controller components with partial state feedback in order to control direction of the aircraft with one control surface (aileron). The direction controller components are [p, psi, phi]. The most important part of method is determining the gain matrix K. To find these K matrix components we have used a MATLAB command “place”. First, the poles of the associated system have been found.

p = [0, -12.9726, 0]

Before the determination of the acceptable pole values by the user, one has to check whether the system is completely controllable or not. It has been found that “psi” is the uncontrollable state of the system. We can perform the pole placement job even though the system is not completely controllable.

Then acceptable poles are selected. The array of desired poles (dpol) is;

dpol =[-5 -10, 0];

Note that the pole associated with the uncontrollable state is left in its original place. After the execution of the command “place” the gain matrix is obtained. The associated gains of the system are given below.

K = [-0.0183, 0, -0.4523]

Unfortunately this gain matrix cannot control the heading signal so we have to modify the gain values similarly as we have done with the PID controller. We have used the same controller model on the non-linear aircraft model. The gains which are applied on the non-linear model are;

K = [-0.0183, -1, -0.4523]

As you will observe, this gain matrix works sufficiently well for our purposes.

We have tested the performance of the direction controller (with the pole placement method) with different reference heading signals and observed highly satisfactory results. The step response of the direction controller is given in Figure 37. For the constant reference heading signal the system response is given in Figure 36. And finally, the reference heading signal which is generated by the lateral position controller is applied to the model and the response of the system is given in Figure 38.

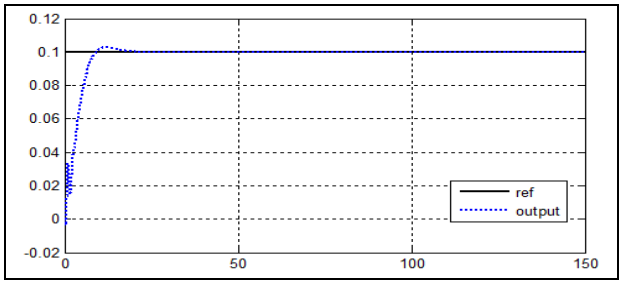

Figure 36 The Response of Heading Pole Placement Controller (1st Signal)

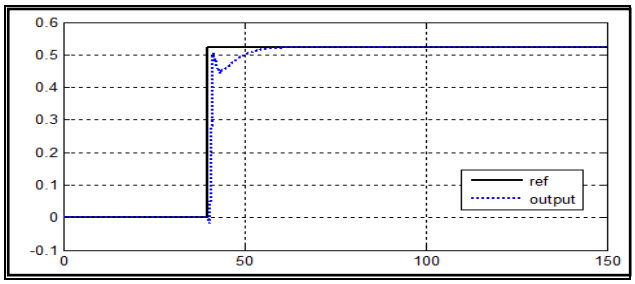

Figure 37 The Response of Heading Pole Placement Controller (2nd Signal)

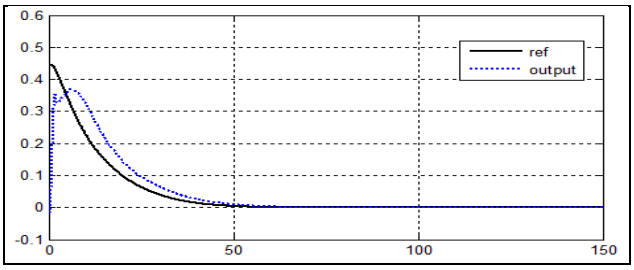

Figure 38 The Response of Heading Pole Placement Controller (3rd Signal)

3.6. Gain Scheduling

The response of the aircraft state controllers will be changed due to the initial altitude and speed values [8]. That means the appropriate controller gains which are generated for defined initial states will not work at any other condition. This information is verified by many applications in the literature and in this thesis work. Also, the observations about this case are explained in the previous parts of this thesis.

In order to solve this difficulty gain scheduling method will be applied. This method provides the generation of appropriate controller gains according to the different scheduling variable values (altitude or speed values).

Regarding the performance of the controller and related response of our UAV the airspeed states are assigned as the gain scheduling variables. As we mentioned before two autopilots are designed for the maximum and minimum cruising speeds. As we observed only the gains of altitude controller are changed. The response of the altitude controller gains due to the changing speed value is given in Figure 44. And we have merged these set of controller gains by the help of linear interpolation between these two sets.

For the interpolation process in the autopilot Simulink model we have used MATLAB/Simulink n-dimensional lookup tables.

According to the system simulations which have been presented in the previous chapters and in this chapter we have concluded that, these two data sets are enough to control the UAV at any initial input state (speed, altitude, and heading).

Then we have considered the response of the system for the gain scheduled autopilot and we have obtained very good results. In the first case the speed of the aircraft is increasing from 30 m/s to 60 m/s at a constant altitude. The reference heading signal is 0.1 rad (1st case). At the end of the simulation when we look at the speed signal response (Figure 39) we have concluded that, the gain scheduling is working properly. Also, the responses of other controlled states are acceptable (Figure 40 and Figure 41).

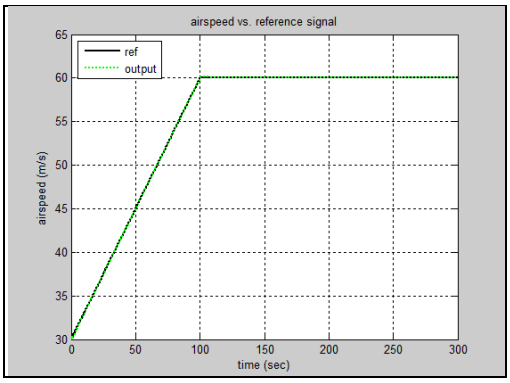

Figure 39 Response of System to Speed Signal (with Gain Sch. 1st case)

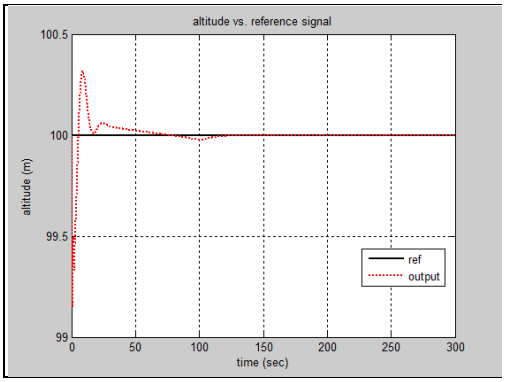

Figure 40 Response of System to Altitude Signal (with Gain Sch. 1st case)

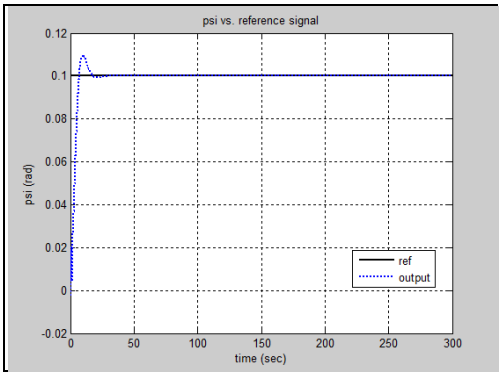

Figure 41 Response of System to Heading Signal (with Gain Sch. 1st case)

In the second case, additionally we have changed the altitude signal as a landing path (2nd case). We have observed that the gain scheduled autopilot is still working properly. The related system responses are given in Figure 42 (altitude response) and Figure 43 (airspeed response). The changing controller gains of altitude controller are given in next figure (Figure 44). The given legends on this figure are Kpa, the proportional gain, Kia, the integrated gain, Kda, the derivative gain.

The deviation on the altitude graph is ± 0.4 m and ±0.8 m/s on the speed graph as can be observed from the simulations below (Figure 42 and Figure 43). Heading signal response has not changed in this case.

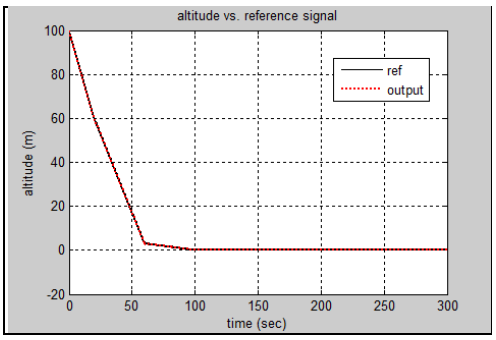

Figure 42 Response of System to Altitude Signal (with Gain Sch. 2nd case)

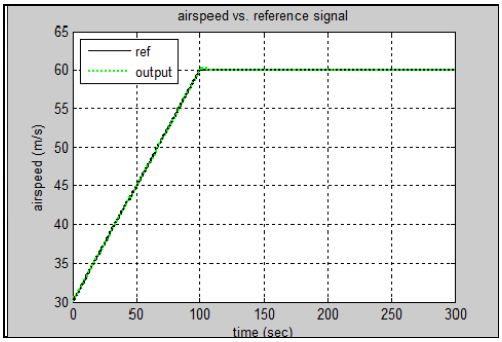

Figure 43 Response of System to Speed Signal (with Gain Sch. 2nd case)

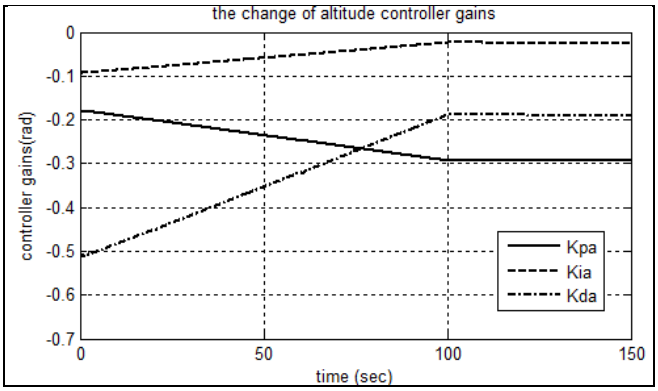

Figure 44 Changing of Altitude Controller Gains

Responses of the other system states and controller surfaces are given below. The longitudinal components; angle of attack, pitch angle, throttle and elevator deflections are changing due to the changing speed value (from 30 m/s to 60 m/s). The break points can be observed on longitudinal components due to the decreasing altitude (from 100m to 0). Due to the decoupled aircraft motions the lateral axis responses are not changed (similar to non-linear model first scenario). The responses of the lateral components are acceptable. The figures (Figure 47 and Figure 49) show that, aircraft tries to keep the direction at a constant value.

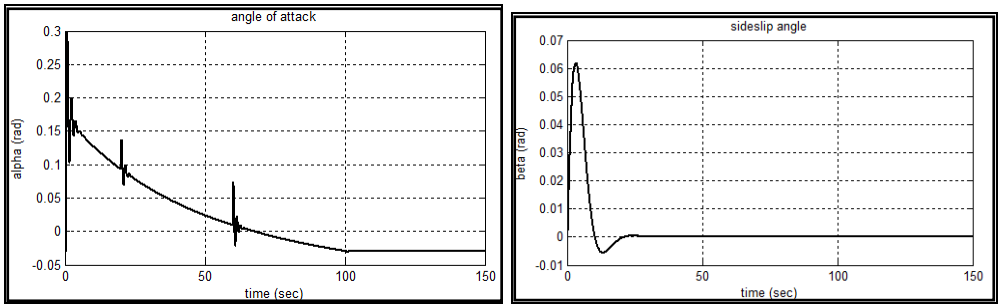

Figure 45 Angle of Attack and Sideslip Angle Responses (with Gain Sch. 2nd case)

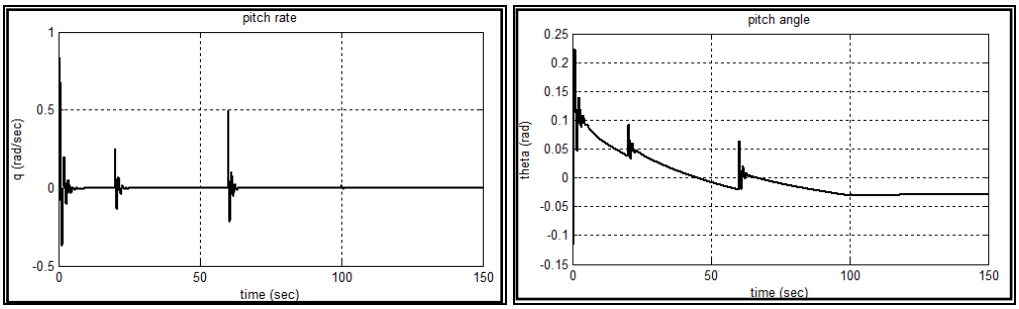

Figure 46 Pitch Rate and Pitch Angle Responses **(**with Gain Sch. 2nd case**)**

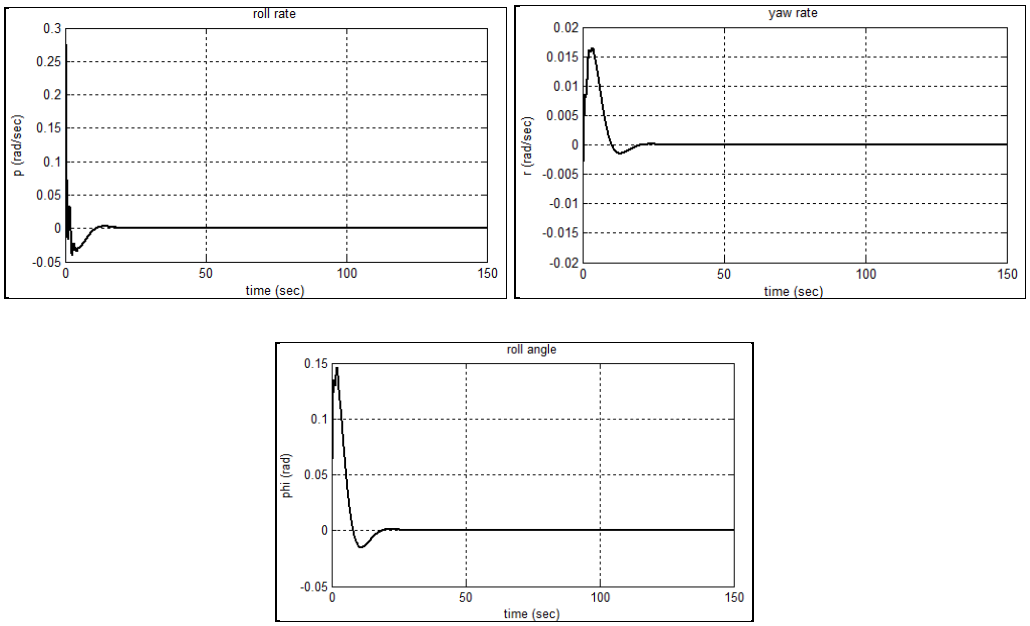

Figure 47 Roll Rate, Yaw Rate and Roll Angle Responses (with Gain Sch. 2nd case)

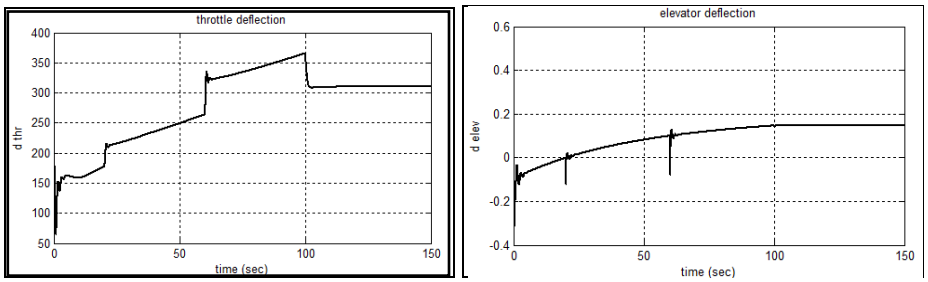

Figure 48 Throttle and Elevator Deflections **(**with Gain Sch. 2nd case**)**

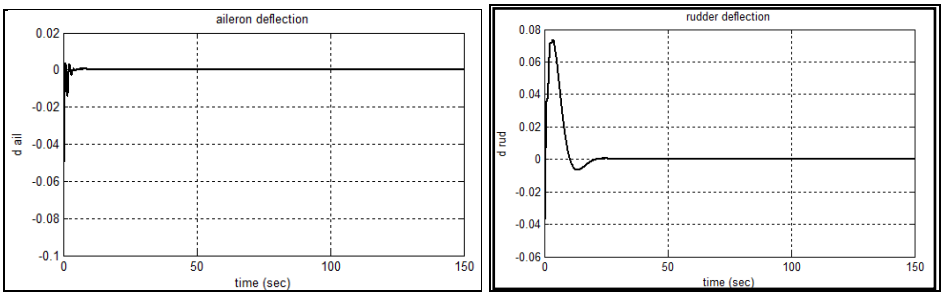

Figure 49 Aileron and Rudder Deflections (with Gain Sch. 2nd case)

Also, according to our performance tests on the simulation model the scheduled autopilot is working up to 80 m/s airspeed. But due to the performance parameters of the UAV, this does not bring us anything.

These scenarios and related results are verifying that the aircraft motions are possible starting from any given initial state (speed, altitude and direction) regarding the performance limitations.

CHAPTER 4

PATH (TRAJECTORY) OPTIMIZATION

Path optimization is realized in order to generate optimum paths, regarding time, fuel costs, and movement area (x-y-z axis) constraints. By the help of path optimization the aircraft is supposed to reach the target point with minimum cost (minimum time, fuel, etc.). Also an optimum path will be generated between two waypoints regarding the limitations about the flight areas (distance, geographic shapes, position of other aircrafts, etc) and the collision risk of aircrafts will be avoided [17].

In this chapter, using optimization, we have generated appropriate landing paths for our UAV. These paths are chosen from inside of the safe landing corridor (See Chapter 2). If the aircraft is in the defined safe landing corridor but not on the main landing path, we concluded that, in such a condition the mission will not be aborted. Aircraft will follow the nearest suitable landing path. For this purpose we have produced many optimized landing paths.

As we mentioned in Chapter 2 some altitude constraints and corresponding lateral areas are defined on the safe landing corridor. These altitude constraints are 49 m, 75 m and 102 m (Figure 8). The corresponding rectangular shaped lateral areas are divided into several segments due to the defined interval values. And we have collected the origin points of these segments in order to use them as starting points of optimization process. Note that, size of each segment is reducing with the decreasing altitude. Also the defined simulation times are decreasing when the altitude is decreasing.

Actually in this step we have generated proper altitude and heading angle reference signals. So, by following these reference signals the aircraft will reach the main landing path disregarding its initial position.

For optimization procedure we have developed separate cost functions that consider longitudinal and lateral axis motions of aircraft. Even so, these functions are in similar forms and at the end, the outputs of each function have been summed.

Main idea of the cost function is minimizing the error between actual values and desired values of the related control states (altitude and heading signals). Then at each iteration of the optimization algorithm, new reference altitude and heading signals are generated and applied on the simulation model. The output states of the simulation are used as input states in the next iteration. This process is prepared in an m-file.

According to the defined altitude and lateral area constraints we have realized the optimization process for different starting points which are tabulated in Table 5.

Table 5 Optimization Starting Points Data Set

At 102m altitude area								
Vertical fixes	60m	80m	100m	120m	140m			
Horizontal fixes	140m	100m	60m	20m	-20m	-60m	-100m	-140m
At 75m altitude area								
Vertical fixes	45m	60m	75m	90m	105m			
Horizontal fixes	130m	78m	26m	-26m	-78m	-130m		
At 49m altitude area								
Vertical fixes	45m	49m	53m					
Horizontal fixes	7m	0	-7m					

During the construction of the optimization problem we have defined the system constraints [26], [28]. All system input states have been considered as optimization constraints. That means, airspeed value is not an optimized parameter but it is used as a constraint whose response is observable at the end of each simulation.

The generalized form of thr cost function and the related constraints are;

$$f1 = \int_0^{tf} w1(x_a - x_d)'Q(x_a - x_d)dt \quad [4.1]$$

$$f2 = \int_0^{tf} w2(y_a - y_d)'R(y_a - y_d)\, dt \quad [4.2]$$

Minimize $f = f1 + f2$

Subject to $-1 \leq \Psi \leq 1\ (rad)$ [4.3]

$26 \leq V \leq 60\ (m/s)$

$H \geq 0\ (m)$

where,

$w1, w2, Q, R$ are all weight constants and matrices

x_a is the actual values of all input states at that moment

x_d is the desired values of all input states at that moment

y_a is the actual values of all related output states

y_d is the desired values of all related output states

V is representing speed and defined as a constraint of the system

H is representing altitude and defined as a constraint of the system

Ψ is representing heading and defined as a constraint of the system

In order to minimize the cost function regarding the constraints a multidimensional search is realized. In this study steepest descent method as a multidimensional search method and parabolic fit as the one dimensional search (line search) method are used. The general iterative form of optimization search method is [27] is given here;

$$x_{k+1} = x_k - \alpha_k g(x_k) \quad [4.4]$$

where, $g(x_k) = \nabla f(x_k)$ is the gradient of the cost function at that point.

It is the direction of the search step which is orthogonal to the previous one, and α_k is the step length which is obtained by the one dimensional search.

Algorithm of the steepest descent iteration is;

- Choose the initial point for x_0 . Then $g(x_0) = -\nabla f(x_0)$
- Determine the step length $\alpha_k = \min f(x_k - \lambda_k g(x_k))$ (one dimensional search is realized at that point)
- Calculate the next value x_{k+1} from [4.4]
- Then calculate gradient (direction) with the new calculated x_{k+1}
- Repeat the steps up to the maximum number of iterations or up to the convergence is observed.

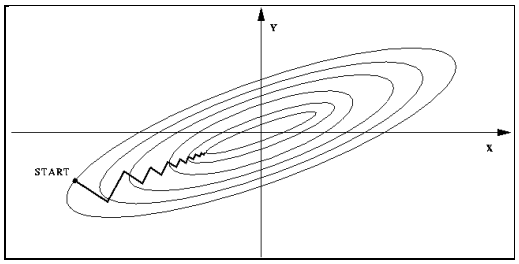

Figure 50 Representation of Steepest Descent Method [27]

We have applied this optimization procedure for altitude and heading reference signals separately. According to the optimization starting points (Table 5) first we have obtained optimized reference altitude signals when the speed and heading states are constant. Then optimized reference heading signals are generated when speed and altitude states are constant. By following this heading signal the aircraft reach the desired position on the y-axis.

According to our observations regarding the response of the system and time durations, we have chosen the number of iterations for steepest descent search as 20 and maximum number of function evaluations during the one dimensional search

(i.e., parabolic fit [35]) as 100. Still, the resultant time duration to obtain a solution is very long.

At the end of the optimization process, we have collected the results corresponding to several initial states and have developed the landing path data base.

In order to consider the optimization results we have presented both reference signals and the system responses for these reference signals. We know that all of the obtained trajectories are inside of the safe landing corridor. So, all the following system response representations are acceptable. By the help of this optimization step we have found the best reference signals that provide the aircraft to reach the main landing path.

For the given 49 m altitude area the optimization starting points at lateral and longitudinal axis are given in Table 6. In this case, 3 reference altitude signal searches and 3 reference heading signal searches have been realized. Note that the initial simulation time is 30 seconds. In Figure 51 obtained optimal reference heading signals are presented. Note that the given reference signal will be smoother if the sample time is chosen as 0.01 instead of 1 second. This is applicable for the following two data sets. When we have applied these reference signals to the direction controller obtained position responses of the UAV are given in Figure 52. Similarly the generated optimal reference altitude signals are given in Figure 53 and related system responses are given in Figure 54. As it is seen from the system response graphs the generated optimal reference signals are suitable for this case. Note that, some other benefits of these optimal trajectories will be explained in the following subchapter.

Table 6 Data Set for 49 m Altitude Area

Vertical fixes	45m	49m	53m
Horizontal fixes	7m	0	-7m

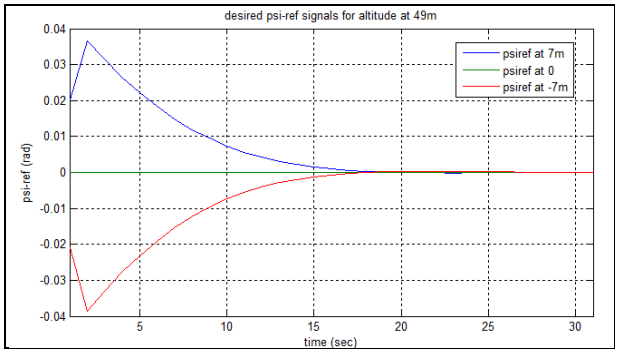

Figure 51 Optimized Heading Reference Signals at 49 m Altitude Area

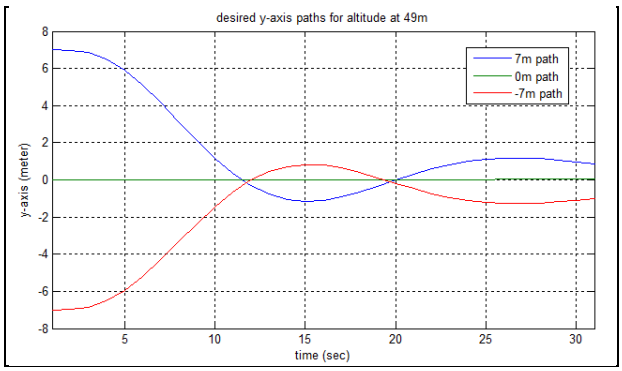

Figure 52 Response of System to Reference Heading Signal at y-axis (at 49 m)

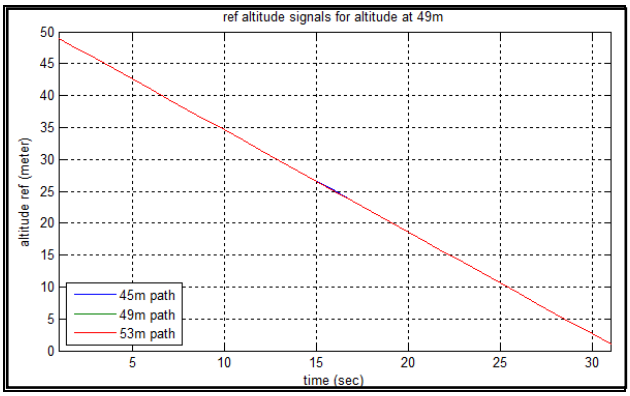

Figure 53 Optimized Altitude Reference Signals at 49 m Altitude Area

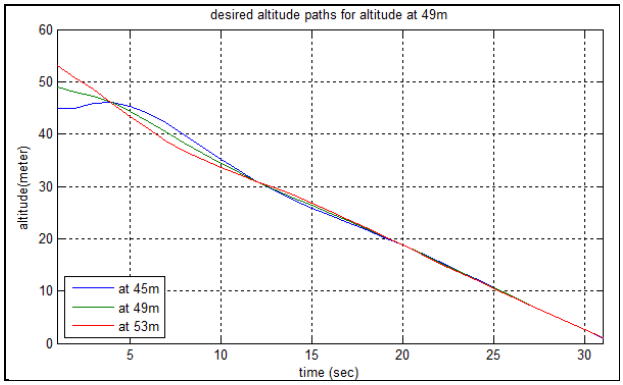

Figure 54 Response of System to Reference Altitude Signal at z-axis (at 49 m)

For the given 75 m altitude area the optimization starting points at lateral and longitudinal axis are given in Table 7. In this case, 5 reference altitude signal searches and 6 reference heading signal searches have been realized. Note that the initial simulation time is 46 seconds. The results are represented similar to the previous altitude area. Generated optimal reference heading signals are given in Figure 55 and related system responses are given in Figure 56. The generated optimal reference altitude signals are given in Figure 57 and related system responses are given in Figure 58. As it is seen from the system response graphs the generated optimal reference signals for this defined area are suitable. In figure 57 the reference altitude signal for 105 m altitude is a little different due to the system response limits. So, related reference signal is generated as given below.

Table 7 Data Set for 75m Altitude Area

Vertical fixes	45m	60m	75m	90m	105m	
Horizontal fixes	130m	78m	26m	-26m	-78m	-130m

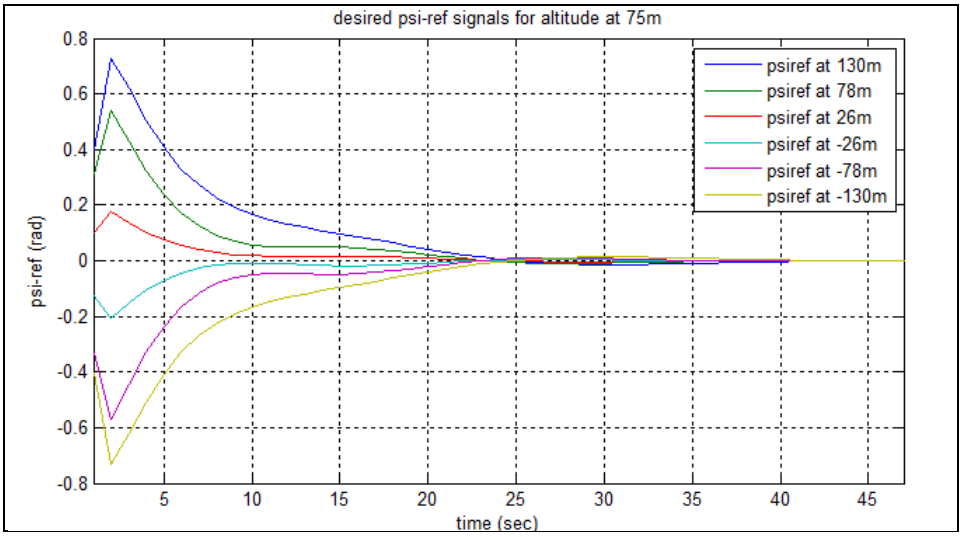

Figure 55 Optimized Heading Reference Signals at 75 m Altitude Area

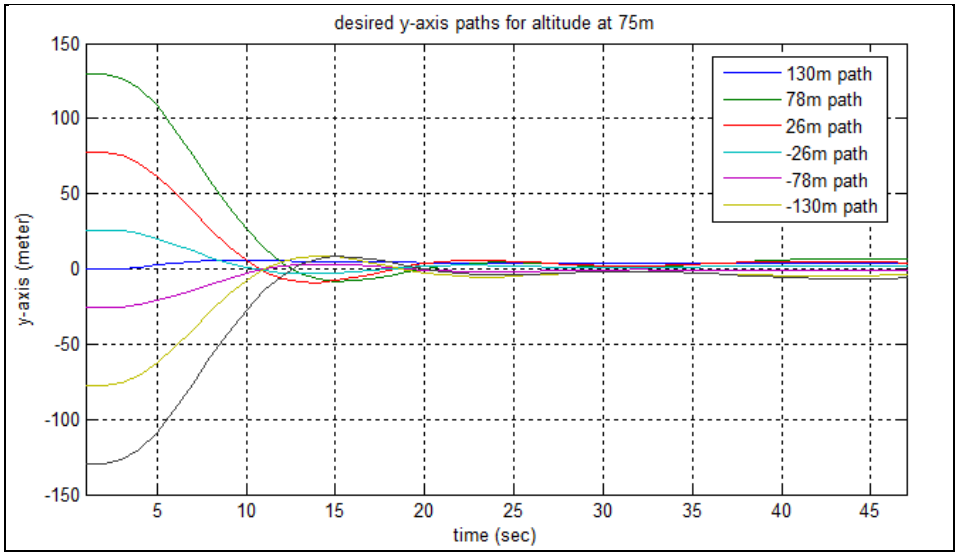

Figure 56 Response of System to Reference Heading Signal at y-axis (at 75 m)

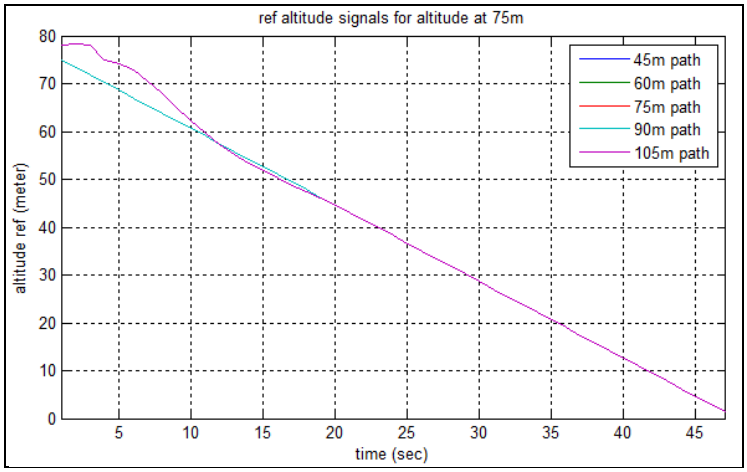

Figure 57 Optimized Altitude Reference Signals at 75 m Altitude Area

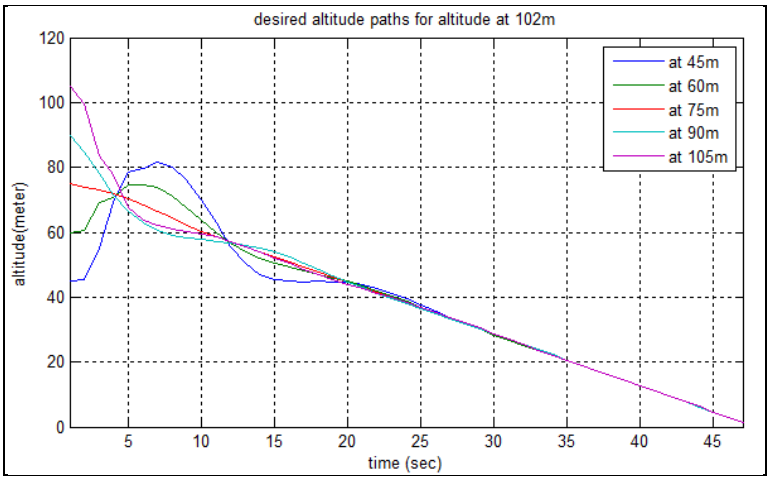

Figure 58 Response of System to Reference Altitude Signal at z-axis (at 75 m)

For the given 102 m altitude area the optimization starting points at lateral and longitudinal axis are given in Table 8. In this case, 5 reference altitude signal searches and 8 reference heading signal searches have been realized due to the larger lateral area. Note that the initial simulation time is 63 seconds. The results are represented similar to the previous altitude areas. Generated optimal reference heading signals are given in Figure 59 and related system responses are given in Figure 60. The generated optimal reference altitude signals are given in Figure 61

and related system responses are given in Figure 62. As it is seen from the system response graphs the generated optimal reference signals for this defined area are suitable. In this case, we did not present the system responses at z = 60 m on graphs, because it is an unacceptable starting condition due to the controller performance. So, the related system response is still unacceptable after the path optimization step.

Table 8 Data Set for 102 m Altitude Area

Vertical fixes	60m	80m	100m	120m	140m			
Horizontal fixes	140m	100m	60m	20m	-20m	-60m	-100m	-140

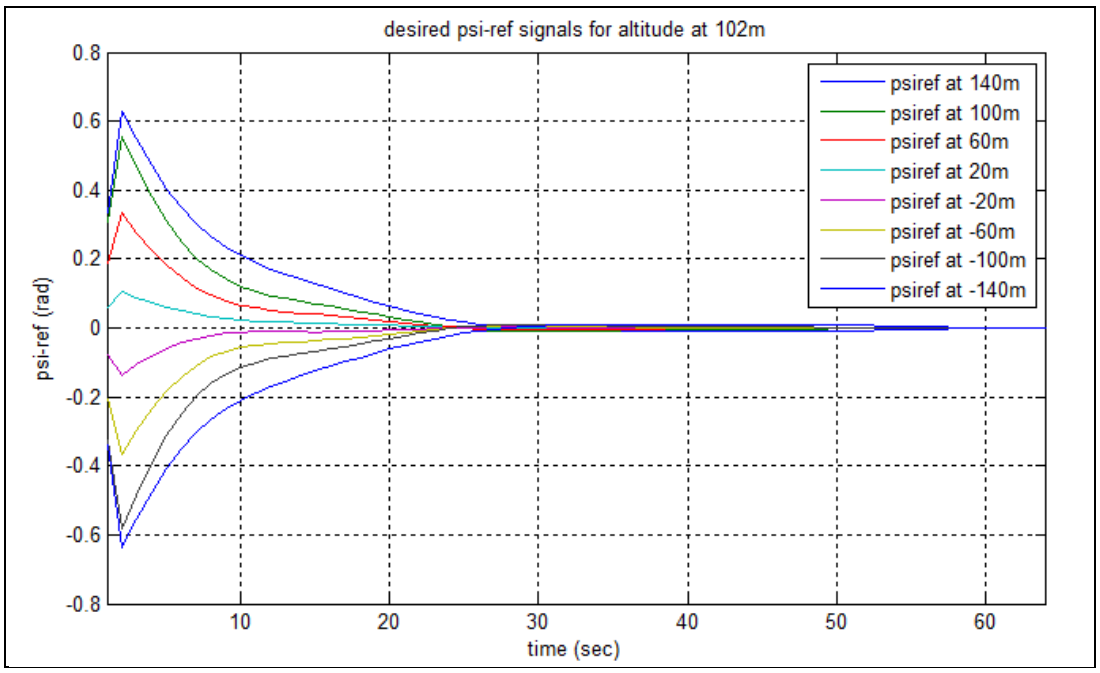

Figure 59 Optimized Heading Reference Signals at 102 m Altitude Area

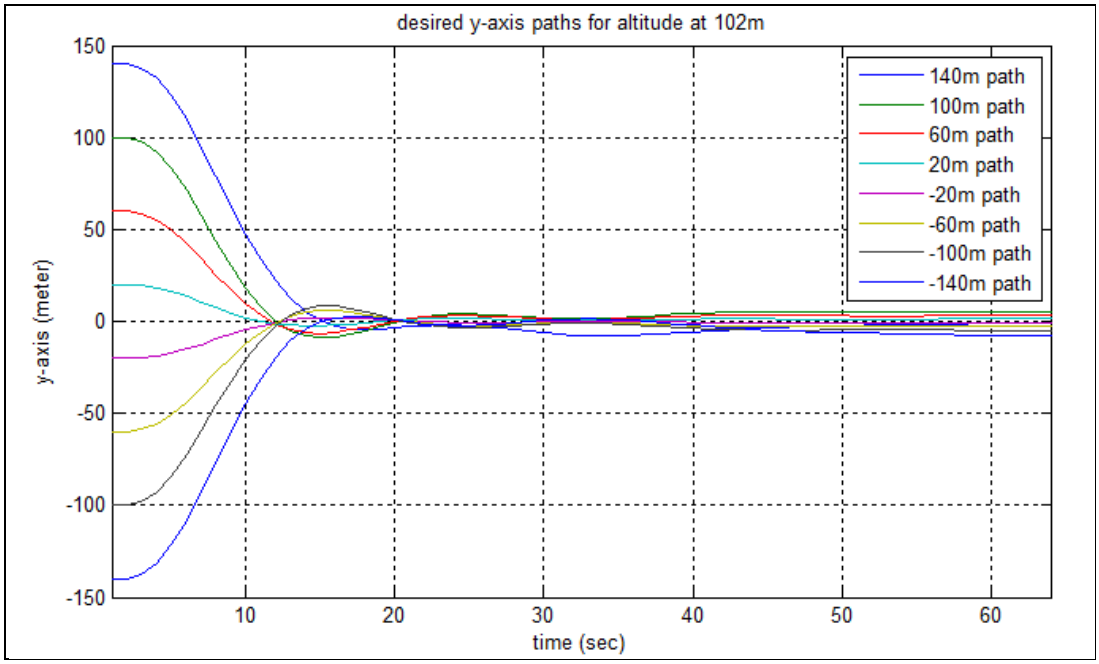

Figure 60 Response of System to Reference Heading Signal at y-axis (at 102 m)

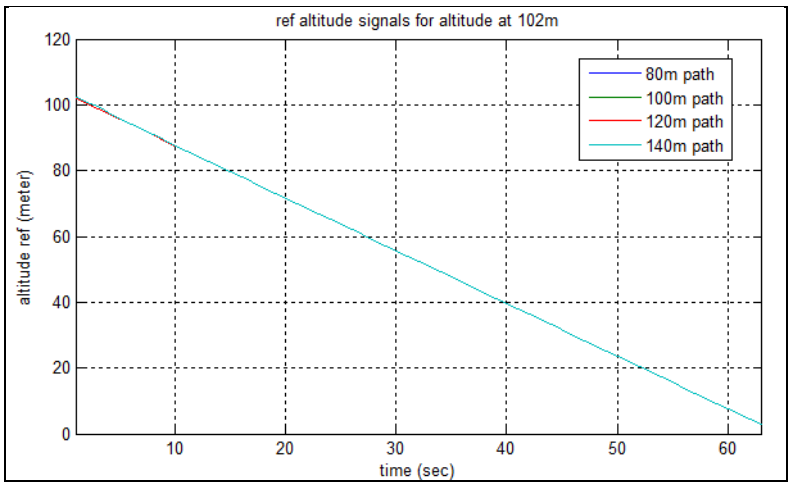

Figure 61 Optimized Altitude Reference Signals at 102 m Altitude Area

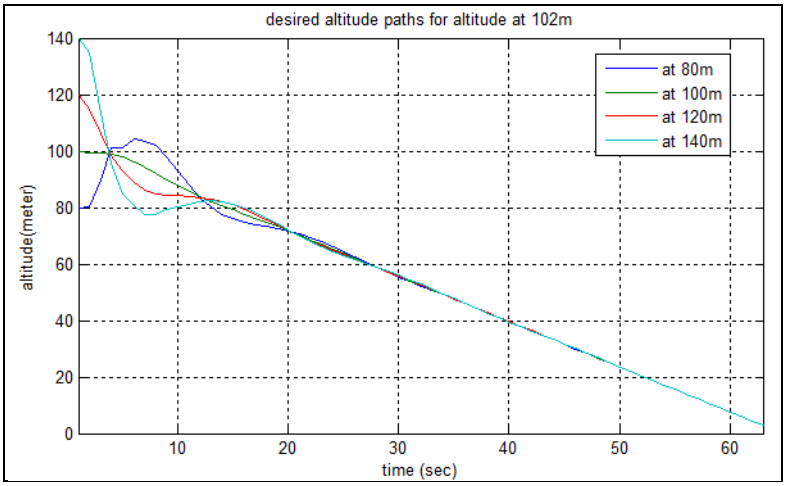

Figure 62 Response of System to Reference Altitude Signal at z-axis (at 102 m)

When the results are criticized; generally, for each defined starting point the main landing path could be reached. This step is very useful to collect reference heading signals. As we have defined before we did not control the aircraft position at lateral axis and for the direction controller we need proper reference heading signals which provides the desired replacement to the aircraft at y-axis. Then, the altitude reference signals and related responses of the aircraft are considered. Again we tried to produce the best reference altitude signals that will provide the aircraft to reach to the main landing path. But when we look at the reference signals and response signal graphs for each altitude area it is seen the reference signals are not changing much due to changing starting points. Similar simulation results will be obtained when the given starting altitude points are applied to the altitude controller directly. This means reference altitude signal optimization will not be required due to these simulation results.

4.1. Interpolation for Optimal Landing Paths

The generated data base of landing paths is a very important and useful tool for us. By using this data base we can cover a big part of the safe landing corridor in terms of the movement of the aircraft. But, some conditions are not covered yet. Thus, in order to consider the remaining parts we should use the linear interpolation method.

By interpolation method we can generate optimal landing paths for every initial position of the UAV.

We applied this method for only lateral axis movement of aircraft. According to the simulation results which are obtained in previous chapter, interpolation is not required for the longitudinal axis movement of the aircraft since optimal landing paths determined are nearly similar for all different starting points.

In order to realize the landing path interpolation a MATLAB code is prepared in an m-file. This code requires aircraft initial positions (x0, y0, z0). In this step speed value will deviate from 30 m/s through the initially defined simulation times.

For example for 49 m altitude, areas' length is 942.04 m (Figure 8). The assumed movement time for this path is 30 sec.

The calculated speed is $x0/time = 942.04/30 = 31.4m/s$ [4.5]

After this step we have tested 2 interpolation methods. At the first interpolation method, we can calculate the required time for landing by the help of the determined speed value and x0 value. That time value is important for us because we have defined the related state values according to this time value. As it is seen from the reference signal graphs the first column of the signal represents time value. The second column represents actual value of the reference signal at that moment. Then we have picked up two boundary y-axis values and corresponding reference heading signals which belong to that time value. We have calculated the interpolation rate at this step. Then we have applied this rate on the boundary reference heading signals. So, we have generated the required reference heading signal. We have inserted zero for the previous values (the values before the calculated time) of the produced reference heading signal.

By this way the simulation is started from the initial x-position. But the simulation results are not so good (not presented here). Then we have to design another interpolation method and presented its results.

As presented in the previous chapter the most effective outputs are obtained at the optimization starting points on y-axis. According to this method we have shifted this optimization starting points on y-axis to the related initial position on x-axis. Similarly we have realized the interpolation between boundary y-axis values and corresponding reference heading signals from the initial (not from the calculated time value). In this case the time value is used to stop the simulation.

Then the interpolated reference heading signals have been applied to the Simulink system model and displacement of the aircraft on the y-axis is observed.

For simulations, we have defined different initial positions from each chosen altitude area. These positions are given before the simulation results. The generated reference heading signals and related system responses are given. We consider the results case by case.

The first initial states are given in Table 9. Then the interpolated reference heading signal (Figure 63) is presented here. As it is explained before, boundary reference heading signals are selected and the required reference heading signal is generated for this initial position of the aircraft. By the help of x0 value the simulation time is calculated. Then the system response to this reference heading signal (Figure 64) is observed from the Simulink system model. When we consider the y-axis response, the aircraft reaches the main path with a negligible deviation.

Table 9 First Initial Position for Interpolation Algorithm

	x0 (m)	y0 (m)	h0 (m)
initial values	-1500	80	102

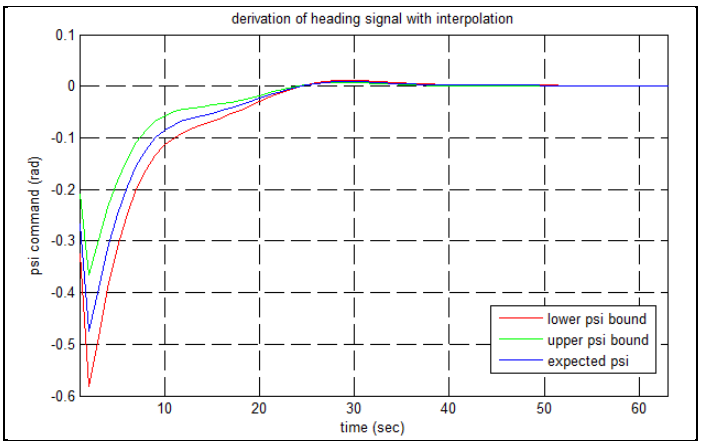

Figure 63 Interpolated Reference Heading Signal for First Initial Position

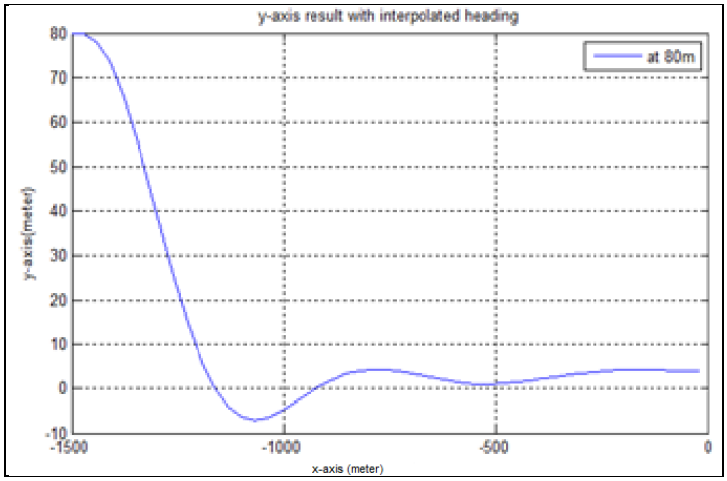

Figure 64 Response of System to Reference Heading Signal at y-axis for First Initial Position

The second initial states are given in Table 10. Similar to the first simulation, in this case the interpolated reference heading signal is presented in Figure 65. Then the system response to this reference heading signal (Figure 66) is observed from the Simulink system model. When we consider the y-axis response, the aircraft reaches the main path with a negligible deviation.

Table 10 Second Initial Position for Interpolation Algorithm

	x0 (m)	y0 (m)	h0 (m)
initial values	-1700	-110	102

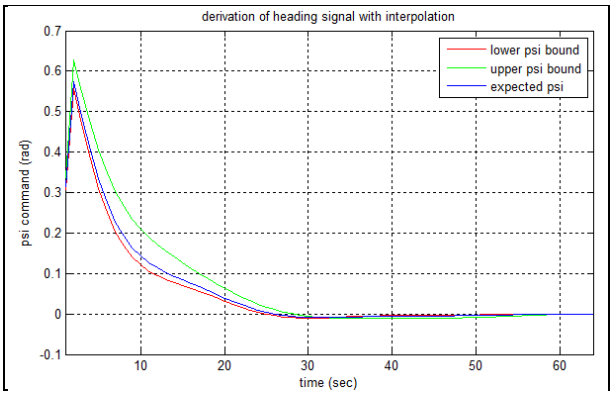

Figure 65 Interpolated Reference Heading Signal for Second Initial Position

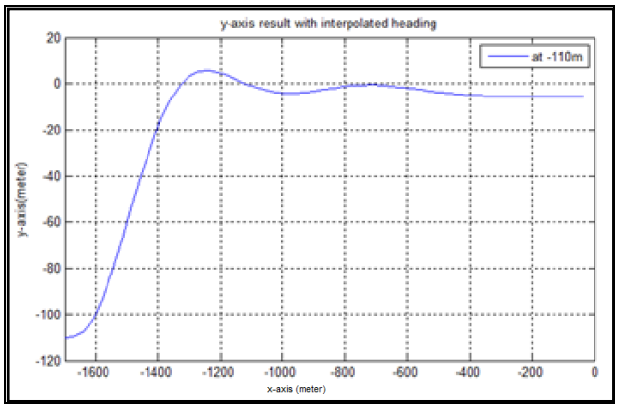

Figure 66 Response of System to Reference Heading Signal at y-axis for Second Initial Position

The third initial states are given in Table 11. Similar to the first simulation, in this case the interpolated reference heading signal is presented in Figure 67. Then the system response to this reference heading signal (Figure 68) is observed from the

Simulink system model. When we consider the y-axis response, the aircraft reaches the main path with a negligible deviation.

Table 11 Third Initial Position for Interpolation Algorithm

	x0 (m)	y0 (m)	h0 (m)
initial values	-1100	50	75

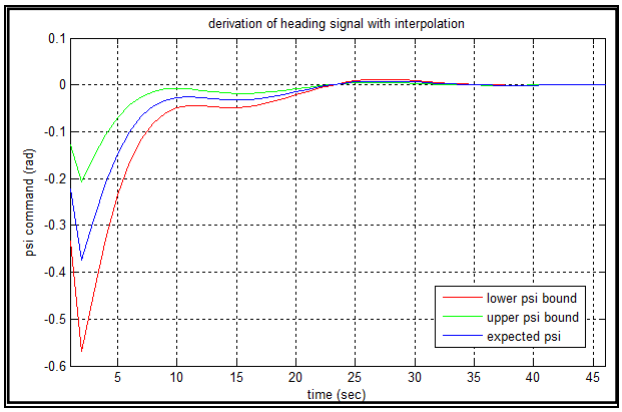

Figure 67 Interpolated Reference Heading Signal for Third Initial Position

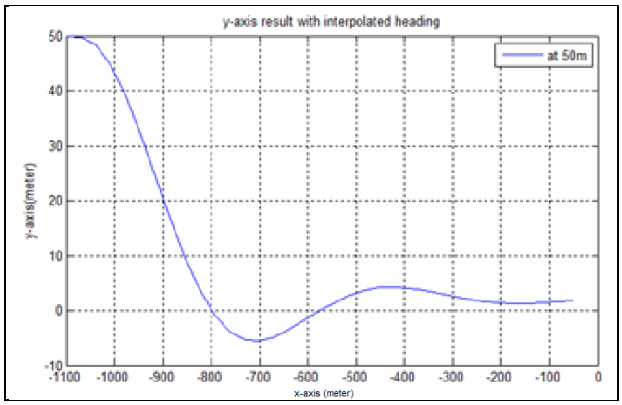

Figure 68 Response of System to Reference Heading Signal at y-axis for Third Initial Position

The last initial states are given in Table 12. Similar to the first simulation, in this case the interpolated reference heading signal is presented in Figure 69. Then the system response to this reference heading signal (Figure 70) is observed from the Simulink system model. When we consider the y-axis response, the aircraft reaches the main path with a negligible deviation.

Table 12 Fourth Initial Position for Interpolation Algorithm

	x0 (m)	y0 (m)	h0 (m)
initial values	-700	-5	49

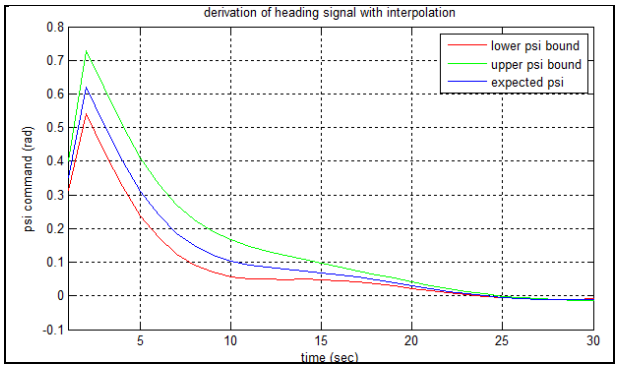

Figure 69 Interpolated Heading Signal for Fourth Initial Position

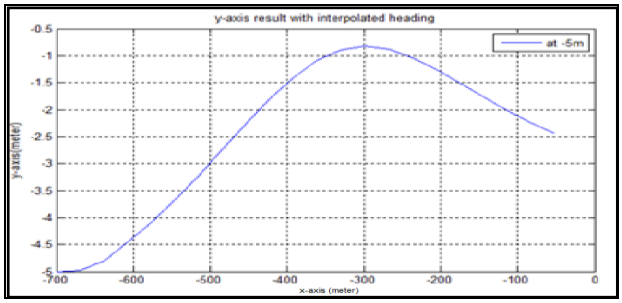

Figure 70 Response of System to Reference Heading Signal at y-axis for Fourth Initial Position

CHAPTER 5

MISSING PATH APPROACH

In previous chapters we have considered the state control of the aircraft when it is inside of the safe landing corridor. In this chapter, we consider the state control of the aircraft when it is outside of the safe landing corridor. For this case we have developed another simple landing procedure. We call it as the missing path approach in general. Actually, the known missing path approach concept which is acceptable in worldwide has some discrepancies. But a basic application is enough for this study.

In this study, we have prepared a flight plan (Figure 71 and Figure 72) and defined some waypoints with determined axis values. For each waypoint the reference command signals are produced by a MATLAB m-file program. Then these command signals are applied to the state controllers in Simulink system model. The details about waypoints and kind of motions are explained below.

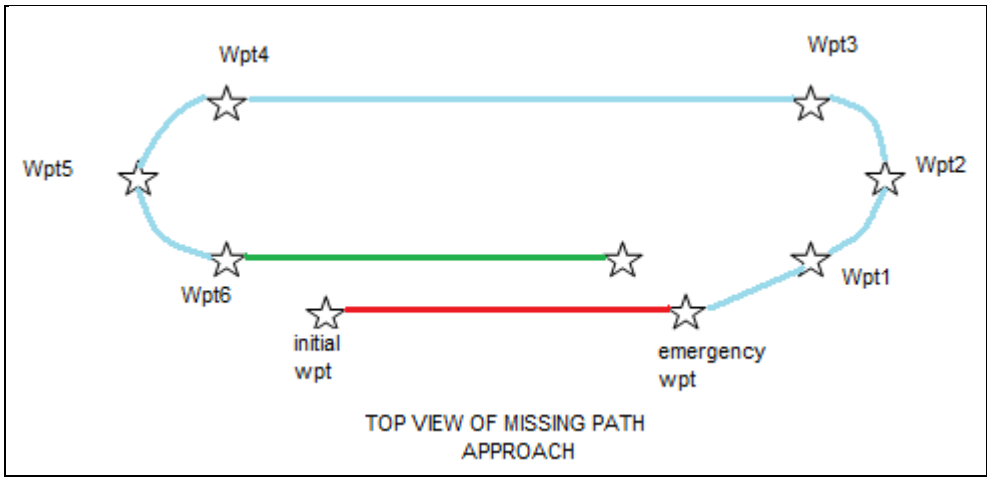

Figure 71 Planned Missing Path Approach Flight Path (Top View)

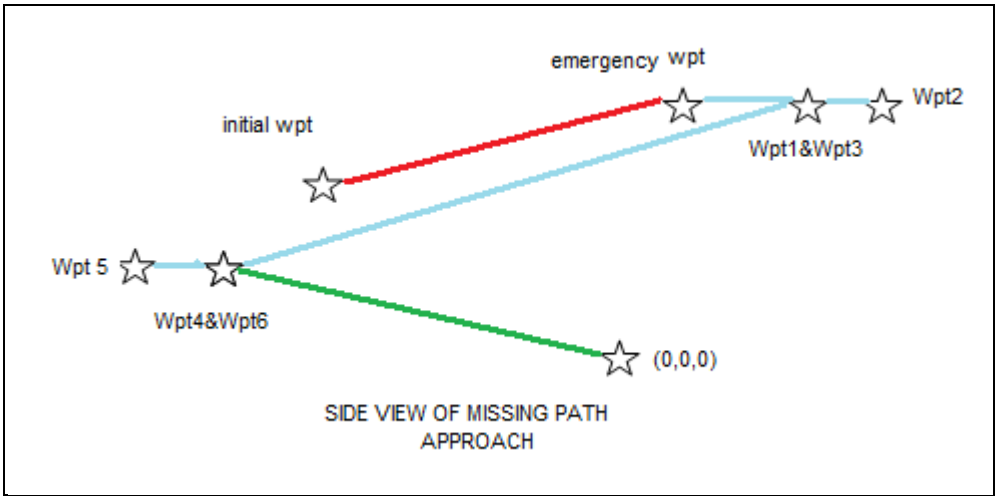

Figure 72 Planned Missing Path Approach Flight Path (Side View)

Initial Waypoint:

It represents the initial position of the aircraft. For this case we have assumed that, aircraft is outside of the safe landing corridor. After this point, aircraft will follow the determined commands which are generated from the waypoints of the path.

Emergency Waypoint:

It is the starting point of the planned flight path and we have named it as the emergency waypoint that has an altitude constraint (300 m). In this case aircraft climbs to this altitude without changing its direction. A climb trajectory as a reference altitude signal will be provided to the altitude controller. Note that, this movement is called as FA (fix to altitude) in FMS (Flight Management System) procedures.

Waypoint 1:

At Waypoint 1 the aircraft is still at same altitude. But if the assigned lateral position values of this point are different from the previous point, the aircraft have to follow the produced reference heading signal. After this step all of the waypoints are constant.

Waypoint 2:

Aircrafts' desired position at Waypoint 2 is given in Table 13 which will be reached by a 90 degrees turn. This movement is called as RF (radius to fix) leg in FMS procedures. Altitude value is not changed.

Waypoint 3:

A 90 degrees turn is repeated. The course is changed to 180 degrees according to our reference axis. Still, altitude value is held constant.

Waypoint 4:

After waypoint 3 a descent phase is started with the same course (180 degrees). The ending value of this descending path is given in Table 13. y-axis value is not changed at this step.

Waypoint 5:

In order to reach Waypoint 5 a 90 degrees turn is commanded.

Waypoint 6:

After an additional 90 degrees turn the aircraft catch the Waypoint 6 which is the desired main landing path starting point.

Zero Point:

It is the end point of the last leg which is the main landing path (between Waypoint 6 and zero). The position coordinates of zero point are (0, 0, 0).

These entire required axis values, related reference command signals and time durations are collected by the help of a MATLAB/m-file program. Then the determined reference command signals are applied to the system controller on Simulink model for the defined time intervals. These time values are generated according to the displacement of the UAV on x-axis and climb/descent performances of the system. Note that the airspeed is 30 m/s. In order to obtain simulation results, initial position of the aircraft is given as input to the m-file program. Then the mentioned reference values are obtained.

Table 13 Generalized Representation of Missing Path Approach Path Waypoints

WAYPOINTS	**X-axis (m)**	**Y-axis (m)**	**Z-axis (m)**
Initial Waypoint	Initial aircraft position	Initial aircraft position	Initial aircraft position
Emergency Waypoint	X2=*	Initial aircraft position	300
Waypoint 1	X3=X2+1000	0	300
Waypoint 2	X4=X3+350	350	300
Waypoint 3	X5=X4-350	700	300
Waypoint 4	X6= -1942-x4	700	102
Waypoint 5	-2272	350	102
Waypoint 6	-1942	0	102
Zero Point	0	0	0

*_ waypoint2 x-axis value is changeable due to the different initial z-axis. That means the required time to reach constant altitude is changing the distance at x-axis.

In Table 14 first initial states of the aircraft and the simulation time are represented. In order to observe the aircraft movement at lateral axis X-Y graph output is presented (Figure 73). When we look at the simulation result the UAV can follow properly the given missing path approach path due to the well calculated reference command signals and time values. At the end of this simulation the UAV comes at the top of the starting point of the main landing path. Also the observed airspeed and altitude responses of the system are given in Figure 74 and Figure 75. The altitude controller is working properly. Because of the climb path the speed controller hold the airspeed at 30 m/s with a bit of difficulty.

Table 14 First Initial Position for Missing Path Aproach Scenario

X0 (m)	Y0 (m)	H0 (m)	V0 (m)	Time duration (sec)
-1400	20	260	30	165

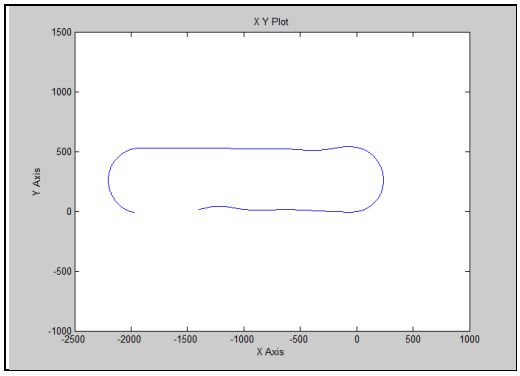

Figure 73 Lateral Movement of Aircraft for First Initial Position

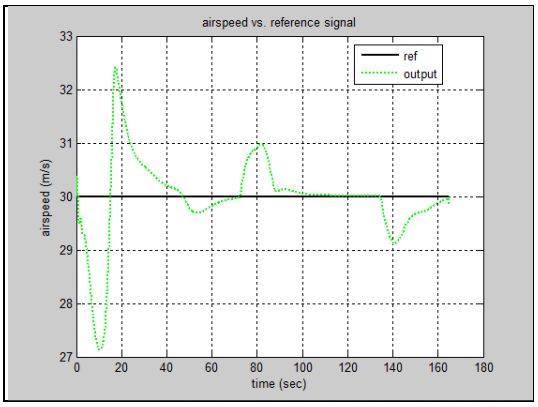

Figure 74 Response of System to Speed Controller for First Initial Position

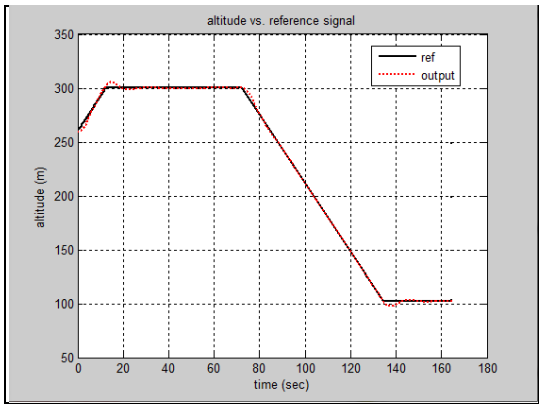

Figure 75 Response of System to Altitude Controller for First Initial Position

For another aircraft position, the initial states and simulation time are given in Table 15. As it is seen from the Figure 76 the UAV can follow properly the given missing path approach path due to the well calculated reference command signals and time values. At the end of this simulation the UAV comes at the top of the starting point of the main landing path. Also the observed altitude, airspeed and heading controller responses of the system are given in Figure 77, Figure 78 and Figure 79. All the responses are acceptable. The altitude controller is working properly. Because of the climb path the speed controller holds the airspeed at 30 m/s with a bit of difficulty. The heading controller responses show the applied heading reference signals on the system.

Table 15 Second Initial Position for Missing Path Approach Scenario

X0 (m)	Y0 (m)	H0 (m)	V0 (m)	Time duration (sec)
-700	-200	100	30	300

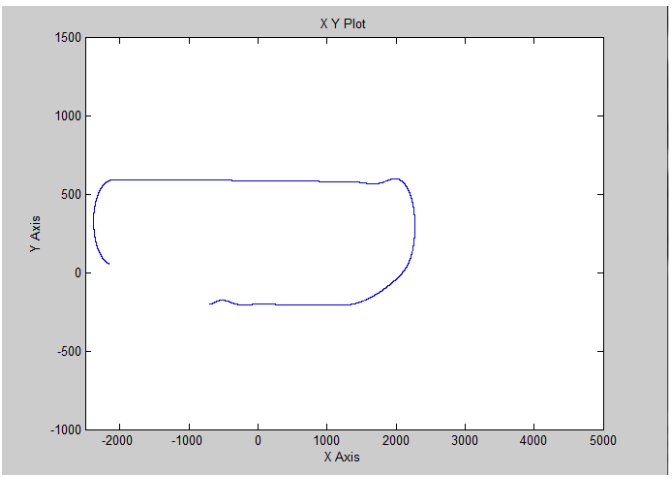

Figure 76 Lateral Movement of Aircraft for Second Initial Position

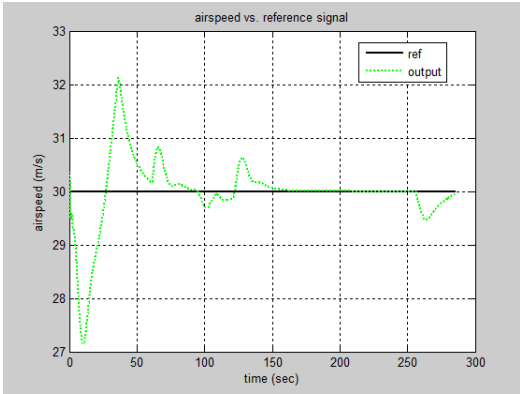

Figure 77 Response of System to Speed Controller for Second Initial Position

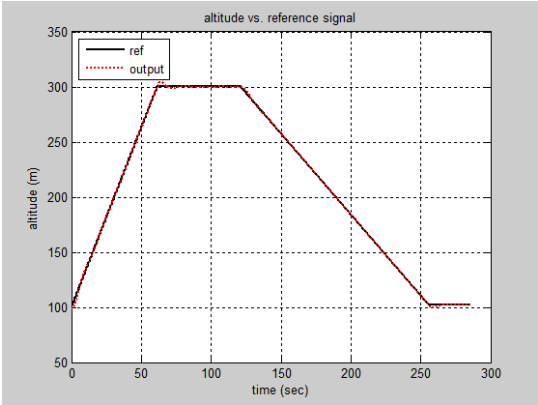

Figure 78 Response of System to Altitude Controller for Second Initial Position

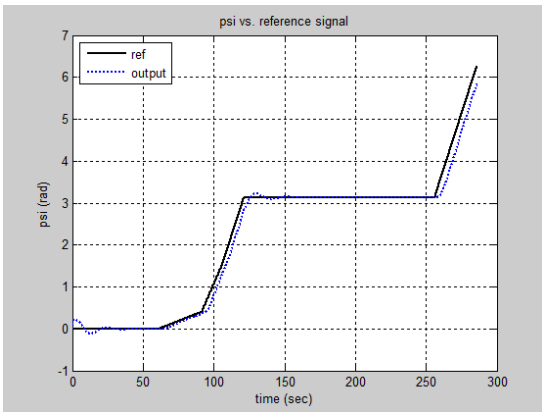

Figure 79 Response of System to Direction Controller for Second Initial Position

In order to test the performance of the missing path approach planning algorithm we have added the main landing path after the 8th waypoint. As it is seen from the results obtained, the system achieves to land the aircraft with acceptable deviations on position states. The related system response graphs are Figure 80, Figure 81, Figure 82 and Figure 83.

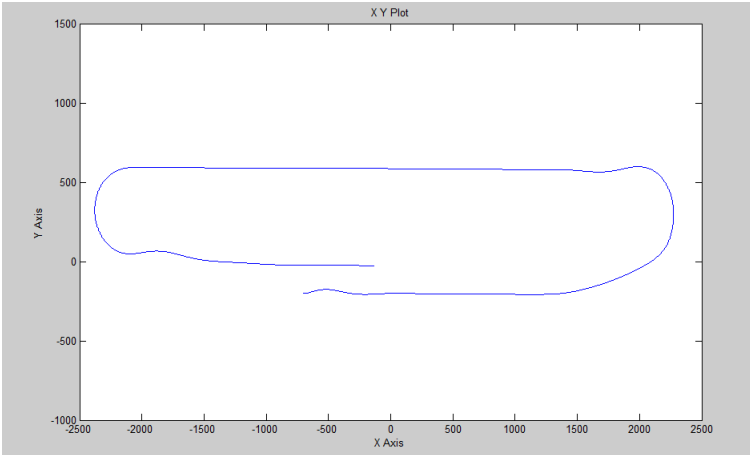

Figure 80 Lateral Movement of Aircraft for Second Initial Positions with Landing Path

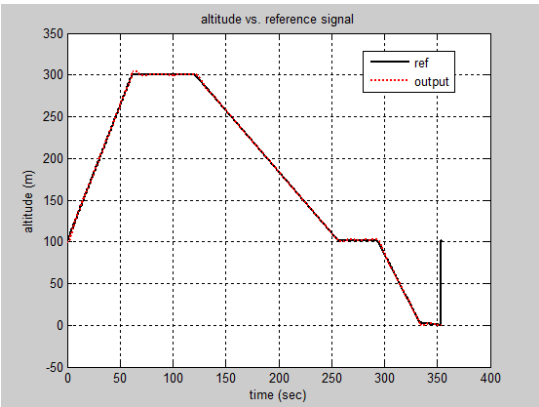

Figure 81 Response of System to Altitude Controller for Second Initial Position with Landing Path

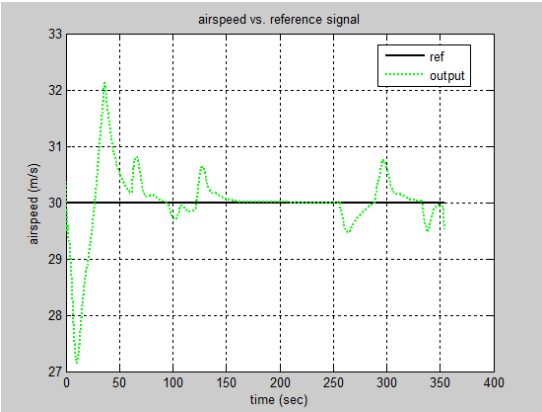

Figure 82 Response of System to Speed Controller for Second Initial Position with Landing Path

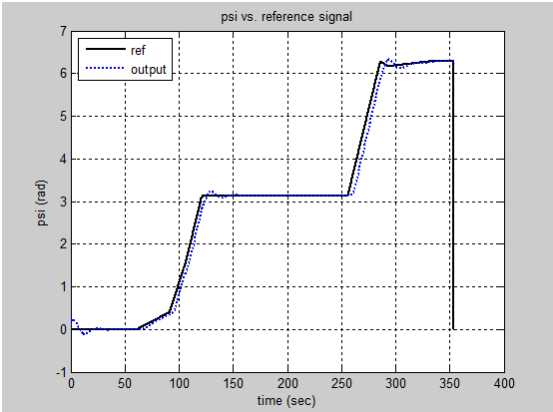

Figure 83 Response of System to Direction Controller for Second Initial Position with Landing Path

At the end of the analysis in this chapter, we have concluded that, in order to construct a missing path approach applied in this thesis too much effort should be spent. It requires very sensitive calculations for the determination of reference command signals and too much simulation time is necessary in order to observe the autopilot and system performances. These issues mentioned above effect the automation level of the proposed method negatively. As an alternative approach, some general lateral position control methods are considered in the next chapter.

CHAPTER 6

LATERAL POSITION CONTROLLER

In this chapter we applied some lateral position control methods which are known as the lateral navigation. According to these methods the main idea is to hold the aircraft position at x and y-axis as it is recommended. For this purpose x-y states are fed back to the lateral position controller block. Then it produces related reference heading signal.

The first presented model [10] provides the movement of the aircraft from any initial point to a desired position. As an assumption, the aircraft is at (0, 200) position and the target value is 0 point at y-axis (we cannot limit x axis due to the aircraft motion). The aircraft initial heading value is zero.

According to the given initial states, the mathematical model of the mentioned method is given here [10]:

The error of y-axis (y_{err}) is:

$$y_{err} = y_{ref} - y_{pre} \qquad [6.1]$$

y_{ref} is the desired value that is decided as 0 here. y_{pre} is the aircraft present position and updated continuously.

Desired inertial y-position is;

$$\dot{y_{err}} = V_0 \sin(\Psi ref - \Psi) \approx V_0(\Psi ref - \Psi) \qquad [6.2]$$

In order to provide smooth decreasing, inertial position is passed from a filter as given below.

$$\dot{y_{err}} = \frac{1}{Td} y_{err} \qquad [6.3]$$

Td is changing according to the aircraft speed. For this UAV we take it 15 seconds. Substitute [6.3] into [6.2]:

$$\frac{1}{Td} y_{err} = V_0(\Psi ref - \Psi) \qquad [6.4]$$

Next, substitute [6.1] into [6.4]:

$$\Psi ref - \Psi = \frac{1}{TdV_0}(y_{ref} - y_{pre}) \qquad [6.5]$$

which is equal to Ψ_{comm}..

We have added this position controller block to the Simulink system model and run the simulation in order to realize the assumed displacement. According to the simulation results we can observe the movement of the aircraft on the y-axis clearly (Figure 85). The aircraft changes its position from 200 m to 0 in y-axis. Also the generated reference heading signal by this block and the system response to this signal is observed (Figure 84). The altitude and airspeed controller responses are very good for this case (Figure 86 and Figure 87).

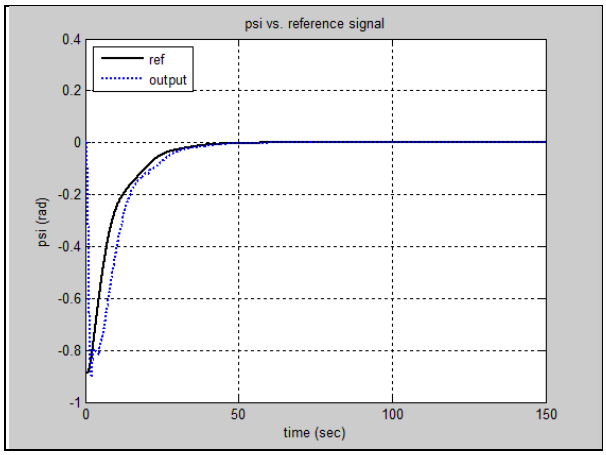

Figure 84 Response of System to Direction Controller with Lateral Position Controller

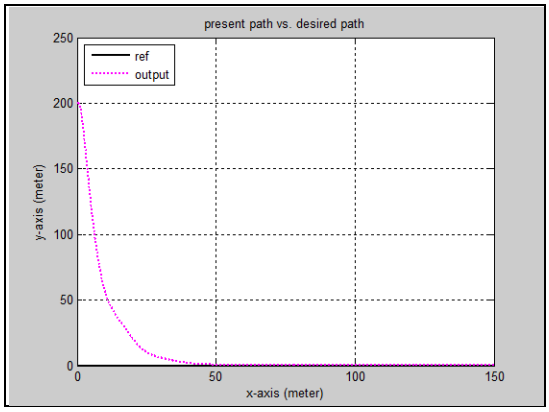

Figure 85 Followed Path by the Aircraft During Replacement

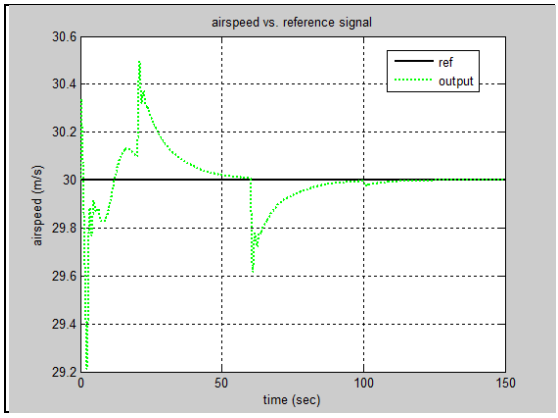

Figure 86 Response of System to Speed Controller with Lateral Position Controller

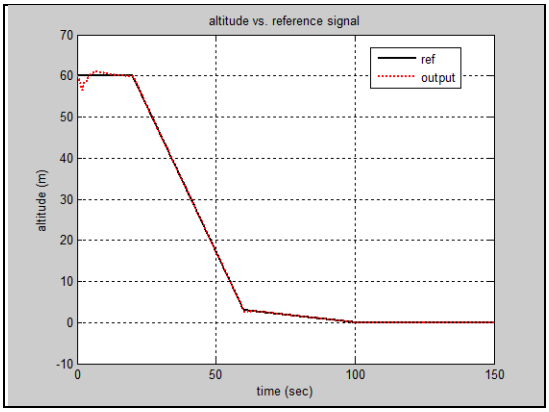

Figure 87 Response of System to Altitude Controller with Lateral Position Controller

6.1. Cross Track Error control

When we consider the main landing path the deviation on y-axis is 0. In case a deviation occurs from the desired flight path at lateral axis, which means the y-axis value is different from the expected value. At this condition the deviation is called as the cross track error. Our concern is to eliminate this error value. The simplified block diagram representation of the explained system is given in Figure 88.

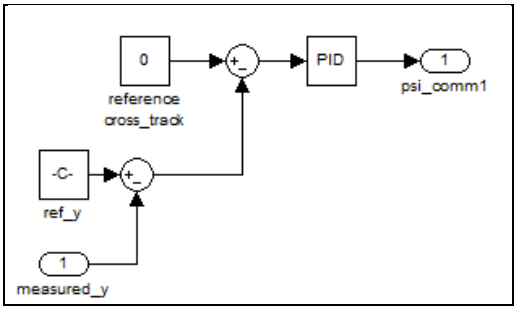

Figure 88 Simulink Model of Cross Track Error Controller

Next, we have added this controller to the Simulink system model and observed the responses of the system. For simulation, it is assumed that initial position at y = -200 m and the reference cross track error is zero. Y-axis response of the system (movement on y-axis) (Figure 89) and the generated reference heading signal (Figure 90) in order to provide this movement are observed and presented here. The other reference states are 30 m/s constant speed and 100 m constant altitude.

Responses of the system to the other reference signals are given below. The response of altitude signal (Figure 91) and speed signal (Figure 92) are acceptable.

Also the responses of other states are given below. When we compare them the previous system responses they are appropriate and acceptable (Figure 93, Figure 94, Figure 95, Figure 96, and Figure 97).

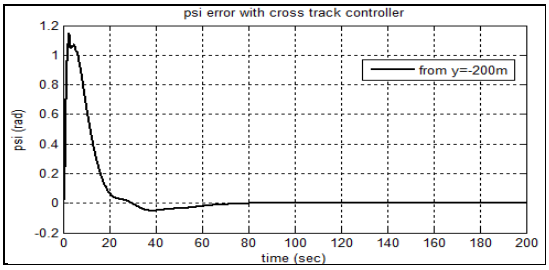

Figure 89 Cross Track Error Compansation Psi Angle Result

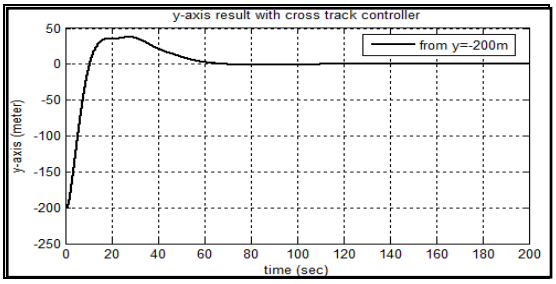

Figure 90 Cross Track Error Compansation y-axis Result

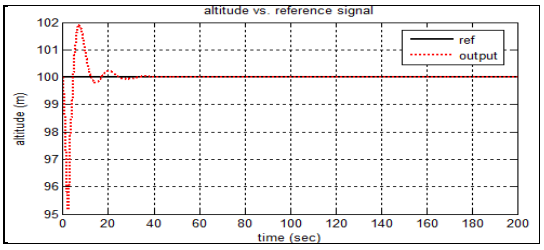

Figure 91 Response of System to Altitude Signal

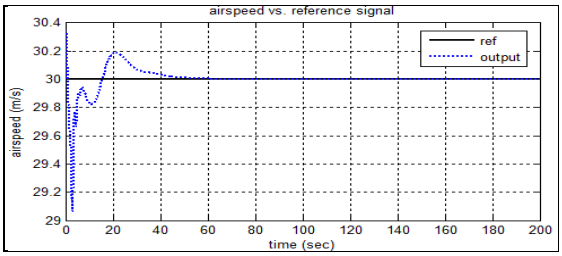

Figure 92 Response of System to Speed Signal

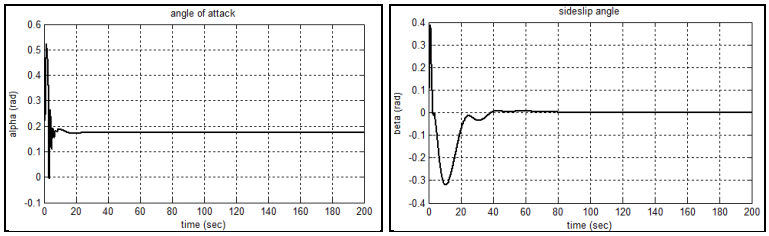

Figure 93 Angle of Attack and Sideslip Angle Responses

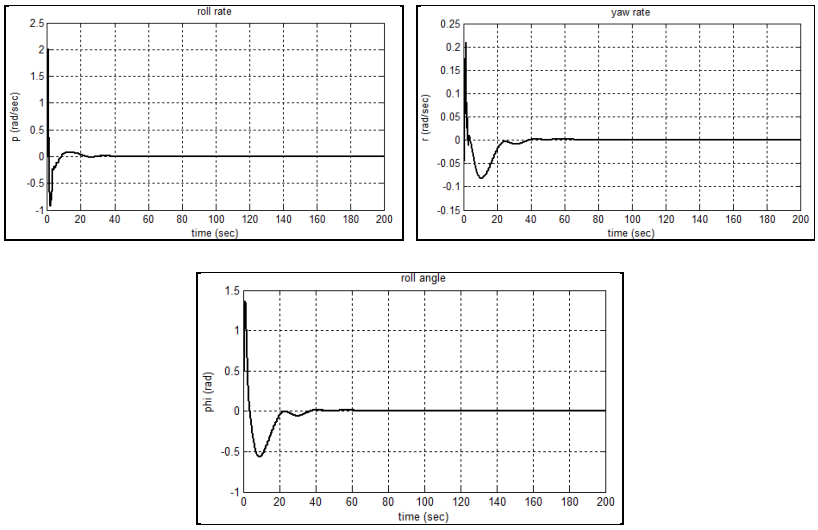

Figure 94 Roll Rate, Yaw Rate and Roll Angle Responses

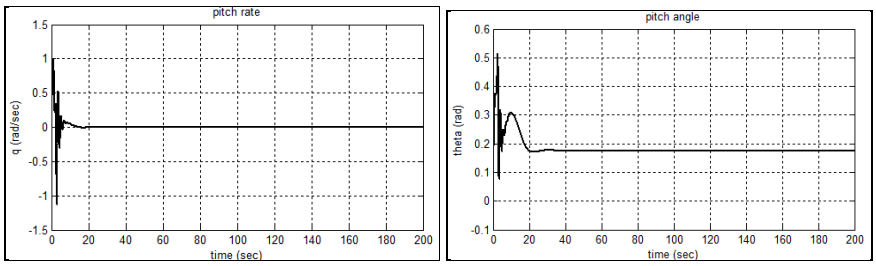

Figure 95 Pitch Rate and Pitch Angle Responses

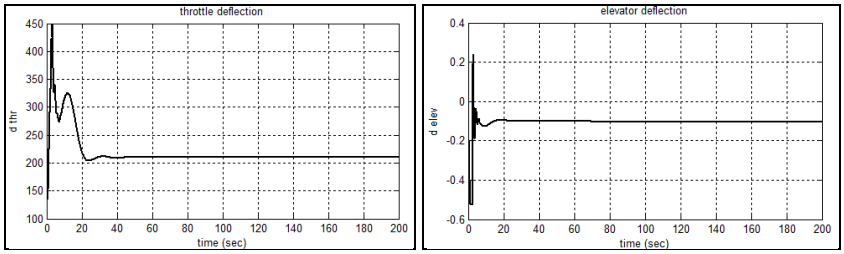

Figure 96 Throttle and Elevator Deflections

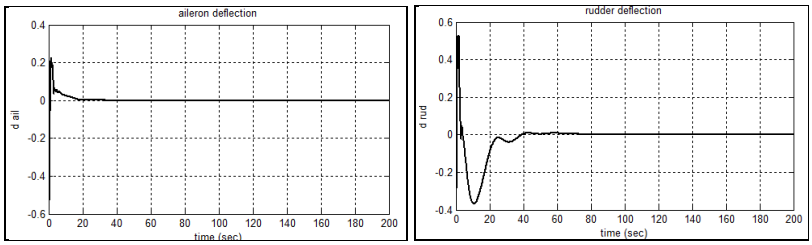

Figure 97 Aileron and Rudder Deflections

6.2. Lateral Track Controller

We can define our landing path with two waypoints where the first one is at the top of the landing path (FAF point) and the second one is at the end of the landing path (flare point) which is called as tract to fix leg. The main idea is to reach the end point before passing through this leg disregarding the present position of the aircraft [12].

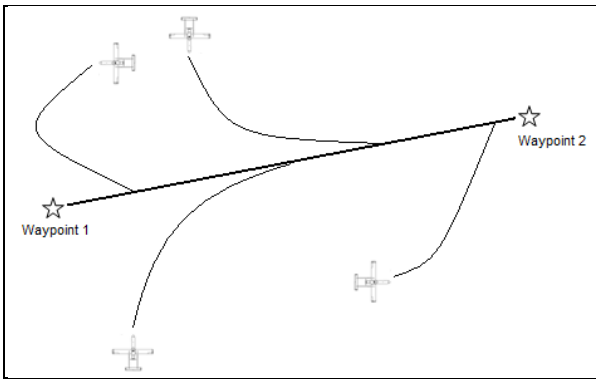

Figure 98 Desired Performance of the Lateral Track Controller

We have studied on the landing path and assumed that the aircraft is deviated from the main landing path at lateral axis. This means the initial y-axis value of the UAV is different than zero for our case. As it is seen from the figure above according to the present position of the aircraft the lateral track controller have to generate appropriate reference heading signal to the direction controller.

Regarding the proposed control strategy in reference [12], a relationship between aircraft actual position and airspeed is constructed;

$$\frac{\dot{X}_{track}}{kX_{track}} = \frac{\dot{Y}_{track}}{kY_{track}} \qquad [6.6]$$

When [6.6] is equated to zero the system error is obtained;

$$Error = k\dot{Y}_{track}X_{track} - \dot{X}_{track}Y_{track} = 0 \qquad [6.7]$$

With a proportional feedback gain the saturated yaw rate is written;

$$r_{comm} = sat(K_r(k\dot{Y}_{track}X_{track} - \dot{X}_{track}Y_{track})) \qquad [6.8]$$

Yaw rate signal is converted to yaw angle due to the system controller (direction controller) properties.

$$\psi_{comm} = \int r_{comm} = \int (K_r(k\dot{Y}_{track}X_{track} - \dot{X}_{track}Y_{track})) \qquad [6.9]$$

The representation of this mathematical model with a drawing is given in Figure 99 and the block diagram representation of the controller is given in Figure 100.

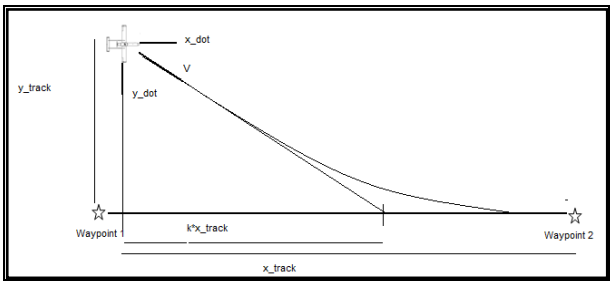

Figure 99 Geometrical Representation of the Lateral Track Controller

The input data $\dot{Y}_{track}$ and $\dot{X}_{track}$ is generated from the derivatives of output states x and y. And, Y_{track} and X_{track} is generated as an error signal. k and K_R are adjustable controller parameters which are 0.2 and 0.000003, respectively. The yaw rate saturation value is defined as 0.26 rad/s. k provides the smoothness of the aircraft movement, when the aircraft is approaching to the target waypoint (target path). At condition $k \geq 1$ the desired behavior is that the aircraft will fly to the second waypoint directly.

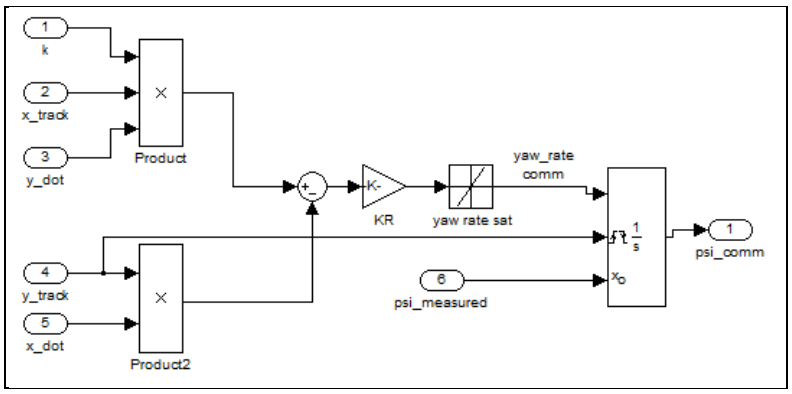

Figure 100 Simulink Model of the Lateral Track Controller

We have added this track controller to the Simulink system model and observed the responses of the system. For simulation, it is assumed that initial position at lateral axis is (0, -200) and the target point is (1000, 300). When we look at the Y-axis response of the system (movement on y-axis) (Figure 101), it is observed that aircraft can reach the target point satisfactorily. But there is no following position command. In that case the aircraft loses the control; probably it tries to turn back to the commanded position (300 m at y-axis). The generated reference heading signal (Figure 102) in order to provide this movement is observed. Due to the lack of following position command the reference heading signal is destroyed after reaching the target point at y-axis. This behavior is not given in this figure. Also x-axis response of the system is presented (Figure 103).

This method will be used in the construction of a flight plan that includes more than 2 waypoints and the results will be successful.

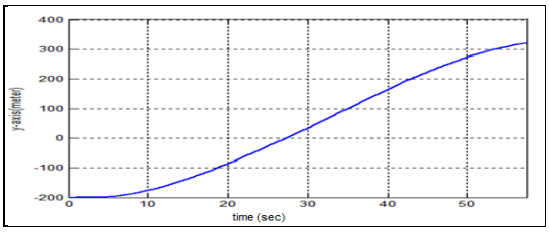

Figure 101 Result of the y-axis Position for the Lateral Track Controller

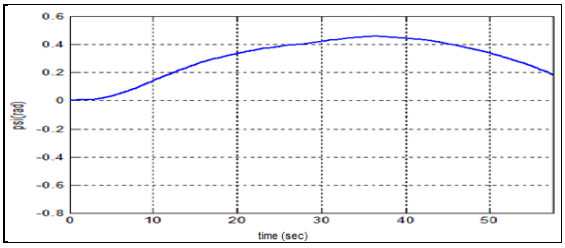

Figure 102 Response of System to Direction Controller for the Lateral Track Controller

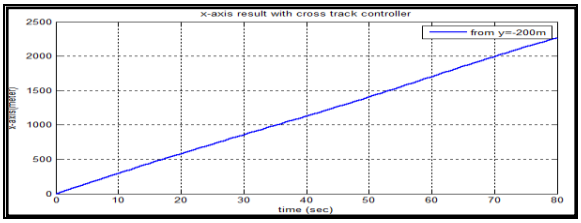

Figure 103 Result of x-axis Position for the Lateral Track Controller

As it is seen, on a landing path there is only one start point and one end point. The first lateral controller method has provided the movement of the aircraft on this path successfully. But, the second method needs a new position command or time limitation in order to give appropriate results. So, we prefer to use the first method as lateral position controller in this thesis.

CHAPTER 7

SHIFTING SAFE LANDING CORRIDOR

In order to expand the movement area of the aircraft we concluded that the defined safe landing corridor can be moved on x-axis. It provides the movement of runway on x-axis. It is not required to consider the movement of runway at y-axis, because as it is seen from the previous system results, the UAV can fit to any commanded y-axis value during flight.

This kind of design about runway is required when the aircraft is not in the defined safe landing corridor which is finishing at (0, 0, 0) point. We have stated initially that, when we apply the proposed method here, the safe landing corridor start to shift up to the defined x-axis constraint. So, by this way we can obtain new safe landing corridor. The new results are reached by a MATLAB/m-file program.

The logic of the proposed algorithm is given below step by step:

1. Consideration of aircraft initial position:
   First, the present position of the aircraft should to be considered. If it is inside of the defined initial safe landing corridor, determination of a new corridor is not a necessity. If it is outside of the corridor the next step will be applied.

2. Definition of x-axis distance constraint:
   We know that the aircraft is outside of the initial safe landing corridor. In this step we consider the longitudinal position of UAV. If aircraft gets over the upper limits we have to shift the corridor through the positive side of our initial axis system or vice versa. Thus, at the top of the execution of the program the positive and negative shifting distance values have to be defined. This limitation is important. It represents the assumed length of the runway. When there is not any limitation, the program executes with endless iteration number.

3. Execution of the program:

   As it is mentioned above the program considers the aircraft initial position according to the initial safe landing corridor limits. Then it starts to iterate up to the defined x-axis distance constraint. The iteration number is found as;

$$\#iteration = (x0 - xexp)/10 \qquad [7.1]$$

   where;

   $\#iteration$ represents number of iterations;

   $x0$ is initial position of aircraft at x-axis

   $xexp$ is x-axis distance constraint (shifting margin value)

   10 is the value of the intervals, that means we make comparison at each 10 meters distance in order to see if the aircraft provides the corridor properties for each axis values (x, y, z).

4. Obtaining resultant values:

   If aircraft is in the initial corridor the program gives a caution as inadequate input". Otherwise, the adequacy of the defined x-axis distance constraint is evaluated. That means at the end of iteration step if the initial point will not be covered by safe landing corridor the program gives a caution as "inadequate x margin". Then preferably for a new search for the x-margin will be changed or missing path approach procedure will be applied.

We have obtained test results of this safe landing corridor shifting program. As it is seen form Table 16 it works properly. In this table you can consider all steps which are explained here. During the position evaluation step of the program 940 m distance at x-axis is an important input for us. Because when we look at the corridor definition graphs (Figure 6, 7, 8) the permitted tolerance angle values are different for 0 /-942.4 m intervals and -942.4 /-1942 m intervals for calculations. This changes the initial position evaluation values.

Table 16 Test Results of Shifting Safe Landing Corridor Algorithm

Initial Values						Resultant values	
X0 (m)	Y0 (m)	Z0 (m)	+x margin	-x margin	Defined #iterations	Xfinal	remarks
-940	6	30	300	-300	30	-930	
-1000	6	30	300	-300	30	-700	Inadequate x-margin
-1440	50	100	300	-300	30	-1710	
-1440	50	105	300	-300	30	-1740	Inadequate x-margin
-1440	62	60	300	-300	30		Inadequate inputs.
-1440	62	90	300	-300	30	-1580	

CHAPTER 8

WIND EFFECT

In the previous parts of this thesis work we have presented many responses of the system to the designed autopilot. But these system models do not include environmental disturbances. That means, the disturbance effect of wind is disregarded for the previous simulations. We have simulated no wind condition by applying zero to the wind input part of the IAI Pioneer Non-linear Model which represents wind velocity and wind rate.

In this chapter we have applied cross wind model on the Simulink system model and tried to control the states of aircraft under wind effect. We have tested the system responses with different wind amplitudes and directions. The results obtained are presented in the following sections.

According to the general autopilot design approach, the controller gains will provide to control of states in spite of the disturbing effects on system [3]. We have tested the Simulink system model with a constant crosswind value (5 m/s) with other reference command signals. In this case reference airspeed is 30 m/s, reference altitude is 100 m and reference heading signal is 0. The expected response of the system is keeping its states constant. When we look at the controlled state results due to the disturbing effect of wind the airspeed reaches to an unacceptable value (Figure 104), the altitude state response is proper (Figure 105). But the heading state response is meaningless (Figure 106). Because it follows another command signal instead of the reference command signal and according to this reference signal the position of aircraft at y-axis is diverging from zero (Figure 107).

We have considered many simulation results of some other lower wind values. But the system did not respond as expected. In order to get the expected results at y-axis we have to add a wind correction angle to the heading input of the direction controller. In that case, some undesired calculations are required.

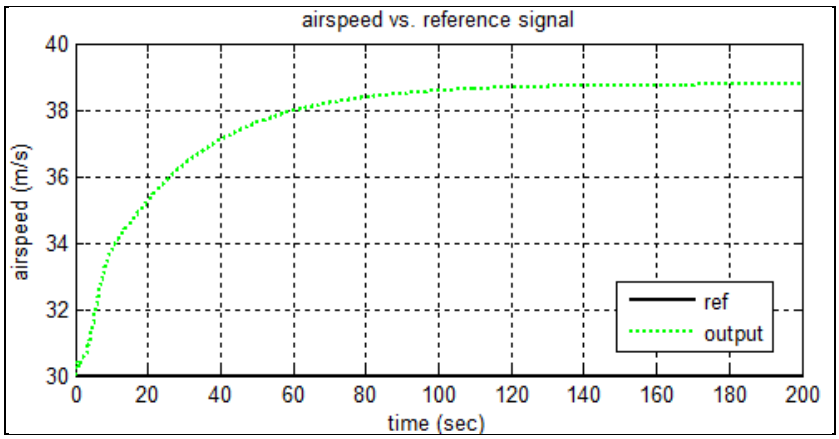

Figure 104 Improper Response of System to the Speed Controller (Wind Effect)

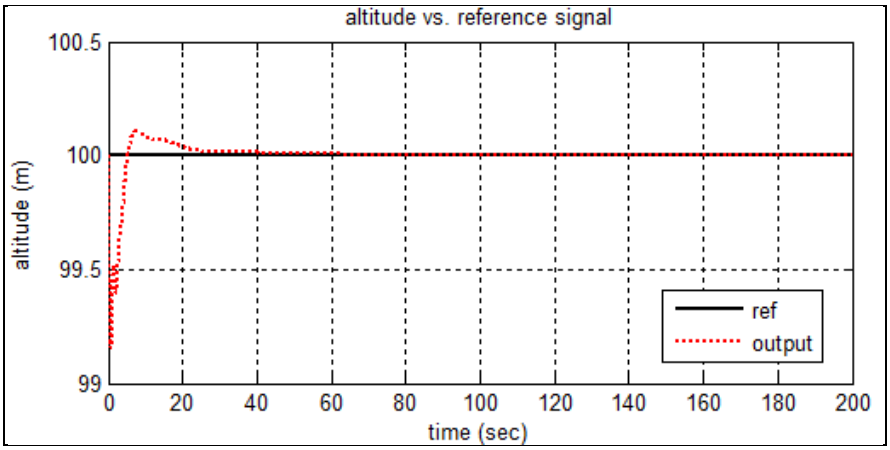

Figure 105 Improper Response of System to the Altitude Controller (Wind Effect)

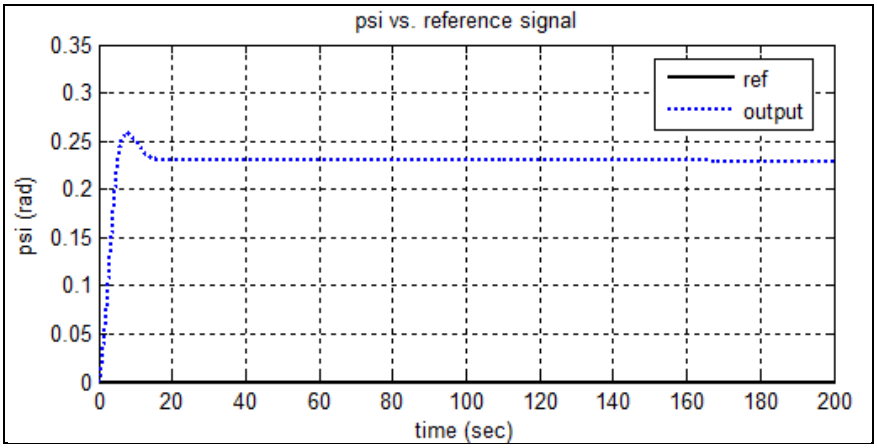

Figure 106 Improper Response of System to the Direction Controller (Wind Effect)

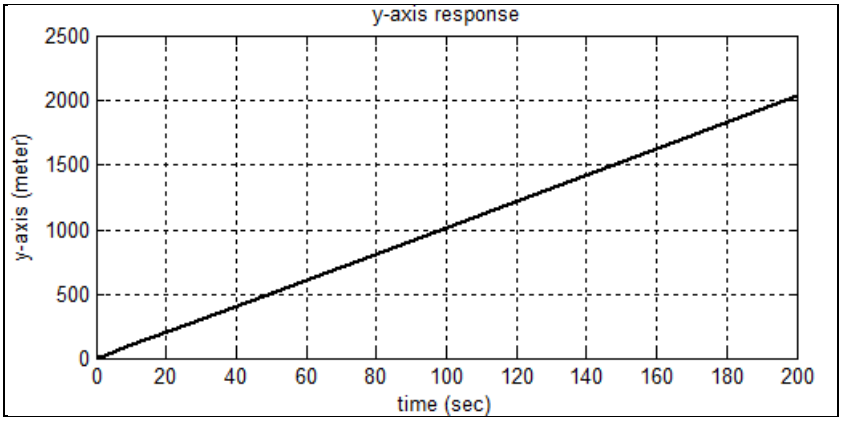

Figure 107 y-axis Result of System (Wind Effect)

Next, we have required testing the performance of the direction controller. We have designed a new direction controller with the pole placement method. The design details of the controller are given in Chapter 3. Similarly the first initial design activities have been realized with the windless Simulink system model. For this case, we have observed the same results similar to the PID direction controller. Then we have added wind component to the simulation model. These controller gains did not work on that model (similar to PID controller), either. But when we changed the gain values we have obtained more meaningful results.

By the help of these results we have concluded that the available controller gains are not suitable for the wind added system. Then we have continued to test the system by changing the PID Direction Controller Gain values. At the end we have found the controller gains that control the system properly.

In order to test the system response for state controllers for a landing scenario, we have defined initial states and produced the reference signal for required states. Initial speed value is 30 m/s and constant up to end of the landing simulation. The initial altitude is 100 m, and a landing trajectory is applied to the altitude controller as a reference altitude signal. Initial y-axis position is 100 m and the desired position is zero according to the main landing path. Due to this lateral deviation we have used cross track error compensation block model and generated related reference heading signal which is applied on the direction controller. Also a 5 m/s crosswind is applied to the Simulink system model. Next the system is tested.

When we look at the speed response (Figure 108) some peak values are observed in the middle of the simulation due to the changing value of reference altitude command. The altitude state response is reasonable (Figure 109). Along y-axis figure we can obtain the elimination of cross track error as expected (Figure 111). The related reference heading signal and system response is shown in Figure 110. As it is seen from these results the aircraft satisfies the desired responses.

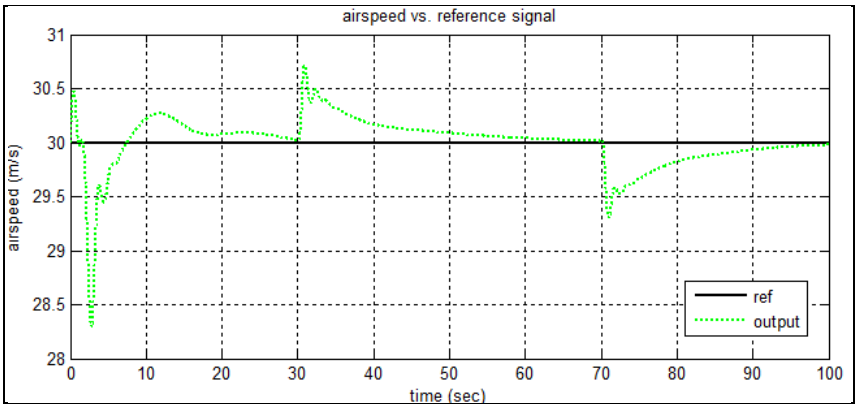

Figure 108 Proper Response of System to the Speed Controller (Wind Effect)

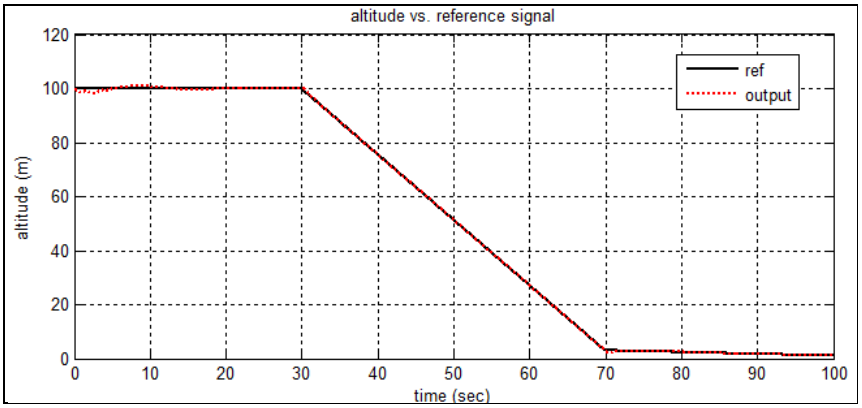

Figure 109 Proper Response of System to the Altitude Controller (Wind Effect)

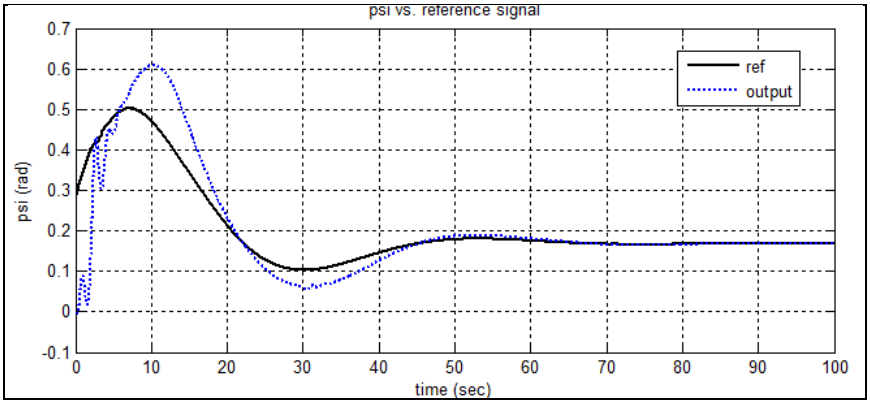

Figure 110 Proper Response of System to the Direction Controller (Wind Effect)

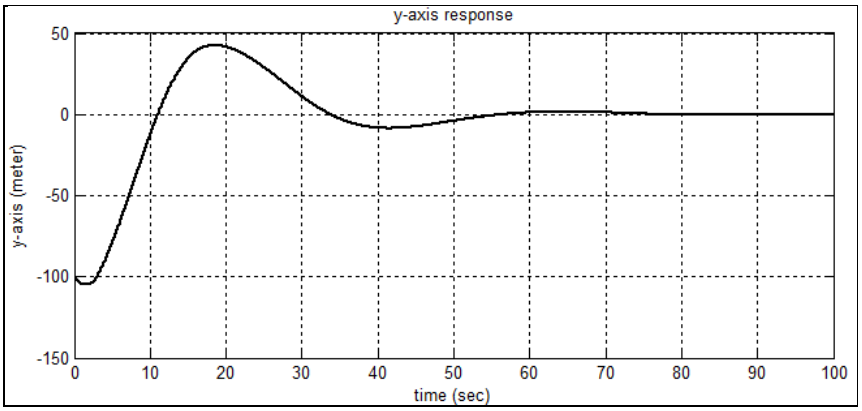

Figure 111 y-axis Result of System (Wind Effect)

Responses of the other system states and controller surfaces are given below. Again for all longitudinal components the effect of the change of reference altitude value is observed (Figure 114 and Figure 115). The system responses are appropriate regarding the controller limiters (Figure 115 – Throttle Deflection). Also, the lateral axis components' responses show that, the aircraft reaches the stability in a longer time due to the no wind effected system (Figure 112, Figure 113, Figure 116).

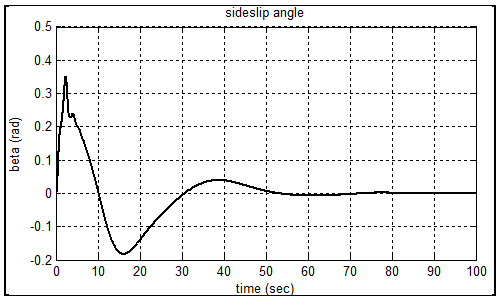

Figure 112 Sideslip Angle Response

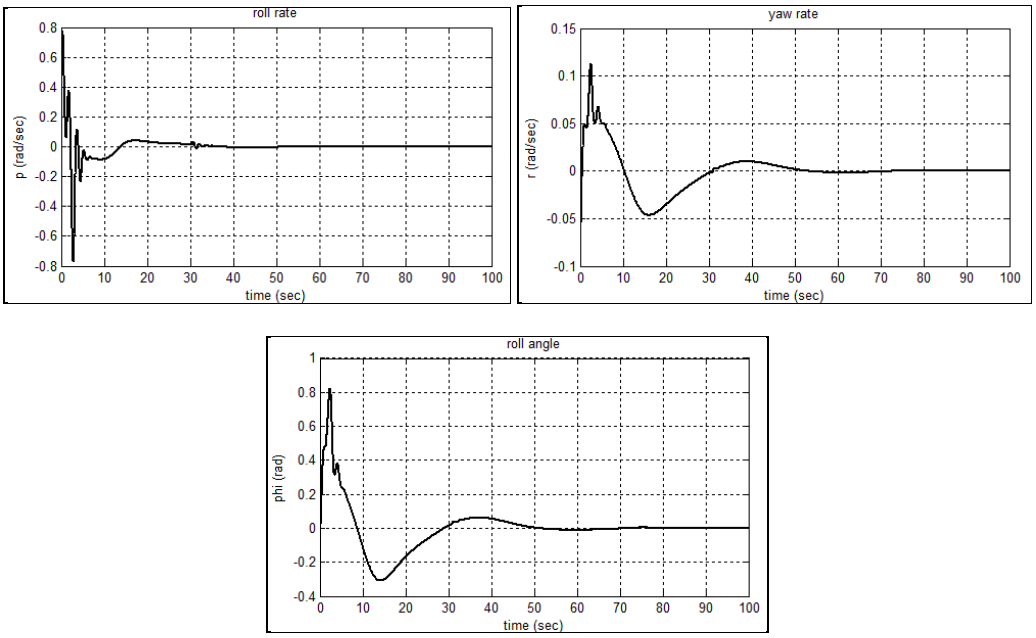

Figure 113 Roll Rate, Yaw Rate and Roll Angle Responses

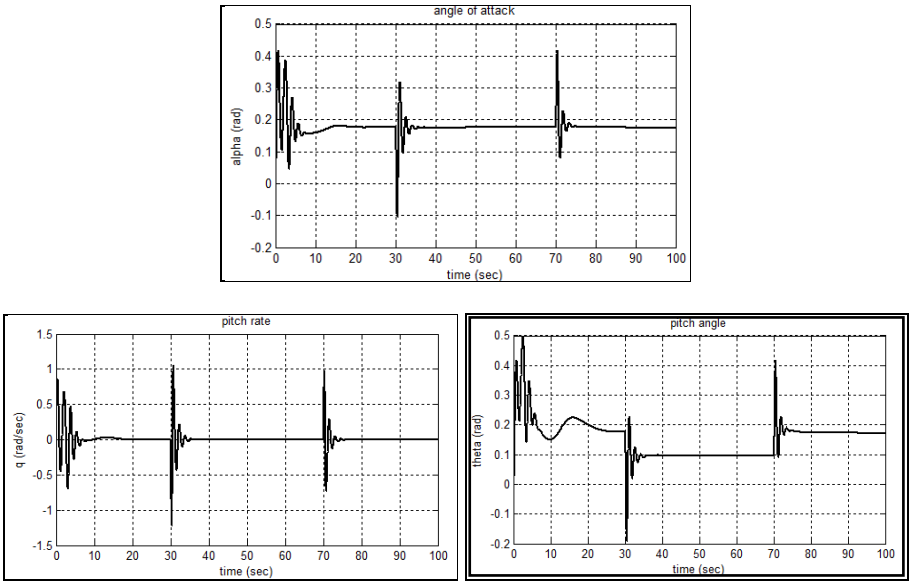

Figure 114 Angle of Attack, Pitch Rate and Pitch Angle Responses

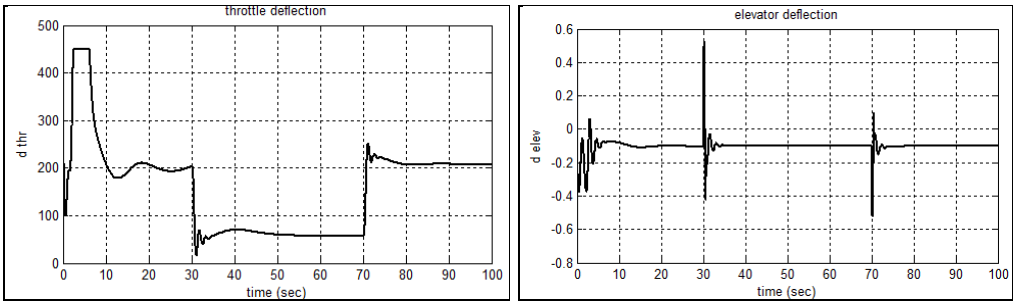

Figure 115 Throttle and Elevator Deflections

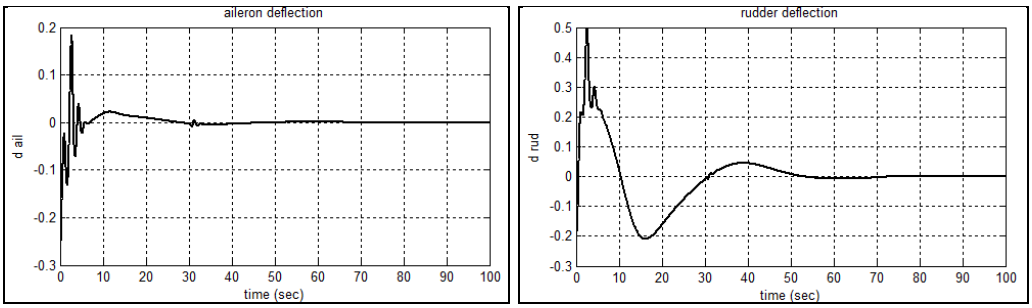

Figure 116 Aileron and Rudder Deflections

We have tested the same system with wind effects whose directions are different. According to all tested cases we have observed that this new controller gain set provides proper control of the related states out of the wind values whose directions are between 160-230 degrees. For the remaining directions (between -150-160 degrees) the system works appropriately.

Then we have tested the simulation model with different wind amplitudes. As it is observed the system works properly up to 20 m/s wind speed. But as we increase the wind speed the responding area of the simulation model is getting narrower due to the changing wind direction. That is, at this speed value the system responds properly for the wind direction values between -100 and 100 degrees. System does not work properly for the other directions, which means the related state controllers try to hold altitude and speed but the heading signal control is not acceptable.

At a rear wind condition the speed of the aircraft is increasing. But during a landing procedure speed of the aircraft will decrease. In our scenarios we kept the airspeed at constant 30 m/s. Under wind effect the actual speed of the aircraft is decreasing up to stall speed. In this case a safe landing is impossible. In other studies in order to avoid the bad effect of the rear wind crab maneuvers are applied [3].

After these considerations about the non-linear model of the UAV, we turned to the linear system analysis with the wind disturbance.

In this case we have repeated each autopilot design step that is explained in Chapter 3 for the linear aircraft models regarding wind effect. Firstly, we have arranged new state space matrices which include the wind components in the input states by using MATLAB Linearization Tool. Again this study is realized for maximum and minimum speeds of the UAV. 30 m/s and 60 m/s speed constraints are determined according to performance parameters. See Chapter 3 for details.

In the first case the non-linear aircraft model is trimmed at 60 m/s speed and 60 m altitude. The obtained initial states are used during the non-linear model linearization. Then we have added the wind input value as 5 m/s. In order to control the system states by the landing autopilot new controller gains are generated for this state. The dedicated reference signals for speed and altitudes are step inputs. By

the help of cross track error compensation block we have observed the position deviation at y-axis due to wind effect and related reference heading signal. The related proper simulation results are given below.

The controller output signals that belong to speed (Figure 117) and altitude (Figure 118) states are generated with so many ripples. This has resulted from the linearization states. That is, 60 m/s is the speed upper limit value of this UAV. Then any disturbance effect can reduce the system performance. But the lateral movement of the aircraft can eliminate the cross track error (Figure 120). In addition the ripples have occurred on the related reference heading signal due to the other controller responses (Figure 119). For these given results the wind speed is 5 m/s.

When we change the direction of the wind, still the system works properly. We have tested the system with different wind speeds. For the crosswinds faster than 7 m/s system does not work. We cannot obtain any meaningful simulation results.

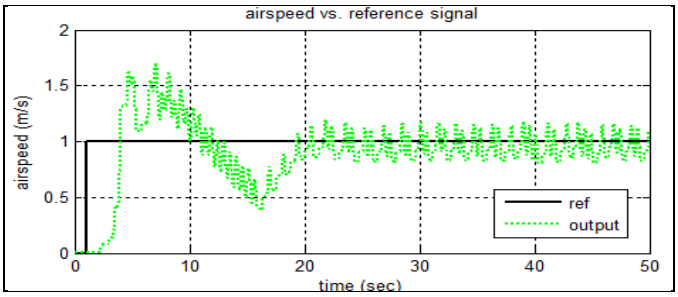

Figure 117 Response of 1st Linear System to Speed Controller with Wind Input

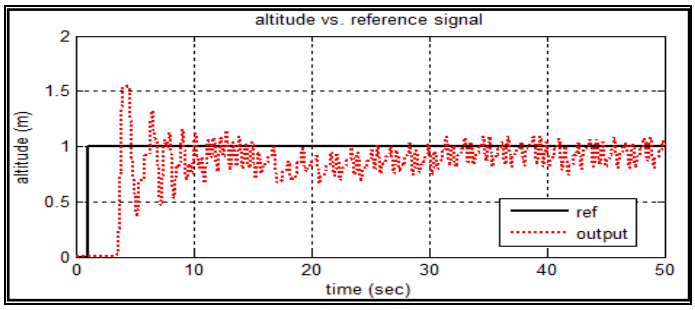

Figure 118 Response of 1st Linear System to Altitude Controller with Wind Input

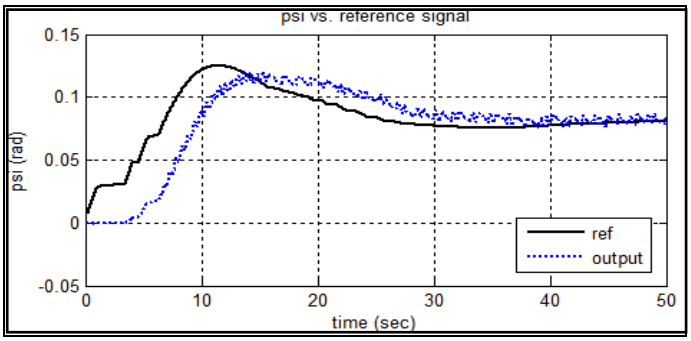

Figure 119 Response of 1st Linear System to Direction Controller with Wind Input

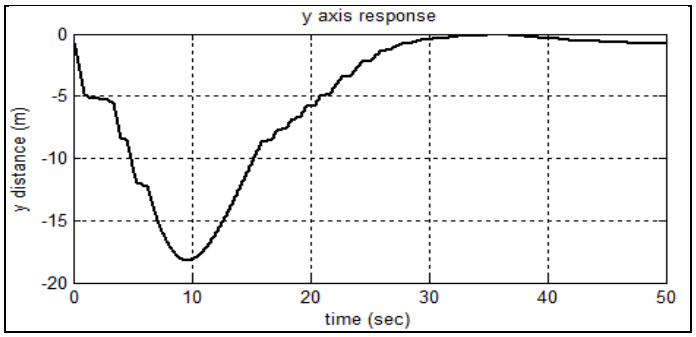

Figure 120 y-axis Response of 1st Linear Model with Wind Input

Then we have repeated the previous non-linear model linearization activities for the new initial states (30 m/s speed and 60 m altitude). Similarly a landing autopilot is designed for these initial states and an appropriate controller gain set observed. By the help of this set the wind effect on the linear system is compensated. For simulations, we have added the same reference state signals that have been used in the other linearized mode. Again the speed of the applied crosswind is 5 m/s.

When we have evaluated system responses, the outputs of speed and altitude state controllers have been observed to be more stable (Figure 121 and Figure 122). Also, cross track error elimination performance of the system is very well (Figure 124). The related reference heading signal is satisfactory (Figure 123).

When we change the direction of the wind, still the system is works properly. We have tested the system with different wind speeds. For the crosswind faster than 7 m/s system is still working. But the obtained results of the controlled states cannot be accepted.

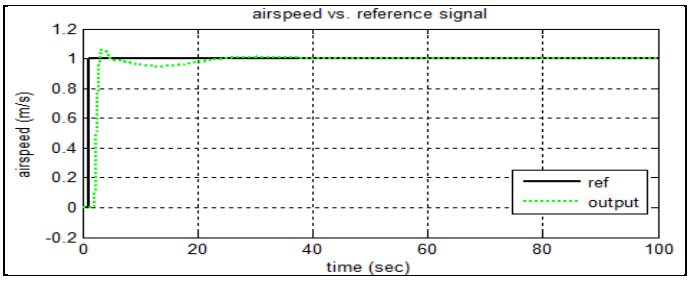

Figure 121 Response of 2nd Linear System to Speed Controller with Wind Input

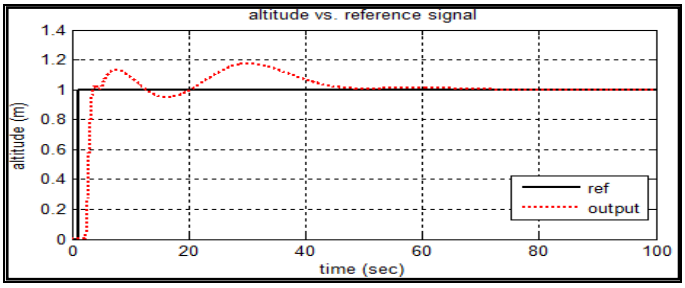

Figure 122 Response of 2nd Linear System to Altitude Controller with Wind Input

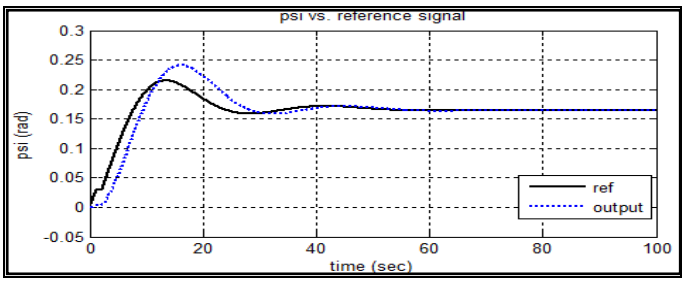

Figure 123 Response of 2nd Linear System to Direction Controller with Wind Input

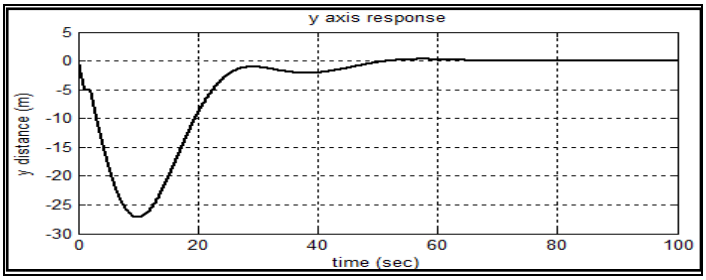

Figure 124 y-axis Response of 2nd Linear Model with Wind Input

By this application, we have considered the limiting values of the given UAV linear models. According to this idea, for different cruising speed values, we can produce corresponding controller gain sets. These sets will be merged similar to gain scheduling method. For the remaining speed values related controller gain set will be generated from this set. When we increase the number of the considered linear models and related controller gain sets, the obtained linear system response converges to non-linear model response.

CHAPTER 9

CONCLUSIONS AND FUTURE WORKS

In this thesis work the landing phase which is one of the most important parts of any flight is considered regarding both lateral and longitudinal states of the aircraft. Also, the related simulation results are presented. For this purpose a non-linear model of IAI Pioneer RQ-2 UAV is used. This model is taken from an available MATLAB Library. System simulation is realized in MATLAB/Simulink.

In order to provide the lateral and longitudinal movement of the UAV a speed, an altitude, and a direction controller are designed. Before the design phase of the autopilot, different trim states are obtained. Regarding the performance of the system two trim points at maximum and minimum speed values were seen to be sufficient. Then, obtained initial state values are used during the linearization of the non-linear model. MATLAB Linearization Tool is used for this purpose. Initially the autopilot is designed for the linear models. Subsequently, the designed autopilot is applied on the non-linear model with the trim input. These steps are repeated for each trim input set. Then the resultant controller gains set are merged with a gain scheduling method where the speed is the scheduling variable. The results of the designed system are acceptable.

In addition to the autopilot design, another important issue for this thesis is generating appropriate landing paths. Firstly, regarding the known flight rules a main landing path is generated. Then a safe landing corridor is defined. Next, aircraft position is considered whether it is inside or outside of this defined area. For inner parts of the corridor a landing path set is obtained by using optimization algorithms. For this purpose some starting points are determined. Next a cost function is defined which tries to express the error between actual position and desired position of the aircraft. Then the optimum paths are generated for movement at y-axis and z-axis. As it is concluded the altitude path optimization is not required, because the

controller holds altitude directly. But it is very useful for lateral position control, because we have only a direction controller. By the help of this reference heading signal data base we produced optimum lateral movement paths which reaches the main landing path at the end. Then we augmented the reference heading signals using linear interpolation. So, for each initial position at y-axis a proper reference heading signal is obtained successfully. For outer part of the safe landing corridor, a simple missing path approach procedure is applied. This movement is realized with a time based data set that includes the heading, altitude and speed values as a reference signal for each waypoint. The controllers follow the given reference states for each case properly.

Also lateral position controllers are designed in order to control the replacement of the aircraft at lateral axis. For each controller the basic idea is producing reference heading signal due to the initial position of the aircraft and position of target point. It has been observed from the simulation results that the controller is working properly.

In order to be able to increase the coverage area of the safe landing corridor its movement is provided regarding the assumed runway length. So, by the help of this design approach the number of possible missing path approach procedures is decreased.

In order to consider the effects of the environmental disturbances we added a crosswind to the system simulation. Although the initial controller gain set did not work for this case, a new gain set is generated. Then, in general we have observed good results but some discrepancies related with the direction of the wind are observed. Finally we considered the wind effect on the linear model of UAV. For this case we obtained expected good result at all wind directions up to 7m/s wind speed.

Suggested items as future works are listed below;

- Adaptive or fuzzy logic controllers/autopilots will be used in order to eliminate gain scheduling and provide the control of the aircraft even under the environmental disturbance (wind) effects.
- Also an online method will be generated that will provide target waypoints during a flight regarding aircraft performance and environmental constraints.

- The Simulink model of the system will be enriched with some sensor models and a landing gear model.
- Landing can be done based on a sliding mode landing autopilot.

REFERENCES

1. H. Grankvist, “Autopilot design and Path Planning for UAV”, FOI-R-2224-SE, Scientific Report, Defense and Security, System and Technology, December, 2006.
2. A. Barrientos, P. Gutiérrez, J. Colorado, “Advanced UAV Trajectory Generation: Planning and Guidance”, Universidad Politécnica de Madrid – (Robotics and Cybernetics Group) Spain, Aerial Vehicles, InTech, 2009.
3. V. Kargın, “Design of an Autonomous Landing Control Algorithm for a Fixed Wing UAV”, M.Sc. Thesis, METU, 2007.
4. J. Juang, B. Lin, K. Chin, “Intelligent Fuzzy Systems for Aircraft Landing Control”, I. Wang, Y. Jin (Eds.) Lecture Notes in Computer Science, Springer-Verlag Berlin Heidelberg, vol.3613/2005, pp. 851 – 860, 2005.
5. F. Küreksiz, “A Real Time Test Setup Design and Realization for Performance Verification of Controller Designs for Unmanned Air Vehicles”, M.Sc. Thesis, METU, 2008.
6. R. S. Christiansen, “Design of an Autopilot for Small Unmanned Aerial Vehicles”, M. Sc. Thesis, Brigham Young University, 2004.
7. M. Oosterom, R. Babusˇka, “Design of a Gain-scheduling Mechanism for Flight Control Laws by Fuzzy Clustering”, Elsevier, Control Engineering Practice, vol. 14, pp. 769-781, 2006.
8. D. McLean, “Automatic Flight Control Systems”, Prentice Hall,1990.
9. S. Suresh, N. Kannan, “Direct Adaptive Neural Flight Control System for an Unstable Unmanned Aircraft” Elsevier, Applied Soft Computing vol. 8, pp 937-948, 2008
10. MIT Open Courseware, “Lecture12 Aircraft Lateral Autopilots”, “URL: http://ocw.mit.edu/courses/aeronautics-and-astronautics/16-333-aircraft-stability-and-control-fall-2004/lecture-notes/lecture_12.pdf” as accurate January 29th 2011.
11. S. Park, J. Deyst, and J. How, “A New Nonlinear Guidance Logic For Trajectory Tracking” Proceedings of the AIAA Guidance, Navigation and Control Conference, AIAA, Paper 2004-4900, August 2004.

12. M. Niculescu, “Lateral Track Control Law For Aerosonde UAV” 39th AIAA Aerospace Sciences Meeting and Exhibit Reno, NV, AIAA Paper 2001-0016, 2001.
13. G.J.J. Ducard, “Fault-Tolerant Flight Control and Guidance Systems Practical Methods for small Unmanned Aerial Vehicles”, H Noura et al. (Eds.), AIC (Advances in Industrial Control), Springer-Verlag, London, 2009.
14. G. Ducard, K. C. Kulling, H. P. Geering, “A Simple and Adaptive On-line Path Planning System for a UAV”, Proceedings of the IEEE 15th Meditarrenean Conference on Control and Automation, Greece, pp. 1-6, 2007.
15. A. Richards, J.P. How, “Aircraft Trajectory Planning With Collision Avoidance Using Mixed Integer Linear Programming”, Proceedings of the American Control Conference, vol. 3, pp. 1936-1941, 2002.
16. A. H. Kassem, “Trajectory Optimization via Simulation Using Incremented Genetic Algorithms” the Canadian Aeronautics and Space Journal, vol.52, No.1, March, 2006.
17. M.D. Ardema, B. C. Asuncion, “Flight Path Optimization at Constant Altitude”, G. Buttazzo, A. Freidiani (Eds.), Variational Analysis and Aerospace Engineering, Springer Optimization and its Applications, vol.33, pp.21-32, 2009.
18. J. Z. Ben-Asher, V. Heymann, “Aircraft Trajectory Optimization in the Horizontal Plane”, Proceedings of the 34th Conference on Decision & Control New Orleans, LA, pp.1879-1880, 1995.
19. “Phase of Flight Definitions and Usage Notes”, CAST-ICAO Common Taxonamy Team, Version 1.0.1, 2006.
20. Federal Aviation Authority, Federal Aviation Rules Part 25: Airworthiness Standards: Transport Category Airplanes. Subpart B-Flight. URL:http://ecfr.gpoaccess.gov/cgi/t/text/text-idx?c=ecfr&sid=2b5d33cc880ea2ec74495e2263005c63&rgn=div5&view=text&node=14:1.0.1.3.11&idno=14, as accurate January 29th 2011.

21. To the Procedures for Air Navigation, “Aircraft Operations”, Amendment No: 14, Doc. 8168, Volume I, Flight Procedures, 5th Edition, International Civil Aviation Organization, June 2005.
22. J. D. Jr Anderson, “Aircraft Performance and Design” McGraw Hill International Editions, 1999.
23. M.V. Cook, “Flight Dynamics Principles”, Elsevier, 2007.
24. V. Nalbantoğlu, “AE 552-Robust Control Lecture Notes”, METU, 2009.
25. A. J. Niven, T. M. Young, “The Standard Handbook for Aeronautical and Astronautical Engineers, Section 10 Aerodynamics, Performance and Stability and Control”, Mc-Graw Hill Digital Engineering Library, 2004.
26. M.S. Bazaraa, H.D. Sherali, C.M. Shetty, “Nonlinear Programming: Theory and Algorithms”, Wiley-Interscience, 2006.
27. URL: http://trond.hjorteland.com/thesis/node26.html, as accurate January 29th 2011.
28. M. Avriel, “Nonlinear Programming Analysis and Methods”, Prentice-Hall, 1976
29. J.G. Juang, H.K. Chiou, L.h. Chien, “Analysis and Comparison of Aircraft Landing Control Using Recurrent Neural Networks and Genetic Algorithms Approaches”, Elsevier, Neurocomputing, vol. 71, pp. 3224–3238, 2008
30. URL: http://www.engin.umich.edu/group/ctm/state/state.html, as accurate January 29th 2011.
31. Copyright Paul Oh, “Hands-on Lab 5 Matlab/Simulink: Designing and Testing Controllers” MEM 351 Dynamic Systems Lab 5, Lecture Notes. URL:http://www.pages.drexel.edu/~pyo22/mem351/mem351Lab-PolePlacementSimulation/mem351Lab-PolePlacementSimulation.pdf, as accurate January 29th 2011.
32. S. Güney, A. Atasoy “An Approach to Pole Placement Method with Output Feedback”, UKACC Control Conference, URL: www.control2008.org/papers/p137.pdf, as accurate January 29th 2011.
33. URL: http://www.ae.illinois.edu/m-selig/apasim/Aircraft-uiuc/pioneerUAV-nl-v2/aircraft.dat, as accurate January 29th 2011.

34. S.C Charpa., R.P. Canale “Yazılım ve Programlama Uygulamalarında Mühendisler İçin Sayısal Yöntemler”, Literatür Yayınları, vol. 82, 2004
35. M. K. Leblebicioğlu, “EE 553-Optimization Lecture Notes”, METU, 2008
36. URL: http://www.aerostudents.com/files/flightDynamics/derivingTheEquationsOfMotion.pdf , as accurate January 29th 2011.